WORKING paper

BANQUE DE FRANCE
EUROSYSTÈME

Inflation and Growth Risk: Balancing the Scales with Surveys

Sarah Mouabbi[1], Jean-Paul Renne[2] & Adrien Tschopp[3]

February 2026, WP #1036

ABSTRACT

Post-pandemic inflation highlighted tensions between price stability and growth objectives. We evaluate this risk using probabilistic responses from professional forecasters' surveys. Our dynamic factor model with time-varying uncertainty and asymmetry captures the joint dynamics of inflation and growth and decomposes them into demand and supply components. We find that tail risk is prominent in US data in the 1980s and during the Great Recession for inflation, and during the 1980s and in the period following COVID-19 for GDP growth. The post-pandemic inflation is driven by temporary adverse supply and persistent positive demand. The model-implied correlation between inflation and growth is time-varying, negatively related to nominal term premiums and on average positive, suggesting that professional forecasters do not have stagflationary beliefs. In 2022, stagflation risks increased after three decades of near-zero probabilities.

Keywords: Dynamic Factor Model with Stochastic Volatility, Uncertainty, Asymmetry, Tail Risk, Inflation, Output Growth, Demand, Supply, Trend, Cycle

JEL classification: C32, E31, E32, E44

[1] Banque de France, sarah.mouabbi@banque-france.fr
[2] University of Lausanne, jean-paul.renne@unil.ch
[3] University of Lausanne, adrien.tschopp@unil.ch

We are grateful to Michael Bauer, Kenza Benhima, Lena Draeger, Michael Ehrmann, Chad Fulton, Erwan Gautier, Domenico Giannone, Pablo Guerron-Quintana, Stephane Guibaud, Marek Jarocinski, Bartosz Mackowiak, Catalina Martinez Hernandez, Elmar Mertens, Krisztina Molnar, Annette Vissing-Jorgensen, to seminar participants at the US Federal Reserve Board, ETH KOF, National Bank of Slovakia, European Stability Mechanism, De Nederlandsche Bank, Bank of England, Banca d'Italia, National Bank of Belgium, European Central Bank, and to participants of the Macro x the pond workshop, Econometrics workshop at the St Louis Fed, Padova Macro talks 2023, Dolomiti Macro Meetings 2023, Annual Villa Research workshop 2023 at the Bank of Finland, 5th Biennial Conference on Uncertainty, Economic Activity, and Forecasting in a Changing Environment (University of Padova), CFE 2023, ESCB Research Cluster on Monetary Economics 7th Annual Workshop, ESSIM 2024, AMSE-BdF workshop 2024, 4th Sailing the MacroWorkshop (Ortygia), PSE Macro Days 2024 and Economics of Risk Workshop (Collegio Carlo Alberto, Turin), IAAE 2025, ESWC2025 for useful comments.

NON-TECHNICAL SUMMARY

Identifying whether macroeconomic fluctuations are mainly attributable to demand or supply factors is essential to setting the appropriate policy mix. A shock like COVID-19 has drawn renewed interest in distinguishing between these determinants because this period is characterized by several large concurrent demand and supply shocks. In this paper, we address this question for the United States (US).

We jointly assess the risks on prices and production by exploiting forward-looking survey information to capture macroeconomic risk perceptions. We identify demand and supply factors for the US by imposing basic theoretical assumptions on a dynamic factor model. Following economic theory, demand factors are those that drive inflation and real activity to move in the same direction. In contrast, supply factors are captured by movements in inflation and economic activity in the opposite direction. The dynamic factor model features time-varying volatility (uncertainty) and asymmetry to study the relationship between inflation and the real economy through the lens of the probabilistic responses of professional forecasters. The use of surveys allows us to study the perception of the joint relationship between inflation and GDP growth of informed market participants that regularly nourish monetary policy discussions. Importantly, such data reveal information beyond past and current realized inflation and GDP growth because they are forward-looking and inform about tail-risk expectations without the need for such fears to materialize, making them a rich and relevant source of information for our analysis.

Beyond standard realized inflation and output growth series, we leverage probabilistic responses of the Survey of Professional Forecasters (SPF) to exploit changes in the entire distribution of future expected inflation and GDP growth. In our setup, we enrich the identification of drivers by allowing changes in the shape of the distribution of expected inflation and GDP growth to inform about the nature (demand/supply) of the shock hitting the economy. Hence, our model features time-varying uncertainty and asymmetry (tail risk) to jointly estimate the dynamics of realized and expected inflation and GDP growth rates and fit the conditional first-, second- and third-order survey-moments at different horizons. Moreover, our model allows for a trend and cycle decomposition, which enables us to study the drivers of prices and real activity at business-cycle and lower frequencies.

We estimate our model on US data spanning the period 1981-2024. Our model can fit realized inflation and growth as well as all three first conditional moments of their forecast distributions. Importantly, the sample includes both calm periods and very large shocks (e.g., 1980s, Great Recession, COVID-19), therefore, our model performs well under any economic condition. Our demand and supply factors capture key events that relate to demand and supply shocks, respectively. Moreover, our volatility factor marks its sharpest increase during the COVID-19 crisis and features peaks around every NBER recession in our sample.

Our findings suggest that the output gap is determined by a mix of demand and supply factors before the Great Recession and in the last quarters of our sample, while it is mainly driven by demand between 2008 and 2020. Moreover, the price gap exhibits a sharp rise in the last quarters of our sample, in line with the idea that high inflation realizations are partly explained by transitory components. Interestingly, the post-Covid increase in inflation is attributed to temporary negative supply factors and more persistent positive demand factors after the COVID crisis. These findings are consistent with the increase in bottlenecks and supply chain disruptions since COVID-19, as well as the large pandemic economic stimulus and relief packages that were implemented in the United States. Finally, we compute the time-varying correlation between inflation and economic activity, revealing the evolving importance professional forecasters assign to aggregate supply and demand. We observe that this correlation varies over time and is negatively related to nominal term premiums, in line with structural modeling of the term structure of interest. On average, the relationship between inflation and economic activity is positive, suggesting that professional forecasters do not have stagflationary beliefs. Computing probabilities of stagflation risk in future horizons, we also show that in 2022, these risks reemerged after three decades of near-zero probabilities.

Figure 1. Time-varying probability of stagflation

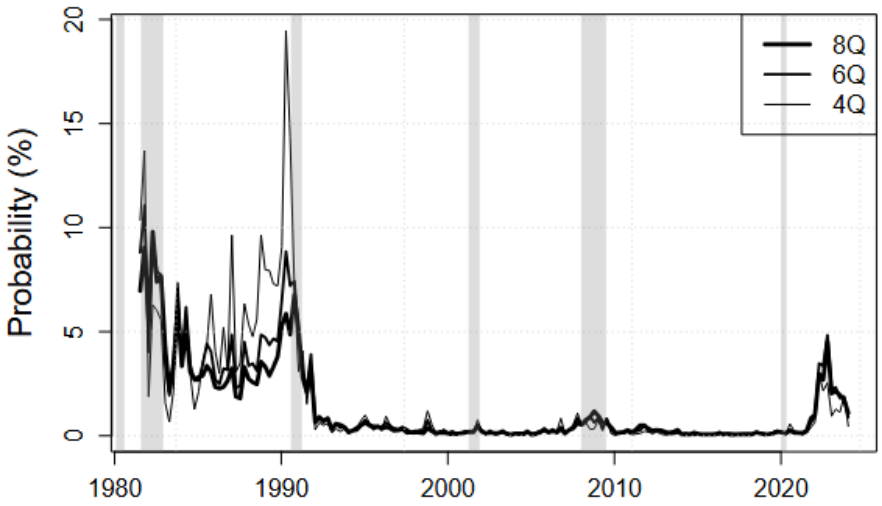

Note: This figure presents the model-implied probabilities of experiencing a stagflation, defined as year-on-year inflation above 4% and year-on-year GDP growth below 0%, across different forecast horizons (4 to 8 quarters ahead). Each series is computed by 10,000 model simulations for each date in the sample, capturing the evolution of stagflation risk over time.

Risque d'inflation et de croissance à travers le prisme des prévisionnistes professionnels

RÉSUMÉ

L'inflation post-pandémie a mis en lumière les tensions entre les objectifs de stabilité des prix et de croissance. Nous évaluons ce risque à l'aide des réponses probabilistes issues des enquêtes auprès des prévisionnistes professionnels. Notre modèle à facteurs dynamiques, intègre la variabilité dans le temps de l'incertitude et de l'asymétrie de la distribution de la dynamique conjointe de l'inflation et de la croissance et les décompose en composantes de demande et d'offre. Nous constatons que les risques extrêmes sont marqués dans les données américaines pour l'inflation dans les années 1980 et durant la Grande Récession, ainsi que pour la croissance du PIB dans les années 1980 et dans la période suivant la COVID-19. L'inflation post-pandémie est portée par des chocs d'offre défavorables temporaires et une demande positive persistante. La corrélation entre inflation et croissance implicite au modèle varie dans le temps, est négativement liée aux primes de terme nominales et est en moyenne positive, ce qui suggère que les prévisionnistes professionnels n'adhèrent pas à des anticipations stagflationnistes. En 2022, les risques de stagflation ont augmenté après trois décennies de probabilités proches de zéro.

Mots-clés : modèle à facteurs dynamiques avec volatilité stochastique, incertitude, asymétrie, risques extrêmes, inflation, croissance de la production, demande, offre, tendance, cycle

1. Introduction

Identifying whether macroeconomic fluctuations are mainly attributable to demand or supply factors is essential to setting the appropriate policy mix. A shock like COVID-19 has drawn renewed interest in distinguishing between these determinants because this period is characterized by several large concurrent demand and supply shocks.

In this paper, we jointly assess the risks on prices and production by exploiting forward-looking survey information to capture macroeconomic risk perceptions. We use a dynamic factor model with time-varying volatility (uncertainty) and asymmetry to study the relationship between inflation and the real economy through the lens of the probabilistic responses of professional forecasters. The use of surveys allows us to study the perception of the joint relationship between inflation and GDP growth of informed market participants that regularly nourish monetary policy discussions (e.g., Grishchenko et al., 2019; Jo and Sekkel, 2019). Moreover, these surveys are documented to have a strong forecast record relative to various time-series models (e.g., Ang et al., 2007). Importantly, such data reveal information beyond past and current realized inflation and GDP growth because they are forward-looking and inform about tail-risk expectations without the need for such fears to materialize, making them a rich and relevant source of information for our analysis.

We identify demand and supply factors for the United States (US) by imposing basic theoretical assumptions. Following economic theory, demand factors are those that drive inflation and real activity to move in the same direction. In contrast, supply factors are captured by movements in inflation and economic activity in the opposite direction. Beyond standard realized inflation and output growth series, we leverage probabilistic responses of Surveys of Professional Forecasters (SPF) to exploit changes in the entire distribution of future expected inflation and GDP growth. In our setup, we enrich the identification of drivers by allowing changes in the shape of the distribution of expected inflation and GDP growth to inform about the nature (demand/supply) of the shock hitting the economy. Hence, our

model features time-varying uncertainty and asymmetry (tail risk) in order to jointly estimate the dynamics of realized and expected inflation and GDP growth rates and fit the term structures of conditional first-, second- and third-order survey-moments.

Another important element in outlining the appropriate response of monetary and fiscal policy is understanding whether a shock is transitory or permanent in nature. This is of particular importance when the economy is hit by a contractionary shock that increases inflation because, in such a situation, the central bank faces a trade-off. The nature (transitory/permanent) of the shock to inflation will dictate whether central banks need to respond aggressively or not to fulfill their price stability mandate. To this end, our model allows for a trend and cycle decomposition, which enables us to study the drivers of prices and real activity at business-cycle and lower frequencies.

Our paper relates to several strands of the literature. First, our paper is related to the literature that quantifies macroeconomic risk (Adrian et al., 2019; Cook and Doh, 2019; Lopez-Salido and Loria, 2024; Adams et al., 2021; Adrian et al., 2022; Carriero et al., 2022; Hilscher et al., 2022). Our contribution to this strand of the literature is twofold: (i) we *jointly* quantify macroeconomic risks arising from inflation and the real economy, and (ii) we propose a novel framework that captures time-varying asymmetry and tail risk. Importantly, this framework entails closed-form solutions to conditional moments that enable us to fit a number of outputs, including conditional moments underlying SPF density forecasts, in a way that is consistent across forecasting horizons. Our framework belongs to a broad class of affine term structure models, which are often featured in the asset pricing literature (e.g., Duffie and Kan, 1996; Dai and Singleton, 2000; Piazzesi, 2010). In our setup, we fit survey density forecasts instead of forward-looking asset prices. The spirit of the modeling approach is similar: while asset prices embed the views of investors regarding future payoffs, density forecasts reflect the views of professional forecasters regarding the future state of the economy. Second, our work speaks to the empirical macroeconomics literature that focuses on distinguishing supply and demand shocks (Shapiro and Watson, 1988; Blanchard and Quah, 1989; Gali, 1992; Shapiro, 2022; Bekaert et al., 2025). Unlike this literature, which mostly uses structural vector

autoregressive models to identify shocks based on macroeconomic observables, our paper aims at estimating (latent) demand and supply factors. Specifically, the labeling of factors (demand versus supply) is based on the signs of their respective factor loadings on output and prices.[1] Our dynamic factor model is, essentially, a vector autoregressive (VAR) model with stochastic volatility and tail risk. What differentiates it from standard VARs is the fact that factors are latent, and estimated via filtering methods within a state-space framework. This flexibility is necessary to jointly fit the distribution of inflation and growth expectations across horizons. Third, our work speaks to the literature that identifies transitory and persistent fluctuations by decomposing macroeconomic variables into trends and gaps (Bullard and Keating, 1995; Cogley et al., 2010; Nason and Smith, 2021; Cascaldi-Garcia et al., 2022). We extend this work by informing this decomposition with forward-looking survey data.

We estimate our model on US data spanning the period 1981-2024. Our model is able to fit realized inflation and growth as well as all three first conditional moments of their forecast distributions. Importantly, the sample includes both calm periods and very large shocks (e.g., 1980s, Great Recession, COVID-19), therefore, our model performs well under any economic condition. Our demand and supply factors capture key events that relate to demand and supply shocks, respectively. Moreover, our volatility factor marks its sharpest increase during the COVID-19 crisis and features peaks around every NBER recession in our sample.

Our findings suggest that the output gap is determined by a mix of demand and supply factors before the Great Recession and in the last quarters of our sample, while it is mainly driven by demand between 2008 and 2020. Moreover, the price gap exhibits a sharp rise in the last quarters of our sample, in line with the idea that high inflation realizations are partly justified by transitory components. Interestingly, the recent increase in inflation is attributed to temporary negative supply factors and more persistent positive demand factors after the COVID crisis. These findings are consistent with the increase in bottlenecks and

[1] For a given set of estimated parameters, this identification is unique, unlike approaches based on sign restrictions within standard vector autoregressive models, which are set-identified.

supply chain disruptions since COVID-19, as well as the large pandemic economic stimulus and relief packages that were implemented in the United States.

Regarding the quantification of macroeconomic risk, we find that, for inflation, uncertainty and asymmetry are prevalent in the 1980s and during the Great Recession, while for GDP growth, these features are in the data in the 1980s and since COVID-19. Finally, we compute the time-varying correlation between inflation and economic activity, revealing the evolving importance professional forecasters assign to aggregate supply and demand. We observe that this correlation varies over time and is negatively related to nominal term premiums, in line with structural modeling of the term structure of interest (e.g., Rudebusch and Swanson, 2012; Bletzinger et al., 2025). On average, the relationship between inflation and economic activity is positive, suggesting that professional forecasters do not have stagflationary beliefs. Computing probabilities of stagflation risk in future horizons, we also show that in 2022, these risks reemerged after three decades of near-zero probabilities.

The remainder of the paper is organized as follows. Section 2 summarizes the rationale behind our approach and the data used in our analysis, Section 3 describes our model, identification strategy and estimation. Section 5 presents empirical results and Section 6 concludes. Finally, the Appendix gathers proofs and technical results and extends the model to include time-varying fourth-order moments.

2. Surveys of Professional Forecasters as a Rich Source of Information

Surveys of Professional Forecasters (SPF) have provided valuable insight for academics and policymakers since the late 1960s. Academic research highlights their strong forecasting accuracy (Ang et al., 2007; Faust and Wright, 2013) and their utility in understanding the term structure of expectations (Aruoba, 2016; Grishchenko et al., 2019) and the expectation formation process (Coibion and Gorodnichenko, 2012; Andrade and Le Bihan, 2013; Andrade et al., 2016). Policymakers often leverage these surveys as a source of subjective expectations of informed market participants to nourish monetary policy decisions.

The importance of these surveys hinges on the fact that they encode relevant information that goes beyond past observations of macroeconomic variables: they are forward-looking, and their probabilistic responses embed information about the perception of (extreme) risks without having to materialize. In particular, probabilistic responses of SPF provide information about the distributions of macroeconomic expectations, and their shape and asymmetry reveal tail risk. Building on recent work that highlights the important role of higher-order dynamics for the business cycle and macroeconomic outlook (Dew-Becker et al., 2021; Iseringhausen et al., 2023; Bauer and Chernov, 2024), our objective is to capture joint risk perceptions in GDP growth and inflation by exploiting changes in the shape of survey distributions, focusing on time-varying asymmetry and tail risk.

2.1. **Extracting SPF-embedded information.** Our approach involves building a factor model that reproduces changes in the aggregate distribution of professional forecasters for future inflation and GDP growth at different horizons. The relevance of this endeavor is based on two assumptions: (a) aggregate forecasts are rational since, in our framework, conditional distributions are consistent with the process posited for inflation and GDP growth; (b) Surveys of Professional Forecasters embed richer information than the one included in past observations of GDP growth and inflation. The present subsection describes the spirit of our filtering approach, which relies on the two previous assumptions.

First, assume that there is a representative professional forecaster. The density forecasts of this forecaster align with the aggregate distribution, which is derived by averaging the distributions of each forecaster.[2]

Second, assume that the state of the economy is captured by a vector X_t. We denote by $\{\underline{X_t}\}$ the set of current and past values of X_t; that is, $\{\underline{X_t}\} = \{X_t, X_{t-1}, \dots\}$. The logarithmic growth rate in the price index and in the GDP between dates $t-1$ and t, respectively, denoted by $\pi_{t-t,t}$ and $\Delta y_{t-t,t}$, are linear combinations of X_t; formally: $\pi_{t-t,t} = \rho^{(\pi)} + \delta^{(\pi)\prime} X_t$, and $\Delta y_{t-t,t} = \rho^{(\Delta y)} + \delta^{(\Delta y)\prime} X_t$. This implies $\{\underline{\pi_{t-t,t}}, \underline{\Delta y_{t-t,t}}\} \subset \{\underline{X_t}\}$.

[2]Sampling from the aggregate distribution can be described by the following steps: (1) randomly select a forecaster and (2) sample from that forecaster's specific distribution.

To simplify the exposition, we assume that the professional forecaster observes $\{\underline{X_t}\}$ on date t, and that she knows the vector of parameters θ that defines the transition dynamics of X_t, that is assumed to be Markovian, that is:

$$X_{t+1}|\underline{X_t} \sim \mathcal{F}(X_t, \theta), \tag{1}$$

where $\mathcal{F}(X_t, \theta)$ is a parametric distribution. In that context, the forecaster can determine $X_{t+h}|\underline{X_t}$ and, equivalently, compute the cumulants characterizing the distribution of any linear combination of X_{t+h} ($\alpha' X_{t+h}$, say), conditional on X_t. Moreover, if X_t follows an affine process, as assumed in the present paper, then these cumulants are affine in X_t.[3] Therefore, under these assumptions, any vector of cumulants of future inflation and GDP growth rates is of the form

$$S_t = A(\theta) + B(\theta)X_t. \tag{2}$$

Although the forecaster does not directly report these cumulants in the SPF, these moments underlie her density forecasts. Consequently, estimates for S_t can be derived using density forecasts. Denoting these estimates by $\tilde{S}_t$, we posit $\tilde{S}_t = S_t + \nu_t$, where ν_t is a measurement error.[4]

Turning to the econometrician, we suppose that she is interested in recovering the conditional distributions that are available to the professional forecasters, which are the $X_{t+h}|\underline{X_t}$ for $h > 0$. Let us first consider the case where she does not observe the SPF; her date-t information set then is $\{\underline{\pi_{t-t,t}}, \underline{\Delta y_{t-1,t}}\}$. Accordingly, she considers the following state-space

[3] See for instance Darolles et al. (2006). Explicit derivations of conditional cumulants to higher orders are rare in the literature. In this regard, the present paper, which explicitly derives conditional moments up to order four (see Appendix E), serves as an exception. Another notable exception is the study by Feunou and Okou (2018), who derive fourth-order cumulants of the risk-neutral conditional distribution of a multivariate process within an asset-pricing context.

[4] The measurement error reflects in particular the fact that it may be necessary to smooth density forecasts before calculating cumulants (see, e.g., Appendix A).

model:

$$\begin{bmatrix} \pi_{t-1,t} \\ \Delta y_{t-1,t} \end{bmatrix} = \begin{bmatrix} \rho^{(\pi)} \\ \rho^{(\Delta y)} \end{bmatrix} + \begin{bmatrix} \delta^{(\pi)\prime} \\ \delta^{(\Delta y)\prime} \end{bmatrix} X_t \tag{3}$$

$$X_t \quad | \quad \mathcal{F}(X_{t-1}, \theta), \tag{4}$$

and uses filtering techniques to estimate θ and X_t based on the dataset $\{\underline{\pi_{t-t,t}}, \underline{\Delta y_{t-1,t}}\}$. Denoting the resulting estimates by $\hat{\theta}$ and $\hat{X}_t$, her estimate for $X_{t+1}|\underline{\pi_{t-t,t}}, \underline{\Delta y_{t-1,t}}$ is $\mathcal{F}(\hat{X}_t, \hat{\theta})$. She can further deduce an estimate for $X_{t+h}|\underline{\pi_{t-t,t}}, \underline{\Delta y_{t-1,t}}$ from $\hat{X}_t$ and $\hat{\theta}$.

However, if the information contained in $\underline{X_t}$ is richer than that in $\{\underline{\pi_{t-t,t}}, \underline{\Delta y_{t-1,t}}\}$, then $\mathcal{F}(\hat{X}_t, \hat{\theta})$ may be a relatively poor estimate for $\mathcal{F}(X_t, \theta)$. In that case, the econometrician may benefit from the information contained in the SPF by increasing the number of measurement equations at her disposal in the state-space model (3)-(4). Formally, the novel measurement equations—that are added to (3)—read:[5]

$$\tilde{S}_t = A(\theta) + B(\theta) X_t + \nu_t.$$

This is the estimation strategy we follow (see Section 4).

2.2. **Asymmetry and tail risk in survey data.** We use inflation (based on the GDP deflator) and GDP growth forecast data from the Survey of Professional Forecasters (SPF), conducted by the Federal Reserve Bank of Philadelphia. In particular, we rely on the probabilistic responses of professional forecasters, which are available for short- and medium-term horizons (5-8 quarters ahead). Our model assumes the existence of a representative forecaster and, therefore, the object of interest in our estimation is the horizon h average density across forecasters, otherwise known as the aggregate probability distribution.

[5]Note that these measurement equations remain linear in the state vector X_t. This property, which arises from the affine nature of the X_t process, simplifies the filtering exercise. It is important to emphasize that the affine property of X_t does not exclude the presence of time-varying higher-order conditional moments, as will be illustrated below (Section 3).

Our approach hinges on the fact that the shape of the aggregate probability distributions of future inflation and GDP growth vary over time and that changes in uncertainty or asymmetry carry important informational content to better understand the drivers of macroeconomic fluctuations. In our setup, uncertainty is measured as the conditional variance of the aggregate probability distribution of the survey forecasts.[6] Similarly, we capture asymmetry as the third cumulant of the aggregate distribution.

The SPF provides us with the cumulative distribution function (CDF) at key points. This information is not sufficient to obtain the variance and third cumulant of the aggregate probability distribution. Therefore, we first apply Gaussian mixtures to the observed aggregated CDF to obtain an estimate of the full distribution (refer to Appendix A). Once equipped with the smoothed CDFs, we proceed in computing the associated conditional higher-order moments, which we fit in Section 3.

Figure 1 shows the aggregate distributions for GDP growth five quarters ahead, at six different dates. The histograms obtained from the raw SPF data are depicted in gray, along with the smoothed aggregate distribution obtained using Gaussian mixtures, in a black dotted line. The first three plots are constructed during a period of relatively low uncertainty. The distributions have a tight support and are symmetric around a positive mean. In contrast, the last three plots are taken from a high uncertainty period. The support of the distribution has more than doubled and the distributions can feature strong asymmetries: positive skewness in 2021Q4 and negative skewness in 2022Q4.

Similarly, Figure 2 shows the aggregate distributions for inflation five quarters ahead. The first four plots are constructed during a period of relatively low uncertainty about inflation, while the last two plots are taken from a high uncertainty period characterized by increased inflation rates. Thus, the distributions are skewed and allocate larger probabilities to high-inflation outcomes.

[6] Based on the law of total variance, the conditional variance of the aggregate distribution is equal to the sum of disagreement (i.e., dispersion across point estimates of forecasters) and of the average of the variances of forecasters' individual probability distributions.

FIGURE 1. Aggregate distributions for GDP growth under low and high uncertainty

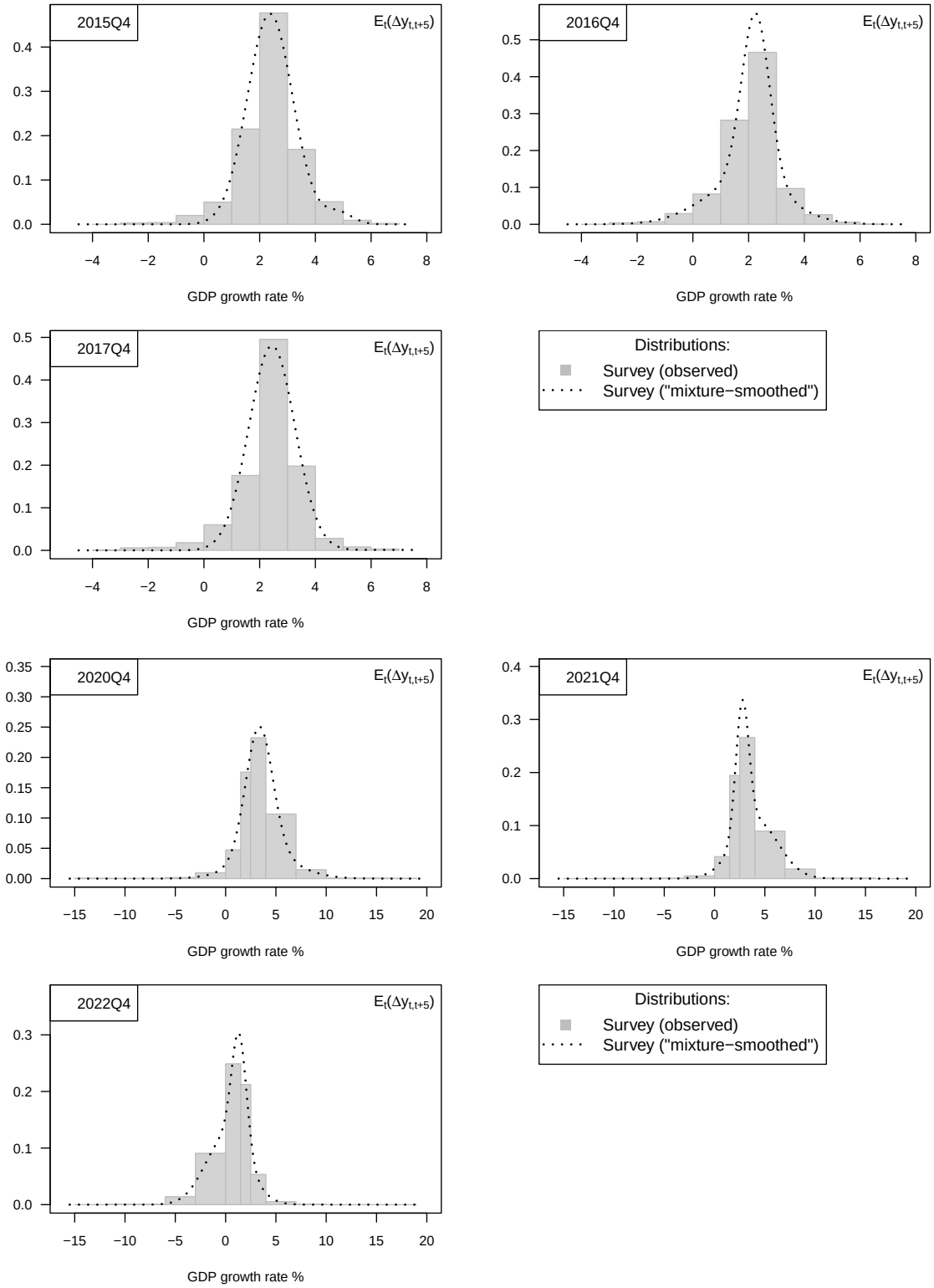

Notes: This figure displays in gray the observed histogram of GDP growth based on the Survey of Professional Forecasters of the Federal Reserve Bank of Philadelphia and in a black dotted line its smooth counterpart obtained using mixtures of Gaussian distributions (refer to Appendix A for details regarding the smoothing approach).

FIGURE 2. Aggregate distributions for inflation under low and high uncertainty

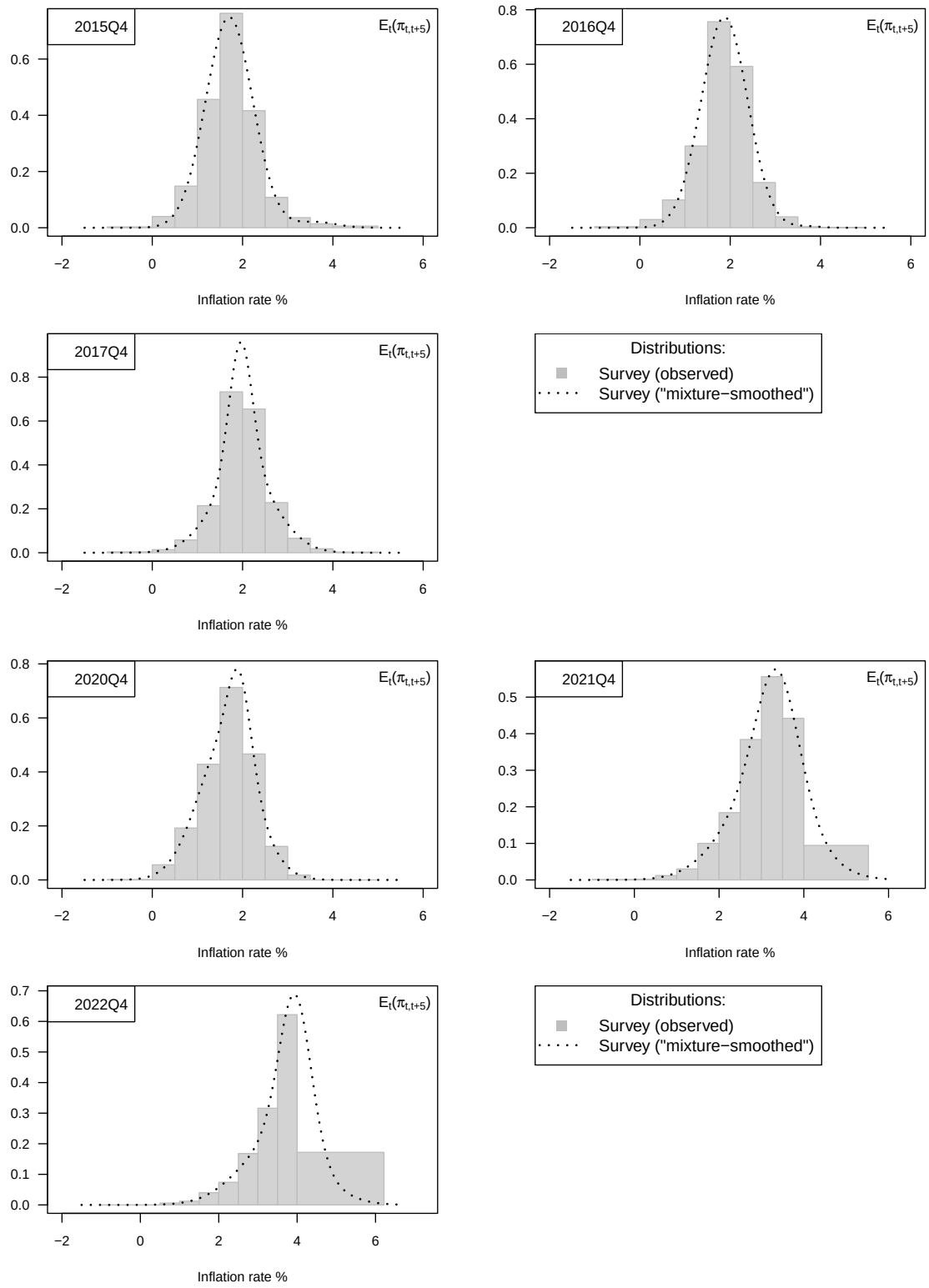

Notes: This figure displays in gray the observed histogram of inflation based on the Survey of Professional Forecasters of the Federal Reserve Bank of Philadelphia and in a black dotted line its smooth counterpart obtained using mixtures of Gaussian distributions (refer to Appendix A for details regarding the smoothing approach).

3. MODEL

In this section, we present our dynamic factor model, featuring time-varying uncertainty and asymmetry, to study the relationship between inflation and the real economy. Our model allows for a trend and cycle decomposition, which enables us to differentiate between transitory and persistent movements in inflation and real activity. Our model jointly estimates the dynamics of realized and expected inflation and GDP growth rates to fit the term structures of first-, second-, and third-order conditional moments. In addition, we outline our identification strategy to disentangle demand and supply factors. Finally, we detail our estimation strategy.

3.1. **Trend Cycle Model.**

The quarterly price index and GDP are denoted, respectively, by P_t and GDP_t, and their logarithms are denoted by p_t and gdp_t. For each of these two variables, we consider a trend-cycle decomposition:

$$p_t = \log(P_t) = T_t^{(\pi)} + C_t^{(\pi)} \tag{5}$$

$$gdp_t = \log(GDP_t) = T_t^{(\Delta y)} + C_t^{(\Delta y)}, \tag{6}$$

where the trends (T_t) are not covariance-stationary, contrary to the cycle components (C_t).[7]

Taking the first differences of p_t and gdp_t, we obtain the quarterly inflation ($\pi_{t-1,t}$) and the real output growth ($\Delta y_{t-1,t}$), respectively. Formally:

$$\pi_{t-1,t} = \Delta T_t^{(\pi)} + C_t^{(\pi)} - C_{t-1}^{(\pi)} \tag{7}$$

$$\Delta y_{t-1,t} = \Delta T_t^{(\Delta y)} + C_t^{(\Delta y)} - C_{t-1}^{(\Delta y)}. \tag{8}$$

[7] Unlike a large body of the literature that uses a trend-cycle decomposition for inflation (Stock and Watson, 2007; Mertens, 2016; Bianchi et al., 2023), we opt for a trend-cycle decomposition of the logarithm of the price index. We do so to preserve a symmetry between the modeling of the price index and GDP, and their respective SPF forecasts. We can draw a parallel with the definition implied by the forecasts of the SPF, where the GDP growth forecast is defined as $\tilde{y}_{t,t+h} = \log\left(\sum_{i=0}^{3} GDP_{t+h-i} / \sum_{i=0}^{3} GDP_{t+h-4-i}\right)$, and where the inflation targeted follows the exact same definition, replacing GDP by the the price index P_t.

We further assume that the cyclical components and the changes in trends are linear combinations of m covariance-stationary factors collected in a vector $\mathcal{Y}_t = [\mathcal{Y}_{1,t}, \ldots, \mathcal{Y}_{m,t}]'$.[8] Factors $\mathcal{Y}_{j,t}$, $j \in \{1, \ldots, m\}$, may be common to inflation and GDP growth; formally:

$$\Delta T_t^{(\pi)} = \rho^{(\pi)} + \delta_T^{(\pi)\prime} \mathcal{Y}_t, \qquad \text{and} \qquad \Delta T_t^{(\Delta y)} = \rho^{(\Delta y)} + \delta_T^{(\Delta y)\prime} \mathcal{Y}_t \tag{9}$$

$$C_t^{(\pi)} = \delta_C^{(\pi)\prime} \mathcal{Y}_t \qquad \text{and} \qquad C_t^{(\Delta y)} = \delta_C^{(\Delta y)\prime} \mathcal{Y}_t. \tag{10}$$

Together, eqs. (5)-(6) and (9)-(10) imply that quarterly inflation and GDP growth rates are given by:

$$\pi_{t-1,t} = \rho^{(\pi)} + \delta_T^{(\pi)\prime} \mathcal{Y}_t + \delta_C^{(\pi)\prime} (\mathcal{Y}_t - \mathcal{Y}_{t-1}) \tag{11}$$

$$\Delta y_{t-1,t} = \rho^{(\Delta y)} + \delta_T^{(\Delta y)\prime} \mathcal{Y}_t + \delta_C^{(\Delta y)\prime} (\mathcal{Y}_t - \mathcal{Y}_{t-1}). \tag{12}$$

If $\mathbb{E}(\mathcal{Y}_t) = 0$, which is the case in the context of the process presented in Subsection 3.2, we have $\mathbb{E}(\pi_{t-1,t}) = \rho^{(\pi)}$ and $\mathbb{E}(\Delta y_{t-1,t}) = \rho^{(\Delta y)}$.

The variables $\pi_{t-1,t}$ and $\Delta y_{t-1,t}$ can be regarded as fundamental growth rates that allow the approximate reconstruction of any other growth rate for inflation and real output. Consider, for instance, the logarithmic annual inflation rate $\pi_{t-4,t} := \log P_t / P_{t-4}$. It is easily seen that it is given by:

$$\pi_{t-4,t} = p_t - p_{t-4} = \pi_{t-4,t-3} + \pi_{t-3,t-2} + \pi_{t-2,t-1} + \pi_{t-1,t}. \tag{13}$$

Turn to GDP growth rates. The associated year-on-year growth rate is expressed as exact linear combinations of the lags of $\Delta y_{t-1,t}$, as follows:

$$\Delta y_{t-4,t} = \Delta y_t - \Delta y_{t-4} = \Delta y_{t-4,t-3} + \Delta y_{t-3,t-2} + \Delta y_{t-2,t-1} + \Delta y_{t-1,t}. \tag{14}$$

3.2. **Dynamics of the state vector.** The dynamics of $\mathcal{Y}_t$ takes the form of a vector autoregressive process that is affected by q non-negative exogenous factors stacked in vector $z_t =$

[8] This implies in particular that the trend components are integrated of order one.

$[z_{1,t}, \dots, z_{q,t}]'$. More precisely, conditional on $\underline{\mathcal{Y}_{t-1}} = \{\mathcal{Y}_{t-1}, \mathcal{Y}_{t-2}, \dots\}$ and on $\underline{z_t} = \{z_t, z_{t-1}, \dots\}$, vector $\mathcal{Y}_t$ evolves as follows:

$$\mathcal{Y}_t = \Phi_{\mathcal{Y}} \mathcal{Y}_{t-1} + \Theta_{\mathcal{Y}}(z_t - \bar{z}) + \text{diag}\left(\sqrt{\Gamma_{\mathcal{Y},0} + \Gamma'_{\mathcal{Y},1} z_t}\right) \varepsilon_{\mathcal{Y},t}, \quad \varepsilon_{\mathcal{Y},t} \sim i.i.d. \mathcal{N}(0, Id_m), \tag{15}$$

where $\text{diag}(x)$ denotes a diagonal matrix whose diagonal entries are the components of vector x, and where $\bar{z}$ is the unconditional mean of z_t, $\Gamma_{\mathcal{Y},0}$ is a $m \times 1$ vector and $\Gamma_{\mathcal{Y},1}$ is a $m \times q$ matrix (m is the dimension of $\mathcal{Y}_t$).

We stress that the conditional and unconditional distributions of the components of $\mathcal{Y}_t$ are symmetric when the matrix Θ_y is null because $\varepsilon_{\mathcal{Y},t}$ follows a symmetric (Gaussian) distribution. In contrast, if the factors z_t exhibit asymmetric conditional distributions and Θ_y is non-null, then asymmetry will be present in the distributions of the components of $\mathcal{Y}_t$.

We close the model by defining the dynamics of z_t. Conditionally on $\underline{z_{t-1}}$, the different components of z_t are assumed to be independent and drawn from non-centered Gamma distributions:

$$z_{i,t} | \underline{z_{t-1}} \sim \gamma_{\nu_i}(\varphi'_i z_{t-1}, \mu_i), \quad i = 1, \dots, q. \tag{16}$$

Hence, z_t follows a multivariate $ARG_\nu(\varphi, \mu)$ process (e.g., Gouriéroux and Jasiak, 2006; Le et al., 2010; Monfort et al., 2017) where $\nu = [\nu_1, \dots, \nu_q]'$, $\mu = [\mu_1, \dots, \mu_q]'$, and $\varphi = [\varphi_1, \dots, \varphi_q]$. In that situation, the dynamics of z_t admits the following (semi-strong) vector autoregressive representation:

$$z_t = \mu_z + \Phi_z z_{t-1} + \text{diag}\left(\sqrt{\Gamma_{z,0} + \Gamma'_{z,1} z_{t-1}}\right) \varepsilon_{z,t}, \tag{17}$$

where $\varepsilon_{z,t}$ is a martingale difference sequence whose covariance, conditional on $\underline{z_t}$, is the identity matrix, and where μ_z, Φ_z, $\Gamma_{z,0}$ and $\Gamma_{z,1}$ are matrices depending on ν, φ, and μ (see Proposition 3).

In our model, the state vector is $X_t = [Y'_t, z'_t]'$, where Y_t is an n-dimensional vector stacked with $\mathcal{Y}_t$ and lagged values of $\pi_{t-1,t}$ and Δy_t. Lagged values of $\pi_{t-1,t}$ and $\Delta y_{t-1,t}$ are added to ensure that the year-on-year growth rate of GDP and the price index are affine functions of

X_t. This facilitates the writing of the measurement equations of the state-space model used at the estimation stage (see Appendix C for more details).

We show in Appendix D.2 that, in this context, X_t admits the following (semi-strong) vector autoregressive dynamics:

$$X_t = \begin{bmatrix} Y_t \\ z_t \end{bmatrix} = \mu_X + \Phi_X X_{t-1} + \Sigma_X(z_{t-1})\varepsilon_{X,t}, \tag{18}$$

where $\varepsilon_{X,t}$ is a $(n+q)$-dimensional unit-variance martingale difference sequence.

The heteroskedastic nature of the process for X_t results from the dependence of Σ_X on z_{t-1}. Within this framework, the conditional higher-order moments of X_t are also influenced by z_t. Notice that while $\varepsilon_{X,t}$ is a martingale difference sequence, its distribution, conditional on $\underline{X_{t-1}} = \{Y_{t-1}, z_{t-1}, Y_{t-2}, z_{t-2}, \dots\}$, depends on z_{t-1}. In particular, as shown in Appendix E.2, the conditional cumulants of X_{t+h}, $h \geq 0$, are affine in z_t.

3.3. **Specific model.** The previous subsection describes a general framework for the dynamics followed by the state vector X_t. In the present section, we present the specific dynamics employed in our empirical exercise.

Given the extensive set of conditional moments that we aim to fit, it is essential to adopt a sufficiently rich specification. Our baseline specification includes four $\mathcal{Y}$ factors (i.e., $m = 4$) and five z factors (i.e., $q = 5$). Although the first two $\mathcal{Y}$ factors are assigned a supply/demand interpretation, we allow the data to dictate the nature of the last two $\mathcal{Y}$ factors. These interpretations relate to the signs of the loadings that connect these variables to inflation and output growth, specifically the signs of the loadings $\delta^{(\pi)}$ and $\delta^{(\Delta y)}$ (see equations 11 and 12). Consistent with common views, a supply (demand) factor influences inflation and output in opposite (the same) directions.

As mentioned above, we impose interpretations on $\mathcal{Y}_1$ and $\mathcal{Y}_2$; specifically, $\mathcal{Y}_1$ is defined as a supply factor, while $\mathcal{Y}_2$ is characterized as a demand factor. Assuming that these two factors exclusively affect the cyclical components of inflation and output growth, the interpretation

of demand/supply of these factors depends on the signs of the first two components of $\delta_C^{(\pi)}$ and $\delta_C^{(\Delta y)}$ (see equation 10). Specifically, the first (respectively second) components of both $\delta_C^{(\pi)}$ and $\delta_C^{(\Delta y)}$ have opposite (resp. identical) signs.

The first two $\mathcal{Y}$ factors are those that drive asymmetry in the conditional distributions of inflation and output growth. This is achieved by using four non-zero values in $\Theta_{\mathcal{Y}}$ (see eq. 15): two in its first row and two in its second row. As mentioned above, $\mathcal{Y}$ needs to feature non-zero entries to accommodate time-varying asymmetry in the $\mathcal{Y}$ factors: As an example, if the (i,j) entry of $\Theta_{\mathcal{Y}}$ is positive, then $z_{j,t}$ positively contributes to the conditional mean of $\mathcal{Y}_{i,t}$, which generates positive skewness in $\mathcal{Y}_{i,t}$. (Note that since z factors are ARG, they are positively skewed.) Hence, to allow for both periods of positive and negative skewness of $\mathcal{Y}_{i,t}$, at least one z factor must positively affect the conditional mean of $\mathcal{Y}_{i,t}$—i.e., one entry of the i^{th} row of $\Theta_{\mathcal{Y}}$ must be positive—and at least one z factor must affect it negatively. With this in mind, we denote the first four entries of z_t with $z^s_{p,t}$, $z^s_{n,t}$, $z^d_{p,t}$, and $z^d_{n,t}$: the exponents s and d respectively refer to supply and demand; the indices p and n respectively refer to positive and negative. For instance, $z^s_{n,t}$ negatively affects the supply factor; that is, the $(1,2)$ entry of $\Theta_{\mathcal{Y}}$ is negative. When this factor ($z^s_{n,t}$) is large compared to $z^s_{p,t}$, then the conditional distribution of the supply factor ($\mathcal{Y}_1$) is negatively skewed. For more flexibility, we further allow for autoregression in $\mathcal{Y}_1$ and $\mathcal{Y}_2$, and we introduce specific Gaussian shocks $\varepsilon_{1,\mathcal{Y}}$ and $\varepsilon_{2,\mathcal{Y}}$ in their dynamics. All in all, this leads to the following dynamics for $\mathcal{Y}_1$ and $\mathcal{Y}_2$, corresponding to the first two equations in (27):[9]

$$\mathcal{Y}_{1,t} = \phi_{1,1}\mathcal{Y}_{1,t-1} + \theta^s(z^s_{p,t} - z^s_{n,t}) + \sqrt{\Gamma_{1,\mathcal{Y},0}}\varepsilon_{1,\mathcal{Y},t}, \tag{19}$$

$$\mathcal{Y}_{2,t} = \phi_{2,2}\mathcal{Y}_{2,t-1} + \theta^d(z^d_{p,t} - z^d_{n,t}) + \sqrt{\Gamma_{2,\mathcal{Y},0}}\varepsilon_{2,\mathcal{Y},t}. \tag{20}$$

For the sake of parsimony, z_t does not intervene in the conditional means of the third and fourth $\mathcal{Y}$. However, a fifth z factor, denoted as $z_{v,t}$, drives the conditional volatility of these

[9] Constructing a real-valued non-Gaussian persistent factor using the difference between two non-negative autoregressive gamma processes ($z_{p,t}$ and $z_{n,t}$) aligns with the approach of Bekaert and Engstrom (2010) and Bekaert et al. (2020).

two factors. Formally, the last two equations in (27) are:

$$\mathcal{Y}_{3,t} = \phi_{3,3}\mathcal{Y}_{3,t-1} + \sqrt{\Gamma_{3,\mathcal{Y},0} + \Gamma_{[3,5],\mathcal{Y},1} z_{v,t}}\,\varepsilon_{3,\mathcal{Y},t}, \tag{21}$$

$$\mathcal{Y}_{4,t} = \phi_{4,4}\mathcal{Y}_{4,t-1} + \sqrt{\Gamma_{4,\mathcal{Y},0} + \Gamma_{[4,5],\mathcal{Y},1} z_{v,t}}\,\varepsilon_{4,\mathcal{Y},t}, \tag{22}$$

where $\Gamma_{[i,j],\mathcal{Y},1}$ denotes the (i,j) entry of matrix $\Gamma_{\mathcal{Y},1}$ (see eq. 15).

We finally assume that $\mathcal{Y}_{1,t}$ and $\mathcal{Y}_{2,t}$ affect only the cyclical parts of GDP and the price index; in other words, the growth rates of the trend components $T_t^{(\pi)}$ and $T_t^{(\delta y)}$ depend only on $\mathcal{Y}_{3,t}$ and $\mathcal{Y}_{4,t}$.

Table 1 summarizes some characteristics of $\mathcal{Y}$'s dynamics, together with the sign restrictions that are imposed on the inflation/GDP loadings at the estimation stage. In addition, Appendix D.3 specifies the matrices $\Phi_{\mathcal{Y}}$, $\Theta_{\mathcal{Y}}$, $\Gamma_{\mathcal{Y},0}$, and $\Gamma_{\mathcal{Y},1}$ (eq. 15) and the vectors $\delta_T^{(\pi)}$, $\delta_C^{(\pi)}$, $\delta_T^{(\Delta y)}$, and $\delta_C^{(\Delta y)}$ (eqs. 9 and 10) associated with these specifications.

TABLE 1. Summary of model factors

	Vol.	Skew.	$z^s_{p,t}$	$z^s_{n,t}$	$z^d_{p,t}$	$z^d_{n,t}$	$z_{v,t}$	$C^{(\pi)}$	$C^{(\Delta y)}$	$T^{(\pi)}$	$T^{(\Delta y)}$
$\mathcal{Y}_{1,t}$	✓	✓	✓	✓				−	+	0	0
$\mathcal{Y}_{2,t}$	✓	✓			✓	✓		+	+	0	0
$\mathcal{Y}_{3,t}$	✓						✓	?	+	?	+
$\mathcal{Y}_{4,t}$	✓						✓	?	+	?	+

Notes: This table summarizes characteristics of the $\mathcal{Y}$ factors. The first two columns show whether the factors feature time-varying volatility and skewness. The table also shows which of the z factors affect the conditional distributions of the $\mathcal{Y}$ factors. In the last two columns, we report the sign that are imposed at the estimation stage; this shows in particular that $\mathcal{Y}_{1,t}$ (resp. $\mathcal{Y}_{2,t}$) is imposed to be a supply (resp. demand) factor. A "?" indicates that the sign of the considered parameter is left unconstrained in the estimation.

4. ESTIMATION STRATEGY

A key property for the tractability of the estimation is the fact that X_t is an affine process. Specifically, in our setup, conditional first-, second- and third-order moments of any linear combination of future values of X_t are available in quasi-closed form, up to recursive formulas. Importantly, these moments also happen to be affine. As detailed below, this allows us to easily cast the model into a linear state-space form, which is the required form of the model

for the Kalman filter algorithm to be applied. These filtering techniques simultaneously estimate the model parameters and the latent factors, $\mathcal{Y}_t$ and z_t.

We stress here that the availability of simple (recursive) linear formulas to compute the conditional moments of $\pi_{t-1,t}$ and $\Delta y_{t-1,t}$ is a fundamental difference between our approach and alternative stochastic volatility models that have been used to model inflation dynamics (e.g., Stock and Watson, 2007; Mertens, 2016). Indeed, while the latter models entail closed-form expressions for the first two conditional moments of inflation, higher-order moments are nonlinear in the unobserved factors; incorporating third-order moments in the estimation—as done here—would therefore substantially complicate the computational burden in these alternative frameworks.[10]

Our state-space model features two types of equations. First, the transition equations describe the dynamics of the state vector X_t; the VAR representation of these equations is given by (18). Second, the measurement equations capture the relationship between observed variables and the state vector. Let us denote by S_t the vector of observations used in our state-space model. We have $S_t = [\pi_t, \Delta y_t, SPF_t', VSPF_t', SSPF_t']'$, where SPF_t, $VSPF_t$ and $SSPF_t$ denote the vectors of means, variances (uncertainty) and third cumulants (asymmetry) of the aggregate probability density functions stemming from the SPF. As mentioned above, in our affine framework, these objects are affine functions of the state vector X_t. Consequently, the measurement equations of the model are of the form:

$$S_t = A + B'X_t + diag(\sigma^S)\eta_t^S,$$

where $\mathbb{V}(\eta_t^S) = Id$.

Conditional on a model parameterization and on observed variables, the Kalman filter computes the distribution of the latent variables. Moreover, a byproduct of the algorithm is the likelihood function. The model parameters can therefore be estimated by numerically

[10] Note that our framework can be extended to include time-varying fourth-order moments, as shown in Appendices B, E and F.

maximizing this function. Once this is done, a last pass of the algorithm provides estimates of the latent variables.

A remark about the performance of our Kalman filter is that, albeit the affine form of our transition and measurement equations facilitates the implementation of the filter, the filter we eventually run is not optimal. (It would be optimal in the absence of z factors, as the state-space model would then be linear and Gaussian.) Therefore, we estimate our model using a quasi-maximum-likelihood (QML) approach based on a modified version of the Kalman filter.[11]

We estimate our model on US data (realized inflation and GDP growth, and their respective aggregate distribution functions at different horizons from the SPF) for the period 1981Q3-2024Q1. Table 2 reports the parameterization of the model. As reported in Panel A, when a latent factor loads with opposite (respectively, same) signs in inflation and GDP growth, we label it a supply (resp. demand) factor.

[11] Our filter algorithm makes use of the standard forecasting and updating steps of the Kalman filter except that, at iteration t, we replace the unobserved covariance matrix of the X_t innovations ($\Sigma_X(z_{t-1})\Sigma_X(z_{t-1})'$) by $\Sigma_X(z_{t-1|t-1})\Sigma_X(z_{t-1|t-1})'$, where $z_{t-1|t-1}$ denotes our filtered estimate of z_{t-1} (using the information up to date $t-1$). Another adjustment we have to make to the filter pertains to the fact that factors z_t are non-negative. For this purpose, after each updating step of the algorithm, negative entries in the estimate z_t are replaced by 0. Monte Carlo analyses performed by Duan and Simonato (1999) and Monfort et al. (2017) suggest that, in the case of linear but heteroscedastic models, this kind of approximation is of limited importance in practice (see also (Duffee and Stanton, 2012)).

TABLE 2. Model parameterization

Panel A - Trend and cycle loadings							
	$\delta_C^{(\pi)}$	$\delta_C^{(\Delta y)}$		$\delta_T^{(\pi)}$	$\delta_T^{(\Delta y)}$		
δ_{C_1}	−1.000	0.087	δ_{T_1}	0.000	0.000		
δ_{C_2}	0.045	1.000	δ_{T_2}	0.000	0.000		
δ_{C_3}	1.221	1.000	δ_{T_3}	0.245	0.263		
δ_{C_4}	−1.019	1.000	δ_{T_4}	−0.052	0.256		
Panel B - Dynamics of $\mathcal{Y}_t$							
	$\Phi_{\mathcal{Y}}$		Θ		$\Gamma_{\mathcal{Y},0}$		$\Gamma_{\mathcal{Y},1}$
$\phi_{1,1}$	0.471	Θ^s	0.136	$\Gamma_{1,\mathcal{Y},0}$	0.086	$\Gamma_{[3,5],\mathcal{Y},1}$	0.066
$\phi_{2,2}$	0.793	Θ^d	0.147	$\Gamma_{2,\mathcal{Y},0}$	0.239	$\Gamma_{[4,5],\mathcal{Y},1}$	0.113
$\phi_{3,3}$	0.990			$\Gamma_{3,\mathcal{Y},0}$	0.004		
$\phi_{4,4}$	0.990			$\Gamma_{4,\mathcal{Y},0}$	0.006		
Panel C - Dynamics of z_t							
	ν		ϕ		μ		
ν_1	0.007	ϕ_{11}	0.990	μ_1	1.000		
ν_2	0.011	ϕ_{22}	0.990	μ_2	1.000		
ν_3	0.052	ϕ_{33}	0.886	μ_3	1.000		
ν_4	0.017	ϕ_{44}	0.973	μ_4	1.000		
ν_5	0.056	ϕ_{55}	0.497	μ_5	1.000		

Notes: This table shows the parameter estimates. We also have: $\rho^{\pi} = 0.721$ and $\rho^{\Delta y} = 0.652$. The first panel shows the trend and cycle loadings. The second shows the dynamics of $\mathcal{Y}_t$. The last panel shows the dynamics of z_t

5. RESULTS

In this Section we present the results of our estimation. We first describe our latent factors, which, through the identification strategy outlined in Subsection 3.3, bear the interpretation of demand, supply or higher-order moments factors. We then provide some stylized facts on survey-based expectations of future inflation and GDP growth in the United States, highlighting that their distributions exhibit time-varying uncertainty and asymmetry (tail risk). Moreover, we provide evidence that our model captures these stylized facts, which are particularly marked in the 1980s, the Great Recession, and since the COVID-19 crisis. We then exploit the joint dynamics of inflation and economic activity in order to decompose their transitory and permanent movements into demand and supply drivers. These decompositions can have important implications for economic policy decisions, as they can inform about the

appropriate policy mix. Finally, we compute the correlation between inflation and economic activity through the lens of professional forecasters. This correlation is found to be time-varying and mostly positive since the Great Recession and most notably at the height of the COVID-19 crisis. This positive relationship suggests that professional forecasters expect the demand drivers to prevail. Importantly, in line with structural models of the term structure of interest rates, this correlation is negatively related to nominal term premiums.

5.1. **Latent factors.** Figure 3 shows the latent factors $\mathcal{Y}_t$, which, thanks to our identification strategy, can be interpreted as supply factors (first and fourth factors, $\mathcal{Y}_{1,t}$ and $\mathcal{Y}_{4,t}$ – where $\mathcal{Y}_{1,t}$ is cyclical and $\mathcal{Y}_{4,t}$ is more persistent) or demand factors (second and third factors, $\mathcal{Y}_{2,t}$ and $\mathcal{Y}_{3,t}$ – where $\mathcal{Y}_{2,t}$ is cyclical and $\mathcal{Y}_{3,t}$ is more persistent). In particular, the largest changes in the cyclical supply factor $\mathcal{Y}_{1,t}$ coincide with large swings in oil prices and with peaks in the uncertainty of the oil price (Abiad and Qureshi, 2023). Moreover, the most pronounced drops in the cyclical and persistent demand factors, $Y_{2,t}$ and $Y_{3,t}$, capture all US recession periods in our sample: 1981-1982, the early 1990s, the early 2000s, the Great Recession, and the COVID-19 crisis. Note that, in the same spirit as Furlanetto et al. (2025), we identify a permanent demand driver. In their analysis, demand shocks can have permanent effects on output through hysterisis, and these are found to be quantitatively important in the US, especially when the Great Recession is included in the sample.

Similarly, Figure 4 plots the latent factors z_t, which broadly drive the time variation in the higher-order moments of $\mathcal{Y}_t$. Specifically, the first two factors ($z^s_{p,t}$ and $z^s_{n,t}$) allow time-varying uncertainty and asymmetry in the cyclical supply factor $\mathcal{Y}_{1,t}$, the third and fourth factors ($z^d_{p,t}$ and $z^d_{n,t}$) allow time-varying uncertainty and asymmetry in the cyclical demand factor ($\mathcal{Y}_{2,t}$), and the fifth factor ($z_{v,t}$) allows time-varying uncertainty (volatility) in persistent factors $\mathcal{Y}_{3,t}$ and $\mathcal{Y}_{4,t}$. We notice that the factors that drive higher-order moments in cyclical supply are prominent in the 1980s and up to the Great Recession. For demand, these factors are prominent in the 1980s and throughout the COVID-19 crisis. Moreover, the volatility

factor marks its sharpest increase during COVID-19 and features peaks around every NBER recession in our sample.

FIGURE 3. Latent Factors Y_t

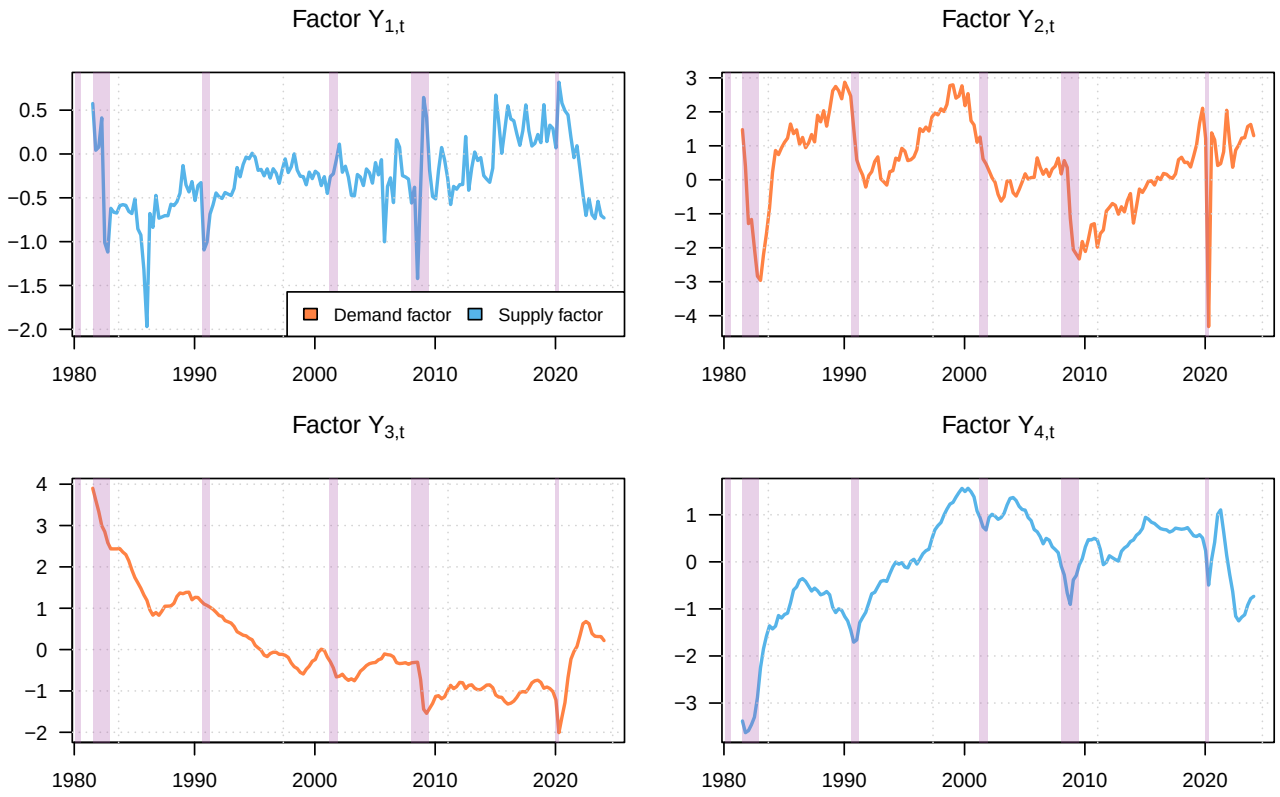

Notes: This figure displays the estimated $\mathcal{Y}_{i,t}$ factors. The dynamics of these factors are described by (19) to (22). These latent factors are estimated by employing Kalman filtering techniques (Section 4). The classification of these factors as demand or supply is based on the sign of the loadings δ^{π} and $\delta^{\Delta y}$ (see Table 1).

5.2. **Model-fit and survey-data stylized facts.** The spirit of our approach is to use a factor model that reproduces changes in the aggregate distribution of professional forecasters for future inflation and GDP growth at different horizons, by fitting conditional moments. Although forecasters do not directly report cumulants in the SPF, these moments underlie their density forecasts. Figure 5 plots, in red, the model-implied densities for the five-quarter ahead real GDP growth histogram (gray bars) and its smoothed counterpart obtained using a Gaussian-mixture (black dotted line) on three different dates: 1985Q4, 2007Q4 and 2017Q4. We observe that our approach of fitting moments is able to fit density forecasts well across time, capturing satisfactorily changes in the conditional distributions of real GDP growth.

FIGURE 4. Latent Factors z_t

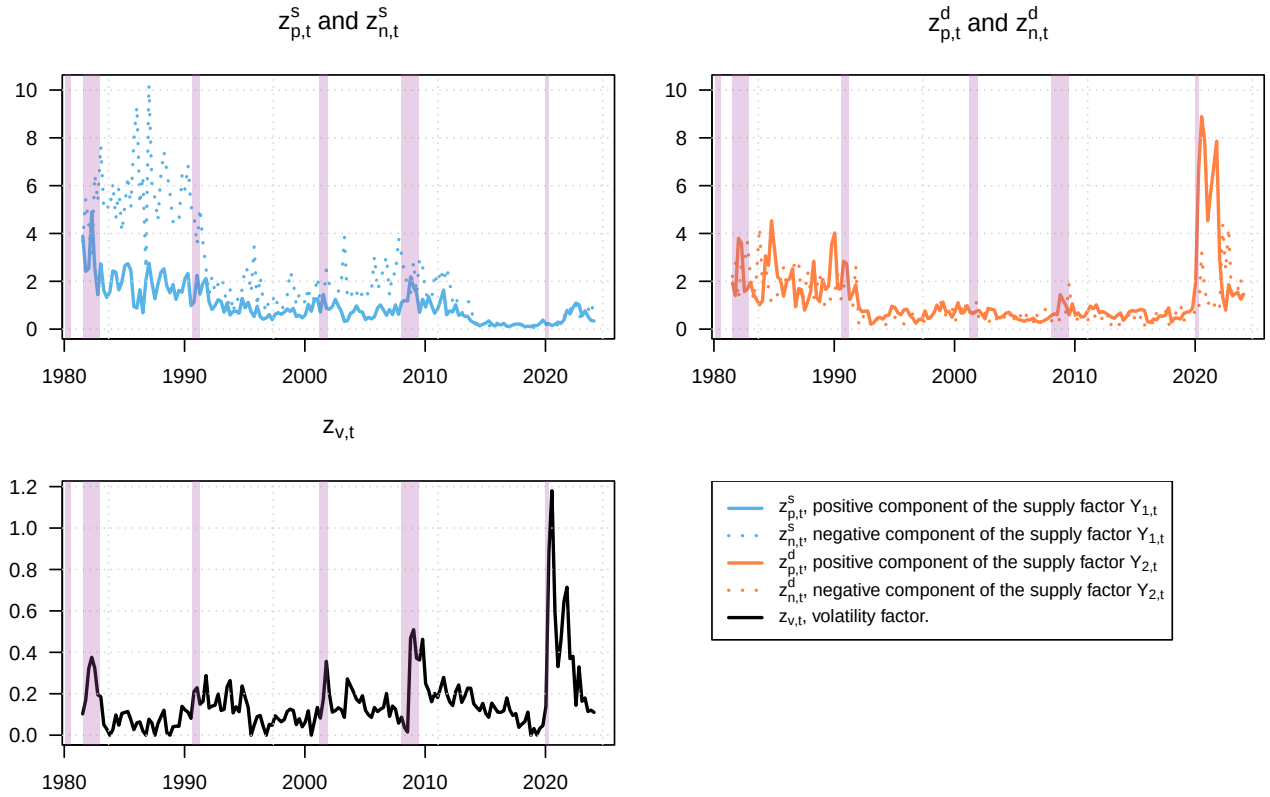

Notes: This figure displays the estimated $z_{i,t}$ factors. These factors follow Auto-Regressive Gamma processes (ARG) (see eq. 16). These latent factors are estimated by employing Kalman filtering techniques (Section 4) and are described in Table 1.

Similarly, Figure 6 shows the model-implied densities for the five-quarter ahead inflation histogram on the same three dates. We observe that the model is able to jointly fit the GDP growth and inflation density forecasts fairly well even when these feature greater uncertainty (wider support) and pronounced asymmetry, as observed in the first panel of Figure 6.

We now proceed to studying the fit of the first three conditional moments for real GDP growth and inflation, respectively. Figure 7 displays the expectation, variance and skewness of the eight-quarter ahead GDP growth distribution over time. The black dots represent the data, while the solid gray line shows the fit implied by the model. Similarly, Figure 8 provides the same figures for inflation. Some observations are worth mentioning. First, the model successfully matches all three conditional moments of the forecast distributions for both growth

FIGURE 5. Observed and model-implied conditional distributions of GDP growth

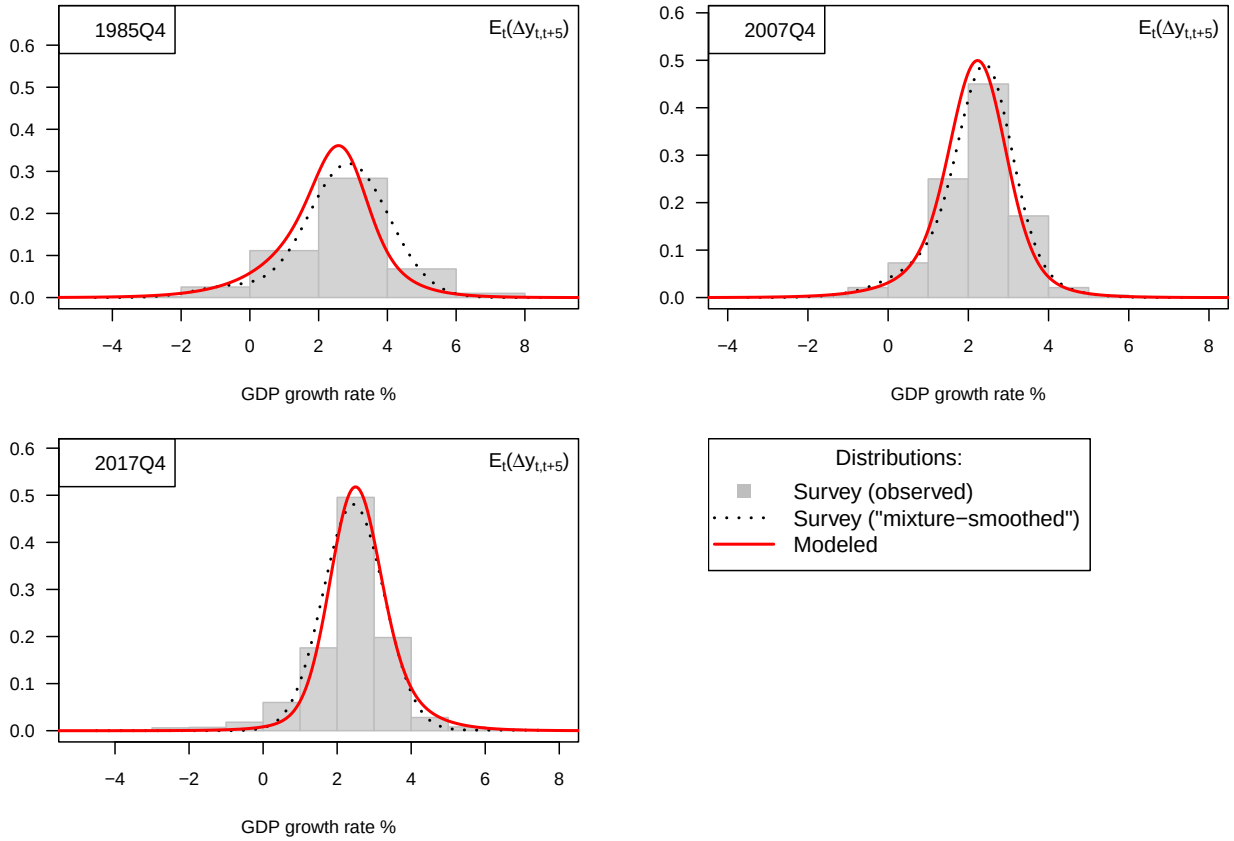

Notes: This figure compares observed and model-implied conditional distributions of GDP growth. The gray histograms is based on the Philadelphia Fed SPF bin forecasts. The black dotted line shows a preliminary interpolation of this histogram relying on mixtures of Gaussian distributions (see Appendix A). The red solid line is the model-implied conditional distribution. The latter is derived by applying inverse Fourier transform to the conditional Laplace transform of the considered GDP growth rate, exploiting the affine property of the model (see, e.g., Proposition 2 of Duffie et al., 2000).

and inflation.[12] Importantly, the sample includes both calm periods and very large shocks (e.g., early 1980s, COVID-19); therefore, our model performs well under any economic condition. Second, conditional expectations of inflation and growth vary throughout the sample period. Third, for inflation, uncertainty and asymmetry are prevalent in the 1980s and during the Great Recession and the skewness is mostly positive, with its inter-quartile range being always positive, across all horizons. For GDP growth, these features are in the data in the

[12]Note that the eight-quarter ahead forecasts are observed only once per year, while our model is estimated at a quarterly frequency. Hence, on quarters when the eight-quarter ahead forecasts are not observed, our model uses observations of other horizon forecasts and exploits its embedded term structure to extrapolate a model-implied eight-quarter forecast.

FIGURE 6. Observed and model-implied conditional distributions of inflation

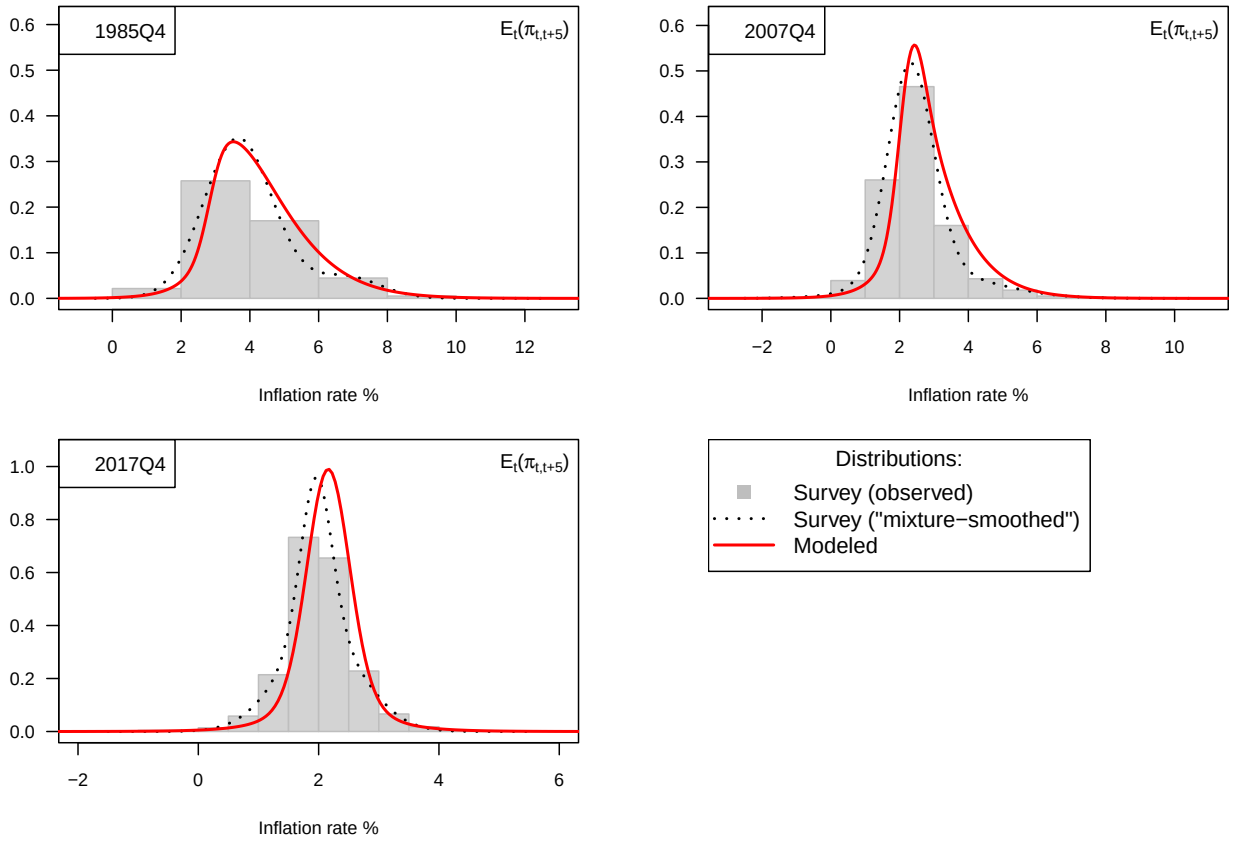

Notes: This figure compares observed and model-implied conditional distributions of inflation. The gray histograms is based on the Philadelphia Fed SPF bin forecasts. The black dotted line shows a preliminary interpolation of this histogram relying on mixtures of Gaussian distributions (see Appendix A). The red solid line is the model-implied conditional distribution. The latter is derived by applying inverse Fourier transform to the conditional Laplace transform of the considered inflation, exploiting the affine property of the model (see, e.g., Proposition 2 of Duffie et al., 2000).

1980s and since COVID-19, and the skewness tends to be negative on average, with the interquartile range capturing both positive and negative skewness at a 5-quarter-ahead horizon and being negative for all other horizons.

5.3. **Exploiting the joint dynamics of inflation and economic activity.** Figure 9 provides the trend and cycle decompositions for the logarithm of the price level (top charts) and the logarithm of GDP (bottom charts). First, we notice that the trend in prices and economic activity slows down around the Great Recession, in line with secular stagnation arguments. Moreover, the cycle component of growth captures the main business cycle fluctuations of

FIGURE 7. Fit of conditional moments of GDP growth survey forecasts

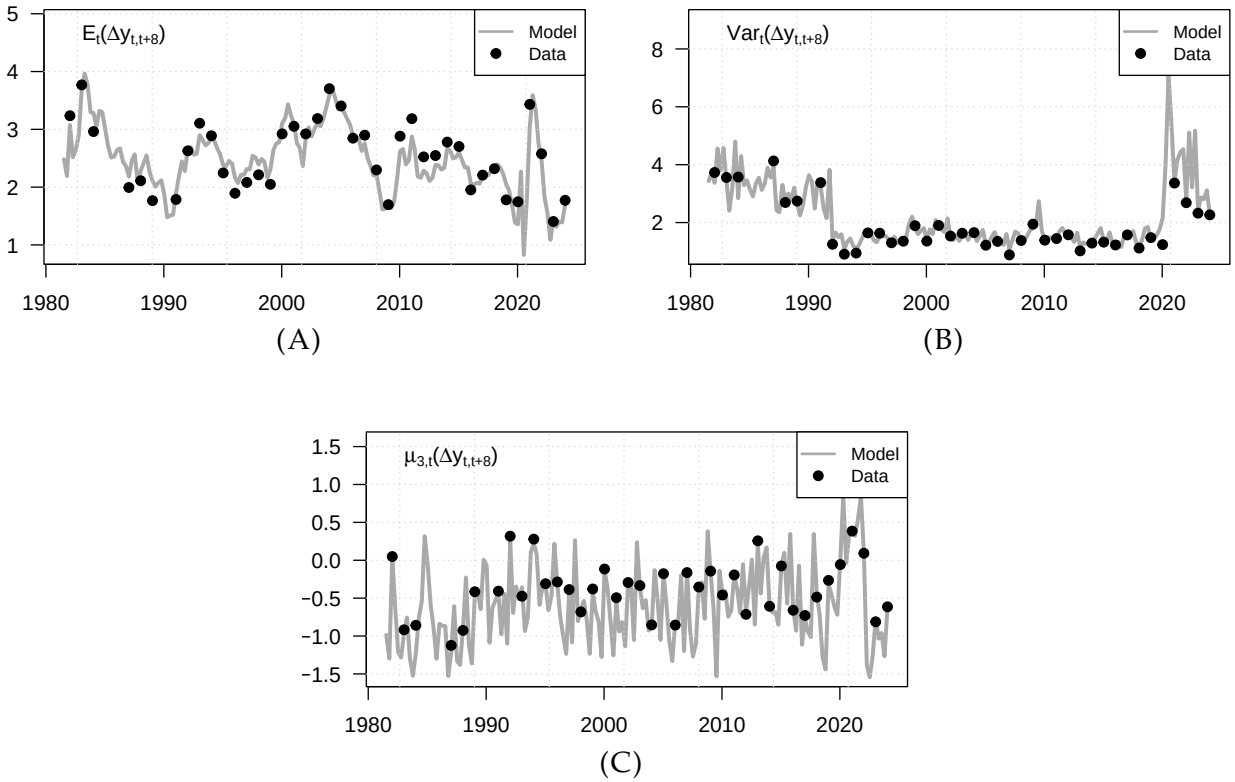

Notes: This figure illustrates the fitting properties of the model, focusing on GDP growth. Black dots correspond to SPF-based observations while gray lines correspond to the model-implied quantities. Panels (A) to (C) respectively correspond to the conditional mean, variance and skewness. (Note that our model fits the conditional 3rd-order cumulant, which we transform, here, for representation purposes to the conditional skewness by dividing it by the conditional variance to the power of 3/2.) The SPF-based cumulants are based on the Gaussian-mixture interpolated distributions (see Appendix A). The horizon is 8 quarters; because the SPF consider calendar years, there is only one observation for this horizon per year.

our sample (1981-1982, the early 1990s, the early 2000s, the Great Recession and the COVID-19 crisis), with the COVID-19 crisis featuring a sharp recovery. Finally, the price gap exhibits a sharp rise since 2021, in line with the idea that high-inflation realizations are partly justified by transitory components. Having said that, the trend in prices has also somewhat steepened in the in the period 2021-2022, implying that there are also some persistent drivers behind the increase in inflation.

Figure 10 decomposes the output gap (top panel) and annual GDP growth (bottom panel) into supply and demand factors. Our analysis suggests that the output gap is determined by a mix of demand and supply factors up to the Great Recession and in the last quarters

FIGURE 8. Fit of conditional moments of inflation survey forecasts

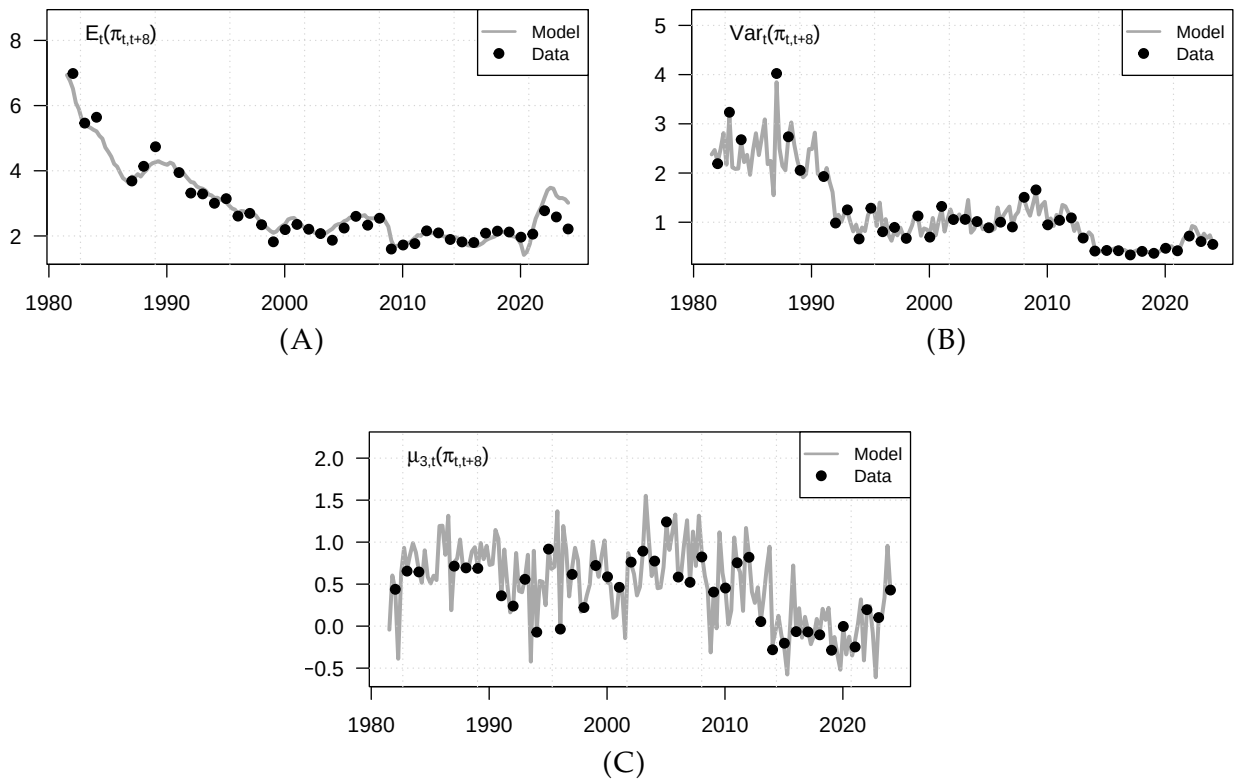

Notes: This figure illustrates the fitting properties of the model, focusing on inflation. Black dots correspond to SPF-based observations while gray lines correspond to the model-implied quantities. Panels (A) to (C) respectively correspond to the conditional mean, variance and skewness. (Note that our model fits the conditional 3rd-order cumulant, which we transform, here, for representation purposes to the conditional skewness by dividing it by the conditional variance to the power of 3/2.) The SPF-based cumulants are based on the Gaussian-mixture interpolated distributions (see Appendix A). The horizon is 8 quarters; because the SPF consider calendar years, there is only one observation for this horizon per year.

of our sample, while it has predominantly been driven by demand factors between 2008-2020. The fact that supply factors have an impact on the output gap echoes arguments in the literature that describe the importance of Keynesian supply shocks, in which sectoral shocks can account for significant fluctuations in the business cycle (Cesa-Bianchi and Ferrero, 2021). Moreover, supply factors are positive from the mid-1990s up to the Great Recession, consistent with globalization and rapid technological change with the advent of the Internet. Focusing on the decomposition of annual GDP growth, we observe that demand factors dominate primarily as a key driver and display striking negative demand movements during recessions. The two first recessions in our sample (1981 and early 1990s) have stronger

FIGURE 9. Trend and cycle decomposition of the price level and GDP

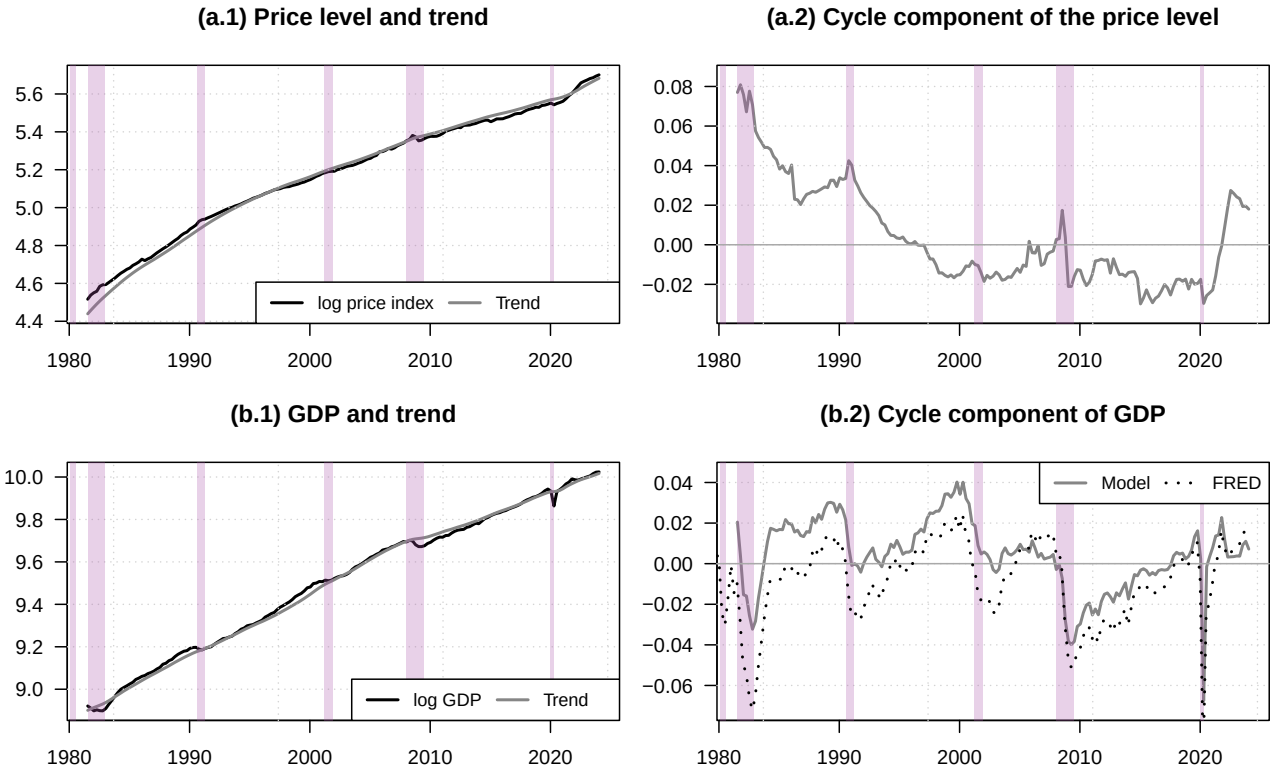

Notes: This figure present the trend-cycle decompositions of the price level and GDP, as described by (5) and (6). Equations (9), and (10) show that the two cyclical components and the changes in the two trend components are affine combinations of $\mathcal{Y}_t$, whose filtered estimates are displayed in Figure 3.

negative supply contributions, which can be explained by the fact that both recessions were driven or exacerbated by oil price movements (Iranian revolution and Kuwait invasion). Our findings are in line with those found by Giannone and Primiceri (2024) for US GDP in the post-pandemic period. Moreover, note that GDP growth is strongly driven by negative persistent demand in all recessions, in line with hysterisis effects, whereby recessions driven by demand shocks may have permanent effects on output (Furlanetto et al., 2025). Similarly, Figure 11 decomposes the price gap and year-over-year inflation into similar demand and supply drivers. Interestingly, the recent increase in prices is attributed to temporary negative supply factors and more persistent positive demand factors after the COVID crisis. These findings are consistent with the increase in bottlenecks and supply chain disruptions since COVID-19, as well as the large pandemic economic stimulus and relief packages that were

implemented in the United States. Although our findings for the post-pandemic period indicate a mix of supply and demand drivers, as in Shapiro (2022) and Giannone and Primiceri (2024), the split in the contributions we obtain is closer to that of Shapiro (2022), where supply factors dominate. In contrast to these papers, our setup further allows us to describe whether these contributions are transitory or persistent. Looking back at the entire sample, we observe that the price gap is largely driven by supply drivers, with one notable exception: the period following the Great Recession up to 2020. Conversely, inflation dynamics are mostly demand-driven, indicating that demand drivers are more persistent in nature. In addition, we study how our different components can be explained by standard variables in the literature that are related to supply and/or demand. Overall, we find that our demand components for inflation and GDP growth can be explained by the World Industrial Production index (Baumeister and Hamilton, 2019) and the Global Economic Conditions Indicator (Baumeister et al., 2022), while supply components are explained by the Global Supply Chain Pressure Index by the Federal Reserve Bank of New York and oil supply news shocks (Kanzig, 2021), with the expected signs.[13]

[13] All regression results are available upon request.

FIGURE 10. GDP: supply and demand factors

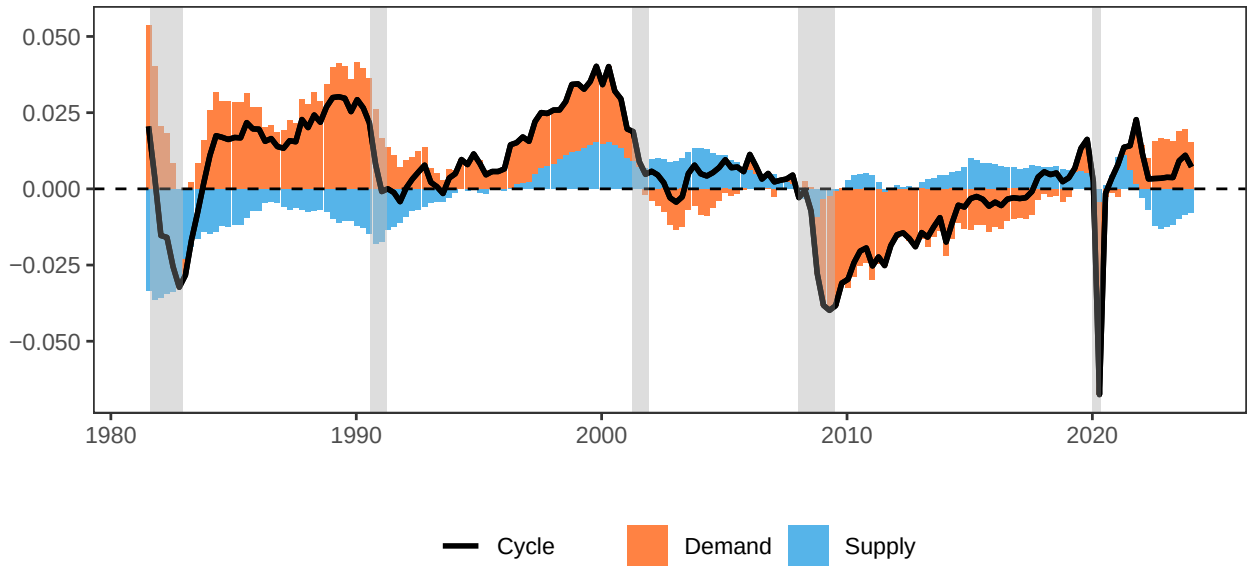

(A)

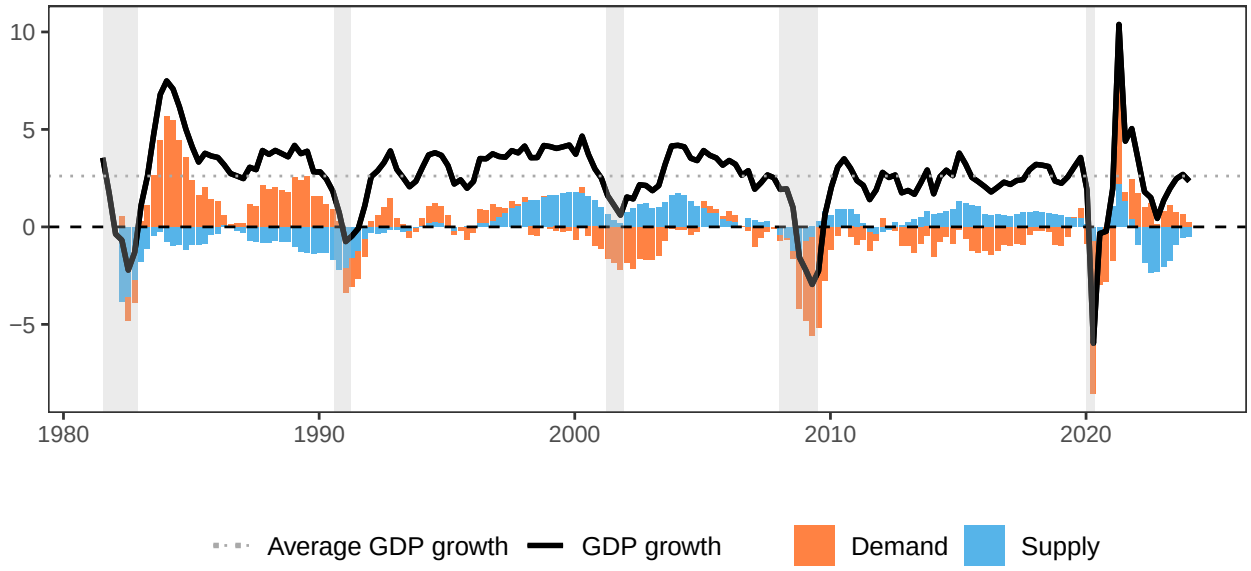

(B)

Notes: Panel (A) illustrates the decomposition of the cyclical component of GDP (or output gap), denoted as $C_t^{(\Delta y)}$ in (6), into demand-driven and supply-driven components. As expressed in (10), $C_t^{(\Delta y)}$ is an affine function of $\{\mathcal{Y}_{1,t}, \ldots, \mathcal{Y}_{4,t}\}$. The classification of these factors as demand or supply is based on the sign of the loadings δ^{π} and $\delta^{\Delta y}$ (see Subsection 5.1). The orange bars (and blue, respectively) indicate the proportion of $C_t^{(\Delta y)}$ attributable to demand-driven factors $\mathcal{Y}_{i,t}$. Panel (B) displays the decomposition of the year-on-year GDP growth rate, which is a linear function of $\mathcal{Y}_t$ and its lags.

FIGURE 11. Inflation: supply and demand factors

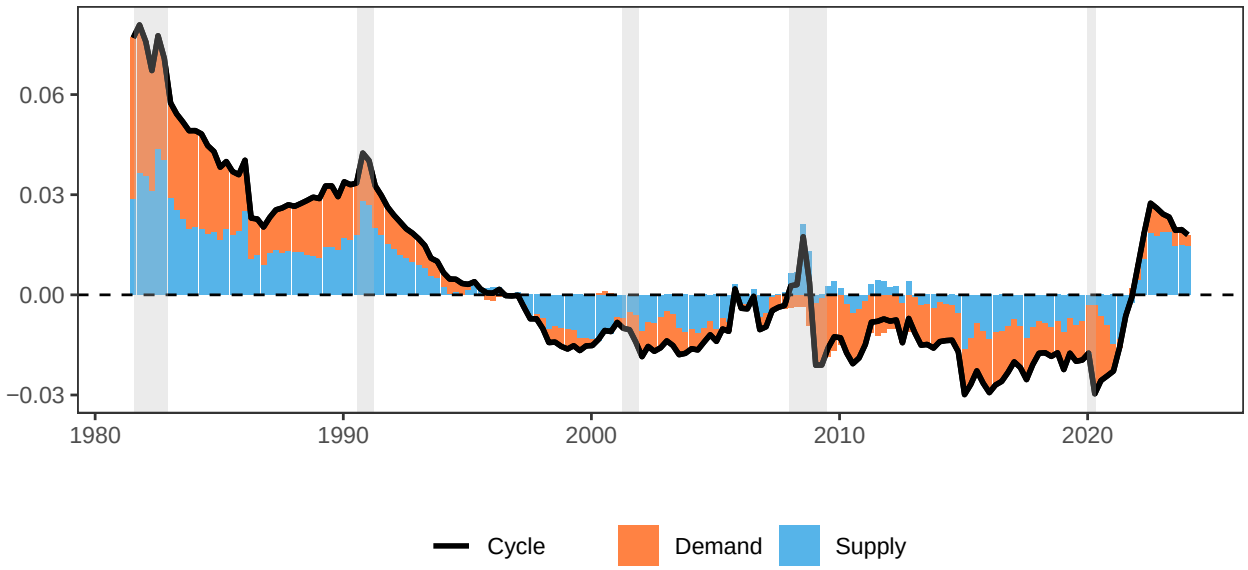

(A)

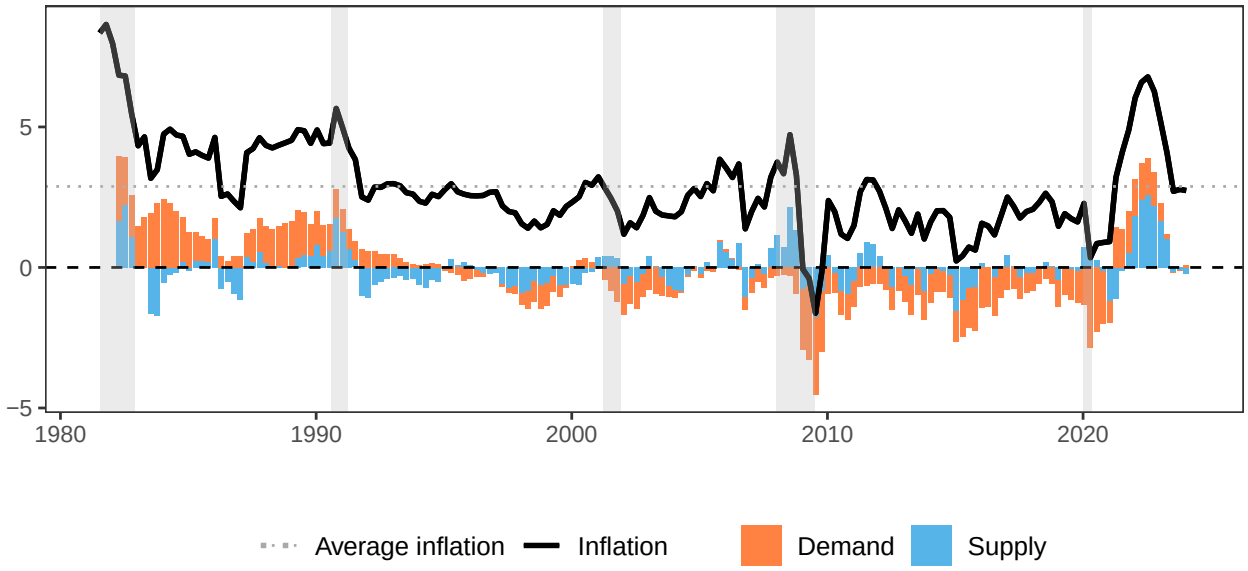

(B)

Notes: Panel (A) illustrates the decomposition of the cyclical component of the price index, denoted as $C_t^{(\pi)}$ in (6), into demand-driven and supply-driven components. As expressed in (10), $C_t^{(\pi)}$ is an affine function of $\{\mathcal{Y}_{1,t}, \ldots, \mathcal{Y}_{4,t}\}$. The classification of these factors as demand or supply is based on the sign of the loadings δ^{π} and δ^{π} (see Subsection 5.1). The orange bars (and blue, respectively) indicate the proportion of $C_t^{(\pi)}$ attributable to demand-driven factors $\mathcal{Y}_{i,t}$. Panel (B) displays the decomposition of the year-on-year inflation rate, which is a linear function of $\mathcal{Y}_t$ and its lags.

Figure 12 displays the time-varying correlation between inflation and economic activity for three horizons, revealing the evolving importance professional forecasters assign to aggregate supply and demand. First, we observe that this correlation varies over time. Moreover, our findings suggest that up until the early 1990s, this correlation is mildly negative or close to zero, implying that supply and demand drivers roughly balance out. Since the Great Recession, demand drivers are dominating, as indicated by the larger and positive relationship between the two variables, with the correlation reaching its peak at the height of the COVID-19 crisis. However, the correlation has decreased sharply since the pandemic, suggesting a shift towards supply factors becoming more influential. Our findings are in line with those of Han (2024) and Kamdar and Ray (2024) that find that, unlike consumers (and firms), professional forecasters do not have supply-side (stagflationary) explanations for their beliefs. Finally, as the horizon increases, the relationship between inflation and economic activity becomes increasingly positive, in line with our findings that demand drivers tend to be more persistent relative to supply drivers. In Figure 13 we plot the model-implied correlation between inflation and growth and a measure of nominal term premiums (Kim and Wright, 2005). Importantly, this correlation is negatively related to nominal term premiums. This is in line with structural models on the term structure of interest rates that show that the more important demand shocks are in an economy, the lower the nominal term premiums (see, e.g., Rudebusch and Swanson, 2012; Bletzinger et al., 2025). Indeed, while the presence of supply shocks pushes up nominal term premiums, the opposite is true for demand shocks.[14] Hence, if the relative importance of demand shocks—as measured by the conditional correlation between GDP and inflation—is high, then nominal term premiums should decrease.

Finally, to illustrate the model's ability to capture the joint dynamics of inflation and output, we compute stagflation probabilities. For each date in the sample, we simulate the model

[14]For example, consider an economy affected solely by supply shocks. In this scenario, the "bad states of the world"—characterized by low activity—also tend to feature high inflation. As a result, agents holding assets with fixed nominal payoffs suffer significant losses during recessions. Consequently, when supply shocks prevail, investors require a high risk premium to hold nominal bonds. This reasoning is reversed for an economy that only features demand shocks. As a result, an increase in the relative importance of demand shocks is expected to be accompanied by a decrease in nominal term premiums.

FIGURE 12. Correlation between inflation and economic activity

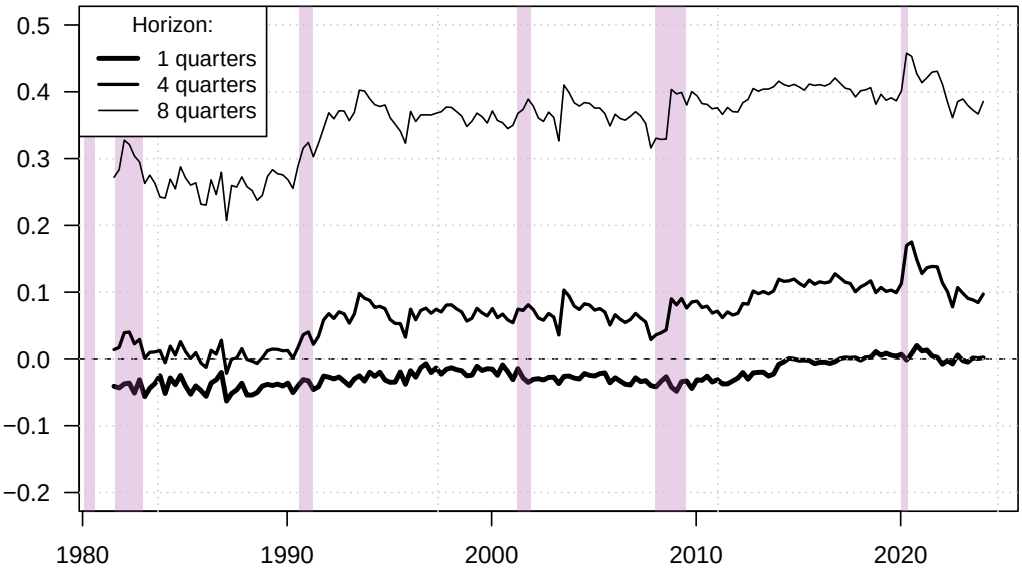

Notes: This figure displays the model-implied conditional correlation between inflation and GDP, at different horizons. More precisely, the plotted correlation is $\mathbb{C}or_t(\Delta y_{t,t+q}, \pi_{t,t+q})$ with $q \in \{1, 4, 8\}$. The calculation of these correlations is based on analytical formulas (provided in Appendix E.2), which are used to determine the second-order conditional moments of the state vector at any horizon.

10.000 times, projecting it eight periods ahead. Using these simulations, we calculate the probability that the economy experiences simultaneously high inflation and negative GDP growth, formally defined as:

$$P\big(\pi_{t+h-4,t+h} > 4\% \;\&\; y_{t+h-4,t+h} < 0\%\big),$$

where $\pi_{t+h-4,t+h}$ and $y_{t+h-4,t+h}$ denote year-on-year inflation and GDP growth over the horizon $[t+h-4, t+h]$, respectively, with $h = 4, \ldots, 8$.

Figure 14 depicts the time-varying probabilities of stagflation at different horizons (4 to 8 quarters ahead). All series move closely together, with correlations ranging between 81.2% and 99.5% (highest between adjacent horizons). During the 1980s and up to the early 1990s, stagflation risks are elevated, with probabilities at short-term horizons reaching up to 20%. Shortly after the early 1990s recession, probabilities drop sharply and remain near zero for most of the subsequent period, consistent with the stabilization of macroeconomic volatility

FIGURE 13. Correlation between inflation and economic activity, and nominal term premium

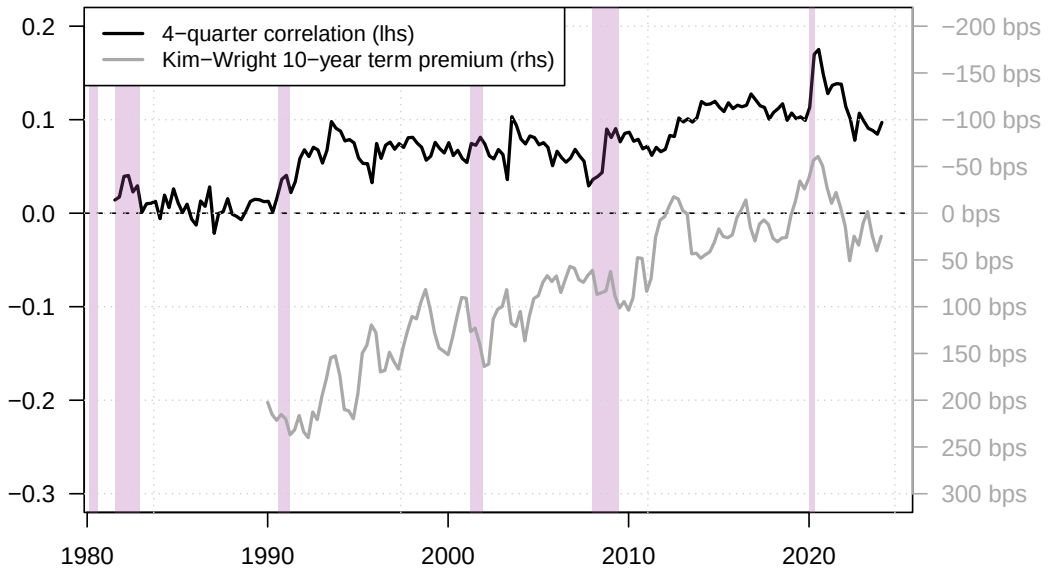

Notes: This figure illustrates the one-year-ahead model-implied conditional correlation between inflation and GDP ($Cor_t(\Delta y_{t,t+q}, \pi_{t,t+q})$), along with the 10-year nominal term premium estimate based on Kim and Wright (2005). The term premium is displayed using an inverted scale.

during the Great Moderation. However, longer horizons display more pronounced peaks during the Global Financial Crisis (slightly above 1.0%) and a larger spike in 2022, reaching around 4.5% before reverting close to zero. These patterns underscore that the risk of medium-term stagflation can exceed the risk of short-term stagflation even when the probabilities in the near term are subdued.

5.4. **Usefulness of higher-order moments.** To highlight the value-added of including higher-order moments we compare the performance of our baseline model in fitting tail risk for inflation and economic activity with that obtained using two alternative specifications of our model. The first specification reduces our baseline model to allow for time variation only in the mean and variance, while the second specification augments the baseline model to further allow for time-variation in the fourth cumulant. Table 3 reports the absolute difference

FIGURE 14. Time-Varying Probabilities of Stagflation

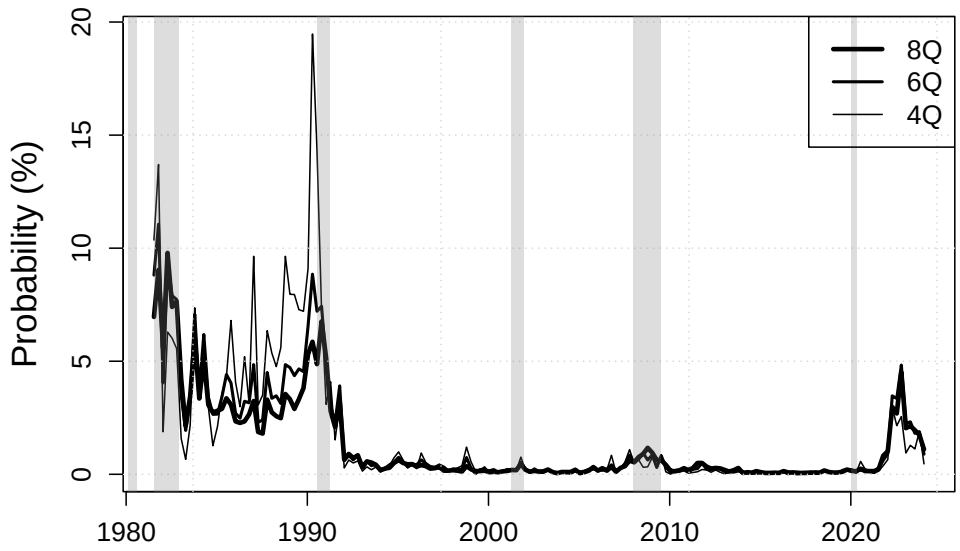

Notes: This figure presents the model-implied probabilities of experiencing a stagflation, defined as year-on-year inflation above 4% and year-on-year GDP growth below 0%, across different forecast horizons (4 to 8 quarters ahead). Each series is computed by 10,000 model simulations for each date in the sample, capturing the evolution of stagflation risk over time.

between model-implied percentiles and those underlying the data (smooth distributions using Gaussian mixtures) for the baseline model and the two alternative specifications. The lower the absolute difference, the better the model is able to capture the tail risk in the data.

We observe that, on average, for inflation, our baseline model performs the best across most horizons, especially in capturing the right tail (95th percentile), in line with the stylized fact that most of the inflation asymmetry in our sample is on the right-hand-side of the distribution. This finding is in line with De Polis et al. (2025) who introduce an econometric model with time-varying asymmetric risk for US inflation and find that it outperforms a state-of-the-art symmetric model in forecasting accuracy, obtaining results comparable to those of professional forecasters.

For output growth, the evidence is more mixed. First, comparing our model with the augmented specification, we observe that fitting the fourth cumulant does not come with any additional benefits in capturing tail risk and that, on average, our baseline model performs better. Now, comparing our baseline model with one that does not allow for asymmetries

in the distribution, we can observe that our model performs very well in capturing upside risk in most horizons. However, our model's performance in capturing the left tail is more heterogeneous, with notable gains at a 6-quarter horizon, but losses at most other horizons. We interpret this mixed evidence as a reflection of the relatively *sparse* prevalence of *strong* asymmetries in the GDP growth expectation data, throughout our sample.[15]

[15]Note that the average skewness for inflation ranges between 0.40 and 0.47 across horizons, while for growth it ranges between -0.23 and -0.43.

TABLE 3. Distance of model-implied percentiles from observed ones

	Baseline (1^{st},2^{nd}, 3^{rd})		All Moments (1^{st},2^{nd},3^{rd},4^{th})		No Higher-Order Mom. (1^{st},2^{nd})	
	5^{th}	95^{th}	5^{th}	95^{th}	5^{th}	95^{th}
(a) Inflation						
horizon = 5 Q						
Min, Max	(0.001, 0.636)	(0.000, 0.634)	(0.000, 0.838)	(0.003, 0.823)	(0.003, 0.831)	(0.002, 0.798)
25th, 75th	(0.111, 0.325)	(0.064, 0.289)	(0.092, 0.339)	(0.071, 0.236)	(0.065, 0.239)	(0.064, 0.333)
Median	0.179	0.124	0.189	0.115	0.143	0.188
horizon = 6 Q						
Min, Max	(0.007, 0.963)	(0.007, 0.953)	(0.009, 0.879)	(0.003, 1.029)	(0.000, 0.798)	(0.021, 0.642)
25th, 75th	(0.071, 0.255)	(0.078, 0.218)	(0.081, 0.250)	(0.061, 0.247)	(0.094, 0.334)	(0.073, 0.283)
Median	0.154	0.140	0.157	0.125	0.201	0.187
horizon = 7 Q						
Min, Max	(0.006, 0.568)	(0.003, 0.739)	(0.018, 0.706)	(0.000, 0.839)	(0.043, 0.588)	(0.002, 0.935)
25th, 75th	(0.072, 0.242)	(0.050, 0.245)	(0.094, 0.290)	(0.112, 0.363)	(0.175, 0.335)	(0.063, 0.410)
Median	0.155	0.137	0.172	0.205	0.278	0.229
horizon = 8 Q						
Min, Max	(0.009, 0.857)	(0.014, 0.663)	(0.003, 0.853)	(0.012, 0.862)	(0.003, 0.415)	(0.012, 0.766)
25th, 75th	(0.151, 0.314)	(0.062, 0.277)	(0.128, 0.372)	(0.094, 0.335)	(0.046, 0.251)	(0.073, 0.259)
Median	0.231	0.165	0.251	0.239	0.147	0.130
Overall						
Min, Max	(0.001, 0.963)	(0.000, 0.953)	(0.000, 0.879)	(0.000, 1.029)	(0.000, 0.831)	(0.002, 0.935)
25th, 75th	(0.083, 0.271)	(0.065, 0.263)	(0.087, 0.298)	(0.076, 0.280)	(0.085, 0.301)	(0.070, 0.314)
Median	0.186	0.143	0.194	0.175	0.191	0.169
(b) Real GDP growth						
horizon = 5 Q						
Min, Max	(0.004, 1.057)	(0.004, 0.962)	(0.010, 1.216)	(0.013, 0.961)	(0.001, 0.821)	(0.007, 1.053)
25th, 75th	(0.135, 0.430)	(0.105, 0.306)	(0.165, 0.526)	(0.084, 0.406)	(0.122, 0.446)	(0.068, 0.335)
Median	0.284	0.202	0.321	0.238	0.205	0.179
horizon = 6 Q						
Min, Max	(0.002, 0.568)	(0.003, 0.229)	(0.023, 1.016)	(0.001, 0.595)	(0.008, 0.650)	(0.003, 1.180)
25th, 75th	(0.169, 0.329)	(0.040, 0.121)	(0.120, 0.279)	(0.072, 0.239)	(0.144, 0.393)	(0.082, 0.221)
Median	0.253	0.083	0.192	0.121	0.211	0.126
horizon = 7 Q						
Min, Max	(0.046, 1.206)	(0.000, 0.884)	(0.003, 1.605)	(0.007, 1.453)	(0.004, 0.868)	(0.002, 1.194)
25th, 75th	(0.273, 0.489)	(0.061, 0.180)	(0.210, 0.548)	(0.112, 0.494)	(0.104, 0.323)	(0.088, 0.269)
Median	0.367	0.100	0.378	0.270	0.203	0.155
horizon = 8 Q						
Min, Max	(0.000, 1.122)	(0.023, 0.587)	(0.002, 0.995)	(0.008, 1.555)	(0.044, 1.122)	(0.001, 0.935)
25th, 75th	(0.196, 0.687)	(0.078, 0.256)	(0.193, 0.763)	(0.133, 0.528)	(0.147, 0.485)	(0.072, 0.344)
Median	0.467	0.154	0.478	0.340	0.374	0.160
Overall						
Min, Max	(0.000, 1.206)	(0.000, 0.962)	(0.002, 1.605)	(0.001, 1.555)	(0.001, 1.122)	(0.001, 1.194)
25th, 75th	(0.178, 0.479)	(0.065, 0.220)	(0.166, 0.532)	(0.093, 0.408)	(0.119, 0.430)	(0.075, 0.305)
Median	0.324	0.115	0.314	0.235	0.235	0.155

Notes: The table reports the absolute difference between model-implied percentiles and those from the smooth distribution using Gaussian mixtures (i.e., data). The table reports key statistics on the ability of our baseline model (with three first conditional moments) to capture the tails (5th and 95th percentiles) of the distributions of future (5 to 8 quarters ahead) inflation and growth. For robustness, we compare its performance against two models: one that uses all four first conditional moments (All Moments) and one that uses only the first two conditional moments (No Higher-Order Mom.).

Finally, in Appendix G we report the decompositions for GDP growth and inflation for each of these three model specifications. We observe that the decompositions are very robust to the model specification. However, there are meaningful differences that arise especially in periods when higher-order moments (asymmetry) gain traction, such as up to the early 1990s and in the post-pandemic period.

6. Conclusion

In this paper, we jointly assess the risks on prices and production by exploiting forward-looking survey information to capture macroeconomic risk perceptions. We use a dynamic factor model that features time-varying uncertainty and asymmetry to study the relationship between inflation and the real economy through the lens of professional forecasters. We exploit the joint dynamics of realized and expected inflation and economic activity in order to identify demand and supply factors for the United States. We use probabilistic responses to surveys of professional forecasters to exploit changes in the entire distribution of future expected inflation and GDP growth. Our model allows for a trend and cycle decomposition, which enables us to study the drivers of inflation and real activity at business-cycle and lower frequencies.

Empirical evidence on US data suggests that the output gap is determined by a mix of supply and demand factors before the Great Recession and since COVID-19, while it is mostly driven by demand between 2008 and 2020. Moreover, the price gap exhibits a sharp increase in the last quarters of our sample, which is attributed to negative supply factors, in line with the idea that high inflation realizations are partly justified by transitory supply components. The trend in inflation has also steepened in the last quarters of our sample, implying that there are also persistent drivers behind the rise in inflation, which are mostly demand-driven. Overall, the recent increase in inflation is attributed to temporary negative supply factors and persistent positive demand factors. Regarding the quantification of macroeconomic risk, we find that, for inflation, uncertainty and asymmetry are prevalent in the 1980s and during the Great Recession, while for GDP growth, these features are in the data in the 1980s and

since COVID-19. Moreover, the model-implied correlation between inflation and growth is time-varying and negatively related to nominal term premiums. On average, the correlation is positive in our sample, implying that professional forecasters do not have stagflationary beliefs. Finally, to illustrate the possible tensions that can arise between the objectives of price stability and growth, we compute probabilities of stagflation at short to medium horizons. In 2022, stagflation probabilities increased sharply, reaching levels not seen in three decades. While still subdued (about a quarter of what they were in the early 1990s) this increase is noteworthy after a 30-year period of near-zero probabilities.

References

Abiad, A. and Qureshi, I. A. (2023). The macroeconomic effects of oil price uncertainty. *Energy Economics*, 125:106839.

Adams, P. A., Adrian, T., Boyarchenko, N., and Giannone, D. (2021). Forecasting macroeconomic risks. *International Journal of Forecasting*, 37(3):1173–1191.

Adrian, T., Boyarchenko, N., and Giannone, D. (2019). Vulnerable Growth. *American Economic Review*, 109(4):1263–1289.

Adrian, T., Grinberg, F., Liang, N., Malik, S., and Yu, J. (2022). The Term Structure of Growth-at-Risk. *American Economic Journal: Macroeconomics*, 14(3):283–323.

Andrade, P., Crump, R. K., Eusepi, S., and Moench, E. (2016). Fundamental Disagreement. *Journal of Monetary Economics*, 83(C):106–128.

Andrade, P. and Le Bihan, H. (2013). Inattentive professional forecasters. *Journal of Monetary Economics*, 60(8):967 – 982.

Ang, A., Bekaert, G., and Wei, M. (2007). Do macro variables, asset markets, or surveys forecast inflation better? *Journal of Monetary Economics*, 54(4):1163–1212.

Aruoba, S. B. (2016). Term Structures of Inflation Expectations and Real Interest Rates. Working Papers 16-9, Federal Reserve Bank of Philadelphia.

Bauer, M. and Chernov, M. (2024). Interest rate skewness and biased beliefs. *The Journal of Finance*, 79(1):173–217.

Baumeister, C. and Hamilton, J. D. (2019). Structural interpretation of vector autoregressions with incomplete identification: Revisiting the role of oil supply and demand shocks. *American Economic Review*, 109(5):1873–1910.

Baumeister, C., Korobilis, D., and Lee, T. K. (2022). Energy markets and global economic conditions. *The Review of Economics and Statistics*, 104(4):828–844.

Bekaert, G. and Engstrom, E. (2010). Inflation and the Stock Market: Understanding the Fed Model. *Journal of Monetary Economics*, 57(3):278–294.

Bekaert, G., Engstrom, E. C., and Ermolov, A. (2020). Aggregate Demand and Aggregate Supply Effects of COVID-19: A Real-time Analysis. Finance and Economics Discussion Series 2020-049, Board of Governors of the Federal Reserve System (U.S.).

Bekaert, G., Engstrom, E. C., and Ermolov, A. (2025). Uncertainty and the Economy: The Evolving Distributions of Aggregate Supply and Demand Shocks. *American Economic Journal: Macroecoomics*, forthcoming.

Bianchi, F., Nicolo, G., and Song, D. (2023). Inflation and real activity over the business cycle. Finance and Economics Discussion Series 2023-038, Board of Governors of the Federal Reserve System (U.S.).

Blanchard, O. J. and Quah, D. (1989). The Dynamic Effects of Aggregate Demand and Supply Disturbances. *American Economic Review*, 79(4):655–673.

Bletzinger, T., Lemke, W., and Renne, J.-P. (2025). Time-Varying Risk Aversion and Inflation-Consumption Correlation in an Equilibrium Term Structure Model. *Journal of Financial Econometrics*, 23(2):110–138.

Bullard, J. and Keating, J. W. (1995). The long-run relationship between inflation and output in postwar economies. *Journal of Monetary Economics*, 36(3):477–496.

Carriero, A., Clark, T. E., and Marcellino, M. (2022). Nowcasting tail risk to economic activity at a weekly frequency. *Journal of Applied Econometrics*, 37(5):843–866.

Cascaldi-Garcia, D., Lopez-Salido, J. D., and Loria, F. (2022). Is Trend Inflation at Risk of Becoming Unanchored? The Role of Inflation Expectations. FEDS Notes 2022-03-31, Board of Governors of the Federal Reserve System (U.S.).

Cesa-Bianchi, A. and Ferrero, A. (2021). The Transmission of Keynesian Supply Shocks. CEPR Discussion Papers 16430, C.E.P.R. Discussion Papers.

Clark, T. E., Ganics, G., and Mertens, E. (2022). What is the Predictive Value of SPF Point and Density Forecasts? Working Papers 22-37, Federal Reserve Bank of Cleveland.

Cogley, T., Primiceri, G. E., and Sargent, T. J. (2010). Inflation-Gap Persistence in the US. *American Economic Journal: Macroeconomics*, 2(1):43–69.

Coibion, O. and Gorodnichenko, Y. (2012). What Can Survey Forecasts Tell Us about Information Rigidities? *Journal of Political Economy*, 120(1):116–159.

Cook, T. R. and Doh, T. ((November 20, 2019)). Assessing macroeconomic tail risks in a data-rich environment. Technical report, Federal Reserve Bank of Kansas City Working Paper RWP 19-12.

Dai, Q. and Singleton, K. J. (2000). Specification analysis of affine term structure models. *Journal of Finance*, 55(5):1943–1978.

Darolles, S., Gouriéroux, C., and Jasiak, J. (2006). Structural Laplace Transform and Compound Autoregressive Models. *Journal of Time Series Analysis*, 27(4):477–503.

De Polis, A., Petrella, I., and Melosi, L. (2025). The taming of the skew: asymmetric inflation risk and monetary policy. Working Paper Series 3028, European Central Bank.

Dew-Becker, I., Tahbaz-Salehi, A., and Vedolin, A. (2021). Skewness and time-varying second moments in a nonlinear production network: Theory and evidence. Working Paper 29499, National Bureau of Economic Research.

Duan, J.-C. and Simonato, J. G. (1999). Estimating exponential-affine term structure models by Kalman filter. *Review of Quantitative Finance and Accounting*, 13(2):111–135.

Duffee, G. R. and Stanton, R. H. (2012). Estimation of dynamic term structure models. *Quarterly Journal of Finance*, 2(2).

Duffie, D. and Kan, R. (1996). A yield factor model of interest rates. *Mathematical Finance*, 6:379–406.

Duffie, D., Pan, J., and Singleton, K. (2000). Transform analysis and asset pricing for affine jump-diffusions. *Econometrica*, 68(6):1343–1376.

Faust, J. and Wright, J. H. (2013). Chapter 1 - Forecasting Inflation. In Elliott, G. and Timmermann, A., editors, *Handbook of Economic Forecasting*, volume 2 of *Handbook of Economic Forecasting*, pages 2–56. Elsevier.

Feunou, B. and Okou, C. (2018). Risk-Neutral Moment-Based Estimation of Affine Option Pricing Models. *Journal of Applied Econometrics*, 33(7):1007–1025.

Furlanetto, F., Lepetit, A., Robstad, O., Rubio-Ramirez, J., and Ulvedal, P. (2025). Estimating hysteresis effects. *American Economic Journal: Macroeconomics*, 17(1):35–70.

Gali, J. (1992). How Well Does The IS-LM Model Fit Postwar U. S. Data? *The Quarterly Journal of Economics*, 107(2):709–738.

Giannone, D. and Primiceri, G. (2024). The drivers of post-pandemic inflation. Working Paper 32859, National Bureau of Economic Research.

Gouriéroux, C. and Jasiak, J. (2006). Autoregressive gamma processes. *Journal of Forecasting*, 25:129–152.

Grishchenko, O., Mouabbi, S., and Renne, J.-P. (2019). Measuring Inflation Anchoring and Uncertainty: A U.S. and Euro Area Comparison. *Journal of Money, Credit and Banking*, 51(5):1053–1096.

Han, Z. (2024). Asymmetric information and misaligned inflation expectations. *Journal of Monetary Economics*, 143:103529.

Hilscher, J., Raviv, A., and Reis, R. (2022). Inflating Away the Public Debt? An Empirical Assessment [Crisis and commitment: Inflation credibility and the vulnerability to sovereign debt crises]. *Review of Financial Studies*, 35(3):1553–1595.

Iseringhausen, M., Petrella, I., and Theodoridis, K. (2023). Aggregate skewness and the business cycle. *The Review of Economics and Statistics*, pages 1–38.

Jo, S. and Sekkel, R. (2019). Macroeconomic uncertainty through the lens of professional forecasters. *Journal of Business & Economic Statistics*, 37(3):436–446.

Kamdar, R. and Ray, W. (2024). Attention-Driven Sentiment and the Business Cycle. CAEPR Working Papers 2024-003 Classification-, Center for Applied Economics and Policy Research, Department of Economics, Indiana University Bloomington.

Kanzig, D. R. (2021). The macroeconomic effects of oil supply news: Evidence from opec announcements. *American Economic Review*, 111(4):1092–1125.

Kim, D. H. and Wright, J. H. (2005). An Arbitrage-Free Three-Factor Term Structure Model and the Recent Behavior of Long-term Yields and Distant-horizon Forward Rates. Finance and Economics Discussion Series 2005-33, Board of Governors of the Federal Reserve System (U.S.).

Le, A., Singleton, K. J., and Dai, Q. (2010). Discrete-time affine-q term structure models with generalized market prices of risk. *Review of Financial Studies*, 23(5):2184–2227.

Lopez-Salido, J. D. and Loria, F. (2024). Inflation at Risk. *Journal of Monetary Economics*, 145(S).

Mertens, E. (2016). Measuring the level and uncertainty of trend inflation. *Review of Economics and Statistics*, 98(5):950–967.

Monfort, A., Pegoraro, F., Renne, J.-P., and Roussellet, G. (2017). Staying at Zero with Affine Processes: An Application to Term-Structure Modelling. *Journal of Econometrics*, 201(2):348–366.

Nason, J. M. and Smith, G. W. (2021). Measuring the slowly evolving trend in US inflation with professional forecasts. *Journal of Applied Econometrics*, 36(1):1–17.

Piazzesi, M. (2010). Affine term structure models. In *Handbook of Financial Econometrics, Volume 1*, chapter 12, pages 389–472. Yacine ait-sahalia and lars peter hansen north holland edition.

Rudebusch, G. D. and Swanson, E. T. (2012). The Bond Premium in a DSGE Model with Long-Run Real and Nominal Risks. *American Economic Journal: Macroeconomics*, 4(1):105–43.

Shapiro, A. H. (2022). Decomposing Supply and Demand Driven Inflation. Working Paper Series 2022-18, Federal Reserve Bank of San Francisco.

Shapiro, M. D. and Watson, M. W. (1988). Sources of business cycle fluctuations. Working Paper 2589, National Bureau of Economic Research.

Stock, J. H. and Watson, M. W. (2007). Why has U.S. Inflation Become Harder to Forecast? *Journal of Money, Credit and Banking*, 39(s1):3–33.

APPENDIX A. SMOOTHING METHOD OF SPF DATA

A.1. **Overview of the method.** Our objective is to develop a model that disciplines the information available in Surveys of Professional Forecasters (SPF). These surveys provide two types of forecast: point estimates and probability-bin forecasts. The first type of forecast corresponds to first-order conditional moments, that is, $\mathbb{E}(x_{t+h}|\mathcal{I}_t)$ for the variable of interest x and an horizon h, where $\mathcal{I}_t$ denotes the information available on date t (the survey date). The second type of forecasts are probabilities of the form $\mathbb{P}(b_k < x_{t+h} \leq b_{k+1}|\mathcal{I}_t)$, where the intervals $[b_k, b_{k+1}]$ are often called "bins". Usually, the lower bound of the first bin ($\underline{b}_0$, say) is $-\infty$, and the upper bound of the last bin ($\underline{b}_{K+1}$, say) is $+\infty$. It is easily seen that observing the probability bin forecasts for the bins $]-\infty, b_1], \ldots,]b_K, +\infty[$ is equivalent to observing forecasters' evaluation of the cumulative distribution function (CDF) at $b_1, \ldots, b_K$ (for a given variable and horizon).[16]

In principle, one could try to directly fit a dynamic model—such as the one we present in Section 3—to the CDF evaluations given in SPF. However, this direct approach is challenging to implement if the CDFs are not available analytically.[17] We adopt an alternative approach that involves fitting the first moments of the targeted conditional distributions, which can be computed relatively easily when the state vector follows an affine process (as is the case in the model proposed in Section 3). However, doing so necessitates the conversion of the probability bin forecasts (which are directly available in SPF) into moments (which are not provided in the surveys). To address that, we consider a parametric distribution function (Section A.3) and look for parameterizations that provide the best possible fit of the CDF, for

[16] For instance, assume that the forecasters attribute probabilities of 1%, 4%, 15%, 30%, 36%, 12%, and 2%, that inflation will fall, respectively, in $]-\infty, 1\%]$, $]1\%, 2\%]$, $]2\%, 3\%]$, $]3\%, 4\%]$, $]4\%, 5\%]$, $]5\%, 6\%]$, and $]6\%, +\infty[$ for a given horizon. This means that we have $F_{SPF}(1) = 0.01$, $F_{SPF}(2) = 0.05$, $F_{SPF}(3) = 0.20$, $F_{SPF}(4) = 0.50$, $F_{SPF}(5) = 0.86$, $F_{SPF}(6) = 0.98$, where F_{SPF} denotes the CDF of the considered distribution.

[17] Formulas exist to compute the cumulative distribution function (CDF) of future linear combinations of the components of an affine multivariate process (Duffie et al., 2000). However, these formulas are not analytical and require the numerical evaluation of an integral. Although this is manageable after estimation, integrating it during the estimation phase—specifically if the likelihood evaluation relies on these numerical formulas for various variables, dates, and horizons—would significantly increase the computational burden.

each variable, date, and horizon. We then compute the moments of the resulting "smoothed" distribution and use these moments to fit our dynamic term-structure model.

It is important to note that the present smoothing exercise is fundamentally different from what is achieved with our dynamic model. In the former exercise, each distribution—through its SPF-based CDF evaluations—is treated independently from the others. In contrast, in the latter case, the dynamic term-structure model produces distributions that are consistent in the time, horizon, and variable dimensions. In other words, the smoothing approach presented in the present section should be regarded as a preliminary processing of the raw SPF data.

Before turning to the numerical procedure used to obtain the smoothed/interpolated density functions, we discuss the approach followed to deal with the recent "bin-compression" issue.

A.2. **Dealing with bins' exterior bounds.** In order to maximize the amount of information contained in the SPF probability bin forecasts, we replace the lower bound of the first (that is $-\infty$) and the upper bound of the last bin ($+\infty$), with non-infinite values, b_0 and b_{K+1}, and assume that $\mathbb{P}(x_{t+h} < b_0) = \mathbb{P}(x_{t+h} > b_{K+1}) = 0$. In other words, denoting with F_{SPF} the SPF-based cumulative distribution function (CDF), we augment the set of targeted CDF values with $F_{SPF}(b_0) = 0$ and $F_{SPF}(b_{K+1})$.

Assigning values to b_0 and b_{K+1} serves two key purposes. First, as elaborated below, we establish these values in a manner that aligns the point estimate given by the forecasters with the mean of the initial rough approximation of the distribution, specifically the histogram supported on the interval $[b_0, b_{K+1}]$ and composed of $K+1$ bins. (Discrepancies between these two representations have often been observed.) Second, and more importantly, this approach addresses the "truncation" of the Survey of Professional Forecasters (SPF) probability bin forecasts that has occurred in recent years. From 2022 to 2023, the upper limits of the bins were not promptly adjusted to reflect the surge in inflation (and inflation expectations), particularly for shorter horizons. For example, even when the one-year-ahead point estimate approached 4% in 2022, the upper limit of the SPF bins remained at $b_K = 4\%$. Consequently,

forecasters ended up allocating significant probabilities to the ">4%" bin. In this context, the SPF probability-bin data offer limited information on the right side of the distribution, as $F_{SPF}(b_1), \ldots, F_{SPF}(b_K)$ primarily provide insights into the left side—given that $F_{SPF}(b_K)$ is considerably less than 1. Our approach seeks to enhance this information by identifying an appropriate value for b_{K+1}, which serves as the upper (finite) boundary of the distribution's support (the 100^{th} percentile). To achieve this, we leverage potentially complementary information embedded in the point estimate. Figure 15 illustrates this generic situation, along with the approach we use to tackle it. This approach is described in the following.

FIGURE 15. Adjusting b_{K+1}

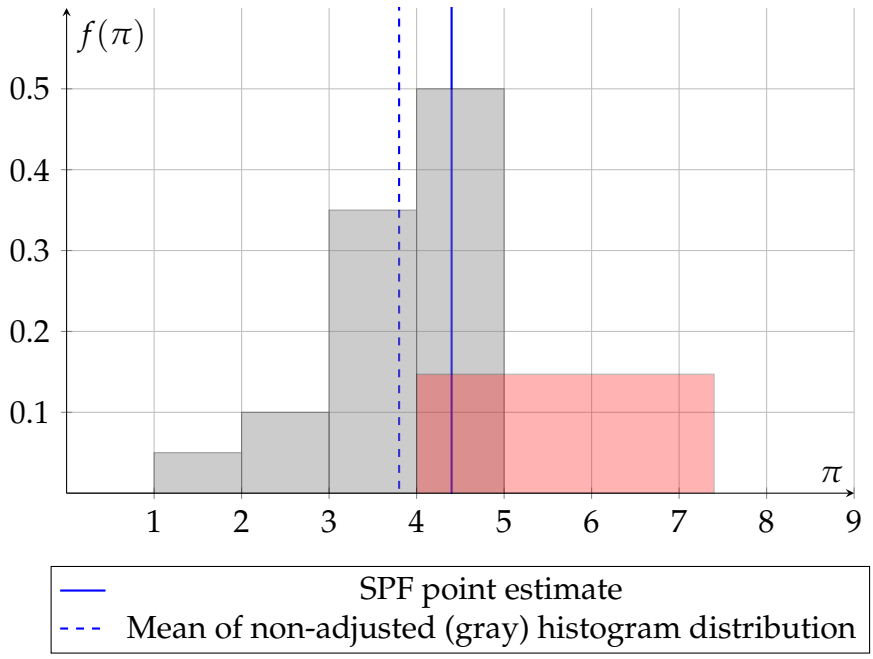

Note — This figure illustrates the methodology we develop to determine b_{K+1} (upper bound of the last bin) when the number of bins is not sufficient to accommodate surge in the variable of interest (inflation π, say). On the chart, the gray shaded bars represent the probabilities extracted from the SPF. The heights of the bars are, respectively: 0.05, 0.10, 0.35, and 0.50, which imply the following values of the cumulative distribution, denoted with F_{SPF}: $F_{SPF}(2) = 0.05$, $F_{SPF}(3) = 0.15$, and $F_{SPF}(4) = 0.50$. (Note that the lower bound of the first bin and the upper bound of the last bin are usually undefined in SPF.) The blue solid line indicates the point estimate, as read in the SPF. The dashed blue line corresponds to the mean associated with the histogram-based distribution, taking $b_0 = 1$ and $b_{K+1} = 5$. It appears that this mean is too low compared to the SPF-based point estimate (solid blue line). The upper limit of the red bar is set so that when the last gray bar is substituted with the red bar, the point estimate aligns with the mean derived from the histogram.

To start with, let us consider the case where the lower bound of the first bin is set to $b_1 - s_{bin}$, where s_{bin} is the size of the other bins, and the upper bound of the last bin is set to $b_K + s_{bin}$. This implies the first and last gray bars in Figure 16. The mean associated with the resulting histogram is:

$$\mu_{hist} = \sum_{k=0}^{K} p_k m_k,$$

where p_k denotes the SPF probability assigned to bin k, and m_k is defined as the midpoint of bin k. For $k \in \{1, \ldots, K-1\}$, we have $m_k = \frac{b_k + b_{k+1}}{2}$, and we have $m_0 = m_1 - s_{bin}$ and $m_{K+1} = m_k + s_{bin}$. In general, μ_{hist} is close but different from the SPF point estimate (PE). Our approach consists in modifying one of the two bounds, b_0 or b_{K+1}, in such a way that the new resulting histogram mean aligns with PE. That is, either b_0 or b_{K+1} is set so as to have:

$$PE = p_0 \frac{b_0 + b_1}{2} + p_{K+1} \frac{b_K + b_{K+1}}{2} + \sum_{k=1}^{K-1} p_k m_k.$$

The previous equation can then be used to obtain either b_0 or b_{K+1} as a function of all other variables. We impose constraints on the resulting extreme bound: (a) the width of the resulting (first or last) bin must be greater than or equal to s_{bin} but less than 5%. Consequently, we have either

$$\begin{cases} b_0 &= b_1 - s_{bin}, \qquad m_0 = \dfrac{b_0 + b_1}{2}, \\ b_{K+1} &= \min\left[\max\left[\frac{2}{p_{K+1}}\left(PE - \sum_{k=0}^{K-1} p_k m_k\right) - b_K, b_K + s_{bin}\right], 5\%\right]. \end{cases}$$

or

$$\begin{cases} b_{K+1} &= b_K + s_{bin}, \qquad m_{K+1} = \dfrac{b_K + b_{K+1}}{2} \\ b_0 &= \max\left[\min\left[\frac{2}{p_0}\left(PE - \sum_{k=1}^{K} p_k m_k\right) - b_1, b_1 - s_{bin}\right], 5\%\right]. \end{cases}$$

A.3. **Gaussian Mixture Distribution and fitting approach.** We rely on mixtures of Gaussian distributions to interpolate and smooth SPF-based probability bin forecasts. The versatility of the mixture of Gaussian distribution is illustrated, in particular, by its ability to attain any

admissible pair of skewness and kurtosis.[18]

Definition 1. *We say that the random variable X follows a mixture of two Gaussian distributions of parameters $(p, \mu_1, \mu_2, \sigma_1, \sigma_2)$, which we denote $X \sim \mathcal{N}_2(p, \mu_1, \mu_2, \sigma_1, \sigma_2)$, if*

$$X = BX_1 + (1 - B)X_2, \quad \textit{with} \quad B \sim \mathcal{B}(p),\ X_1 \sim \mathcal{N}(\mu_1, \sigma_1),\ \textit{and}\ X_2 \sim \mathcal{N}(\mu_2, \sigma_2),$$

where $\mathcal{B}(p)$, with $0 \leq p \leq 1$, denotes the Bernoulli distribution of parameter p, and where B, X_1, and X_2 are independently distributed.

The probability density function of X is given by:

$$f(x; \theta) = p\phi\left(\frac{x - \mu_1}{\sigma_1}\right) + (1 - p)\phi\left(\frac{x - \mu_2}{\sigma_2}\right), \tag{23}$$

where ϕ denotes the probability density function of $\mathcal{N}(0, 1)$ and where $\theta = [p, \mu_1, \mu_2, \sigma_1, \sigma_2]'$.

As explained above, for each variable, date, and horizon for which SPF are available, we look for a mixture of Gaussian distributions that yields the best possible fit of the SPF-based CDF evaluations at $b_0, \ldots, b_{K+1}$, which define the bounds of the SPF's bins. Denoting the SPF-based CDF with F_{SPF} and denoting the CDF of the mixture of Gaussian distribution with F_θ, our approach involves the following optimization:

$$(p, \mu_1, \mu_2, \sigma_1, \sigma_2) = \underset{\theta \in \Theta}{\operatorname{argmin}} \sum_{k=0}^{K+1} (F_\theta(b_k) - F_{SPF}(b_k))^2, \tag{24}$$

where Θ is the set of parameters $(p, \mu_1, \mu_2, \sigma_1, \sigma_2)$ satisfying:

(i) $\mu_1 \in [b_0, PE]$ and $\mu_2 \in [PE, b_{K+1}]$.

(ii) $\sigma_1, \sigma_2 \in [\sigma_{\min}, \sigma_{\max}]$, where

$$\sigma_{\min} = \max\left(0.25, \frac{\min(\{b_{k+1} - b_k\}_{k=1,\ldots,K-1})}{2}\right) \quad \text{and} \quad \sigma_{\max} = \frac{(b_K - b_1)}{6}.$$

[18] The set of admissible skewness (s) and kurtosis (k) associated with a given distribution is the set $\{(k, s), k \geq 1 + s^2\}$. (Thus, in particular, $k > 1$.)

(iii) $p = \dfrac{\mu_2 - PE}{\mu_2 - \mu_1}$.

These constraints are imposed to facilitate the numerical convergence and to ensure the economic relevance of the resulting smoothed distributions.

FIGURE 16. Smoothing approach

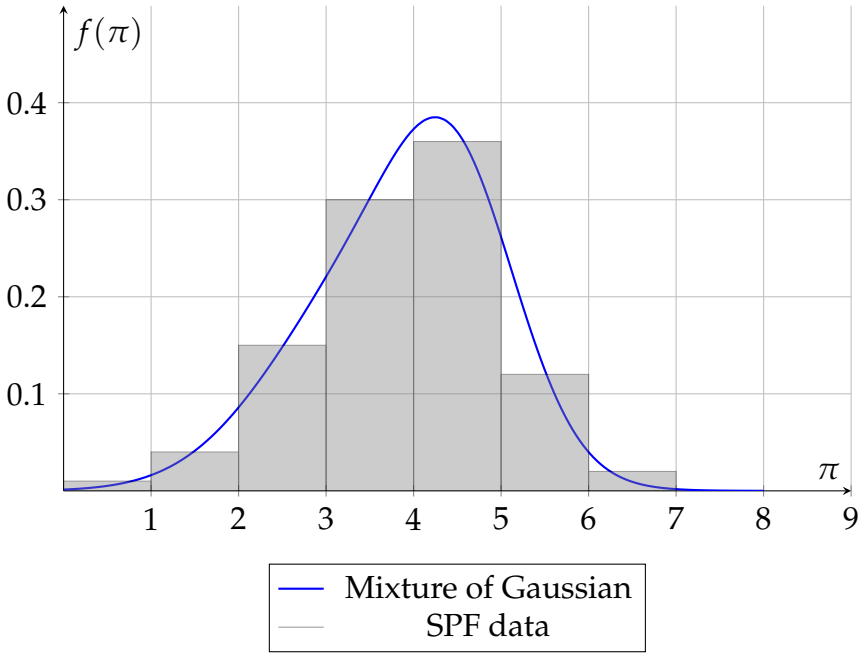

Note — This figure illustrates the methodology we develop to convert SPF's probability bin forecasts into smoothed distributions. On this chart, the gray shaded bars represent the probabilities extracted from the SPF. The heights of the bars are, respectively: 0.01, 0.04, 0.15, 0.30, 0.36, 0.12, and 0.02, which imply the following values of the cumulative distribution, denoted with F_{SPF}: $F_{SPF}(1) = 0.01$, $F_{SPF}(2) = 0.05$, $F_{SPF}(3) = 0.20$, $F_{SPF}(4) = 0.50$, $F_{SPF}(5) = 0.86$, $F_{SPF}(6) = 0.98$. (Note that the lower bound of the first bin and the upper bound of the last bin are usually undefined in SPF.) The blue line is the fitted probability density function of the mixture of Gaussian distribution (see eq. 23), obtained by looking for the parameters of the mixture, namely $(p, \mu_1, \mu_2, \sigma_1, \sigma_2)$, that provide the best fit of the CDF.

APPENDIX B. AUTO-REGRESSIVE GAMMA (ARG) PROCESS

In our model, the process z_t follows a vector autoregressive gamma process (V-ARG). This section describes the useful properties of this process. We start by defining the non-centered Gamma distribution, which is needed to further define ARG processes.

Definition 2 (Non-central gamma distribution)**.** *Variable W is drawn from the non-centered gamma distribution $\gamma_\nu(\lambda, \mu)$ if and only if there exists a Poisson-distributed variable Z that is such that:*

$$Z \sim \mathcal{P}(\lambda) \quad \textit{and} \quad W|Z \sim \gamma_{\nu+Z}(\mu),$$

where $\gamma_\nu(\mu)$ denotes the gamma distribution of scale μ and shape ν.

Remarkably, although the probability density functions of a non-centered-gamma variable is complicated, its Laplace transform admits a simple form:

Proposition 1. *If W is non-centered gamma $\gamma_\nu(\lambda, \mu)$ (see Def. 2), its log-Laplace transform is given by:*

$$\psi_t(u) := \log(\mathbb{E}_t[\exp(uW)]) = a_w(u) + b_w(u),$$

where

$$a_w(u) = -\nu \log(1 - \mu u) \quad \textit{and} \quad b_w(u) = \lambda \left(\frac{u\mu}{1 - u\mu} \right).$$

The first four moments of the non-centered gamma distribution are available in closed form:

Proposition 2. *If W is non-centered gamma $\gamma_\nu(\lambda, \mu)$ (see Def. 2), its first four cumulants are given by:*

$$\mathbb{E}(W) = \mu(\nu + \lambda), \qquad \mathbb{V}(W) = \mu^2(\nu + 2\lambda)$$
$$\mu_3(W) = \mu^3(2\nu + 6\lambda), \qquad \mu_4(W) = \mu^4(6\nu + 24\lambda).$$

Proof. It is well-known that the cumulants of a distribution coincide with the evaluation of the derivatives of its log-Laplace transform at zero. Computing the derivatives of $\psi_t(u)$ with

respect to u (using Prop. 1) gives:

$$a'_w(u) = \frac{\nu\mu}{1-\mu u} \qquad b'_w(u) = \frac{\lambda\mu}{(1-u\mu)^2}$$
$$a''_w(u) = \frac{\nu\mu^2}{(1-\mu u)^2} \qquad b''_w(u) = \frac{2\lambda\mu^2}{(1-u\mu)^3}$$
$$a'''_w(u) = \frac{2\nu\mu^3}{(1-\mu u)^3} \qquad b'''_w(u) = \frac{6\lambda\mu^3}{(1-u\mu)^4}$$
$$a''''_w(u) = \frac{6\nu\mu^4}{(1-\mu u)^4} \qquad b''''_w(u) = \frac{24\lambda\mu^4}{(1-u\mu)^5},$$

which proves the proposition. □

Definition 3 (Vectorial-ARG)**.** *The q-dimensional vector z_t follows an autoregressive gamma process if, conditionally on $\underline{z_{t-1}} = \{z_{t-1}, z_{t-2}, \dots\}$, the different components of z_t are independently drawn from the following non-centered Gamma distributions:*

$$z_{i,t}|z_{t-1} \sim \gamma_{\nu_i}(\varphi_i' z_{t-1}, \mu_i), \quad i = 1, \dots, q.$$

This process is denoted $ARG_\nu(\varphi, \mu)$, where $\nu = [\nu_1, \dots, \nu_q]'$, $\mu = [\mu_1, \dots, \mu_q]'$, and $\varphi = [\varphi_1, \dots, \varphi_q]$.

If z_t follows an $ARG_\nu(\varphi, \mu)$ process, its dynamics admits a vector autoregressive (VAR) representation.

Proposition 3. *If vector z_t follows an $ARG_\nu(\varphi, \mu)$ process (see Def. 3), its log-Laplace transform is affine in z_t. More precisely:*

$$\log \mathbb{E}(\exp(u' z_{t+1})|\underline{z_t}) = a_z(u) + b_z(u)' z_t,$$

where

$$a_z(u) = -\sum_{i=1}^{q} \nu_i \log(1-\mu_i u_i), \quad \textit{and} \quad b_z(u) = \sum_{i=1}^{q} \frac{\mu_i u_i}{1-\mu_i u_i}\varphi_i.$$

Hence process z_t is affine. Its dynamics admits the following (semi-strong) vector autoregressive representation:

$$z_t = \mu_z + \Phi_z z_{t-1} + diag\left(\sqrt{\Gamma_{z,0} + \Gamma'_{z,1} z_{t-1}}\right) \varepsilon_{z,t}, \tag{25}$$

where $\varepsilon_{z,t}$ is a martingale difference sequence whose covariance, conditional on $\underline{z_t}$, is the identity matrix, and where we use the following notations:

$$\mu_z = \mu \odot \nu, \quad \Phi_z = (\mu \mathbf{1}_{q\times 1}) \odot \varphi', \quad \Gamma_{z,0} = (\mu \odot \mu) \odot \nu, \quad \Gamma_{z,1} = 2[(\mu \odot \mu)\mathbf{1}_{q\times 1}] \odot \varphi',$$

denoting the element-wise (Hadamard) product with $\odot$.

Proof. See Monfort et al. (2017). □

Proposition 4. *If z_t follows a multivariate $ARG_\nu(\varphi, \mu)$ (see Def. 3), then:*

$$\mu_{3,t}(\alpha' z_{t+1}) = 2(\alpha^3)'(\nu \odot \mu^3) + 6(\alpha^3)' diag(\mu^3)\varphi' z_t$$
$$\mu_{4,t}(\alpha' z_{t+1}) = 6(\alpha^4)'(\nu \odot \mu^4) + 24(\alpha^4)' diag(\mu^4)\varphi' z_t.$$

Proof. Using Proposition 18, we get $\mu_{3,t}(\alpha' z_{t+1}) = \sum_{i=1}^q \mu_{3,t}(\alpha_i z_{i,t+1}) = \sum_{i=1}^q \alpha_i^3 \mu_{3,t}(z_{i,t+1})$, and $\mu_{4,t}(\alpha' z_{t+1}) = \sum_{i=1}^q \alpha_i^4 \mu_{4,t}(z_{i,t+1})$. The results follow from Proposition 2. □

Appendix C. The extended Y_t vector

This section details the vector Y_t. As explained in Section 3.2, the definition of this vector is guided by the fact that we need, for estimation purposes, the year-on-year inflation rate (see eq. 13) and the year-on-year growth rate of GDP to be affine functions of Y_t.

Consider first the inflation rate. We have:

$$\begin{aligned}
\pi_{t-4,t} &= p_t - p_{t-4} = \sum_{i=0}^{3} \pi_{t-i-1,t-i} \\
&= \rho^{(\pi)} + \delta_T^{(\pi)'} \mathcal{Y}_t + \delta_C^{(\pi)'} (\mathcal{Y}_t - \mathcal{Y}_{t-1}) + \sum_{i=1}^{3} \pi_{t-i-1,t-i} \\
&= \overline{\pi} + \delta'_\pi [\mathcal{Y}_t, \mathcal{Y}_{t-1}, \hat{\pi}_{t-2,t-1}, \hat{\pi}_{t-3,t-2}, \hat{\pi}_{t-4,t-3}]',
\end{aligned}$$

where $\hat{\pi}_{t-1,t}$ denotes the demeaned version of $\pi_{t-1,t}$, i.e., $\hat{\pi}_{t-1,t} := \pi_{t-1,t} - \rho^{(\pi)}$, and where

$$\overline{\pi} = 4\rho^{(\pi)}, \quad \text{and} \quad \delta_\pi = \left[(\delta_T^{(\pi)} + \delta_C^{(\pi)})', (-\delta_C^{(\pi)})', 1, 1, 1\right]'.$$

Turn to the GDP growth rate. The year-on-year GDP is given by $\widetilde{GDP}_t = \sum_{i=0}^{3} GDP_{t-i}$. Its year-on-year growth rate $\Delta y_{t-4,t} := \log(GDP_t/GDP_{t-4})$ can be approximated with

$$\Delta y_{t-4,t} \approx \overline{\Delta y} + \delta'_{\Delta y}[\mathcal{Y}_t, \mathcal{Y}_{t-1}, \Delta\hat{y}_{t-2,t-1}, \ldots, \Delta\hat{y}_{t-4,t-3}]',$$

where $\Delta\hat{y}_{t-1,t}$ is the demeaned version of $\Delta\hat{y}_{t-1,t}$, i.e., $\Delta\hat{y}_{t-1,t} := \Delta y_{t-1,t} - \rho^{(\Delta y)}$, and where

$$\overline{\Delta y} = 4\rho^{(\Delta y)}, \quad \text{and} \quad \delta_{\Delta y} = \frac{1}{4}\left[(\delta_T^{(\Delta y)} + \delta_C^{(\Delta y)})', (-\delta_C^{(\Delta y)})', 1, 1, 1\right]'.$$

What precedes implies that year-on-year inflation and the GDP year-on-year growth rate can be written as approximate linear combinations of Y_t, with:

$$Y_t = [\mathcal{Y}_t, \mathcal{Y}_{t-1}, \hat{\pi}_{t-2,t-1}, \hat{\pi}_{t-3,t-2}, \hat{\pi}_{t-4,t-3}, \Delta\hat{y}_{t-2,t-1}, \ldots, \Delta\hat{y}_{t-4,t-3}]'. \tag{26}$$

More precisely, we have:

$$\begin{bmatrix} \pi_{t-4,t} \\ \Delta y_{t-4,t} \end{bmatrix} \approx \begin{bmatrix} \overline{\pi} \\ \overline{\Delta y} \end{bmatrix} + \begin{bmatrix} \delta^{(\pi)\prime} \\ \delta^{(\Delta y)\prime} \end{bmatrix} Y_t,$$

with

$$\begin{aligned} \delta^{(\pi)} &= \left[(\delta_T^{(\pi)} + \delta_C^{(\pi)})', -(\delta_C^{(\pi)})', 1, 1, 1, 0, 0, 0\right]' \\ \delta^{(\Delta y)} &= \frac{1}{4}\left[(\delta_T^{(\Delta y)} + \delta_C^{(\Delta y)})', (-\delta_C^{(\Delta y)})', 0, 0, 0, 1, 1, 1\right]'. \end{aligned}$$

Note that, in our model, we use $\pi_{t-1,t}$ and $\Delta y_{t-1,t}$ as observables:

$$\begin{bmatrix} \pi_{t-1,t} \\ \Delta y_{t-1,t} \end{bmatrix} = \begin{bmatrix} \rho^{(\pi)} \\ \rho^{(\Delta y)} \end{bmatrix} + \begin{bmatrix} \delta^{(\pi_1)\prime} \\ \delta^{(\Delta y_1)\prime} \end{bmatrix} Y_t,$$

with,

$$\delta^{(\pi_1)} = \begin{bmatrix} \delta_T^{(\pi)} + \delta_C^{(\pi)} \\ -\delta_C^{(\pi)} \\ 0 \\ \vdots \\ 0 \end{bmatrix}, \qquad \delta^{(\Delta y_1)} = \begin{bmatrix} \delta_T^{(\Delta y)} + \delta_C^{(\Delta y)} \\ -\delta_C^{(\Delta y)} \\ 0 \\ \vdots \\ 0 \end{bmatrix}.$$

APPENDIX D. MATRIX REPRESENTATION OF THE MODEL

This appendix expands the different matrices that characterize the dynamics of $X_t = [Y_t', z_t']'$, whose VAR representation is given in (18). We consider the specific model described in Section 3.2.

D.1. **Process Y_t.** Considering the dynamics (15) of $\mathcal{Y}_t$, and since Y_t is defined in (26), it comes that Y_t follows

$$Y_t = \Phi_Y Y_{t-1} + \Theta(z_t - \bar{z}) + \text{diag}\left(\sqrt{\Gamma_{Y,0} + \Gamma_{Y,1}' z_t}\right) \varepsilon_{\mathcal{Y},t}, \quad \varepsilon_{\mathcal{Y},t} \sim \textit{i.i.d.}\, \mathcal{N}(0,\, I_d), \tag{27}$$

where Φ_Y, $\Gamma_{Y,0}$, and $\Gamma_{Y,1}$ depend on $\Phi_{\mathcal{Y}}$, $\Gamma_{\mathcal{Y},0}$, and $\Gamma_{\mathcal{Y},1}$ (characterizing eq. 15), specifically:

$$\Phi_Y = \begin{bmatrix} \Phi_{\mathcal{Y}} & 0_{m\times m} & 0_{m\times 2} & 0_{m\times 1} & 0_{m\times 2} & 0_{m\times 1} \\ I_{d_{m\times m}} & 0_{m\times m} & 0_{m\times 2} & 0_{m\times 1} & 0_{m\times 2} & 0_{m\times 1} \\ \left(\delta_T^{(\pi)} + \delta_C^{(\pi)}\right) & -\delta_C^{(\pi)} & 0_{1\times 2} & 0_{1\times 1} & 0_{1\times 2} & 0_{1\times 1} \\ 0_{2\times m} & 0_{2\times m} & I_{d_{2\times 2}} & 0_{2\times 1} & 0_{2\times 2} & 0_{2\times 1} \\ \left(\delta_T^{(\Delta y)} + \delta_C^{(\Delta y)}\right) & -\delta_C^{(\Delta y)} & 0_{1\times 2} & 0_{1\times 1} & 0_{1\times 2} & 0_{1\times 1} \\ 0_{2\times m} & 0_{2\times m} & 0_{2\times 2} & 0_{2\times 1} & I_{d_{2\times 2}} & 0_{2\times 1} \end{bmatrix},$$

and

$$\Gamma_{Y,0} = \begin{bmatrix} \Gamma_{\mathcal{Y},0} \\ 0_{(m+6)\times 1} \end{bmatrix}, \quad \Gamma_{Y,1}' = \begin{bmatrix} \Gamma_{\mathcal{Y},1}' \\ 0_{(m+6)\times q} \end{bmatrix}.$$

D.2. **Process X_t.** The state vector $X_t = [Y_t', z_t']'$ follows an affine process whose semi-strong VAR representation is given in (18). In the latter, matrices μ_X, Φ_X, and function Σ_X are given by:

$$\mu_X = \begin{bmatrix} -\Theta\Phi_z(I_d - \Phi_z)^{-1}\mu_z \\ \mu_z \end{bmatrix}, \quad \Phi_X = \begin{bmatrix} \Phi_Y & \Theta\Phi_z \\ 0 & \Phi_z \end{bmatrix}, \tag{28}$$

where μ_z and Φ_z are given in Proposition 3, Φ_Y is given in Subsection D.1, and

$$\Sigma_X(z_{t-1})\Sigma_X(z_{t-1})' = \begin{bmatrix} \Sigma_{11}(z_{t-1}) & \Sigma_{12}(z_{t-1}) \\ \Sigma_{12}(z_{t-1})' & \Sigma_{22}(z_{t-1}) \end{bmatrix}, \tag{29}$$

with

$$\begin{cases} \Sigma_{11}(z_{t-1}) &= \Theta \text{diag}\left(\Gamma_{z,0} + \Gamma_{z,1}' z_{t-1}\right)\Theta' + \text{diag}\left(\Gamma_{Y,0} + \Gamma_{Y,1}'(\mu_z + \Phi_z z_{t-1})\right), \\ \Sigma_{22}(z_{t-1}) &= \text{diag}\left(\Gamma_{z,0} + \Gamma_{z,1}' z_{t-1}\right), \\ \Sigma_{12}(z_{t-1}) &= \Theta\Sigma_{22}(z_{t-1}), \end{cases}$$

where $\Gamma_{z,0}$ and $\Gamma_{z,1}$ are given in Proposition 3, and $\Gamma_{Y,0}$ and $\Gamma_{Y,1}$ are given in Subsection D.1.

D.3. **Parameterization of the model presented in Subsection 3.3.** The general representation of the dynamics of $\mathcal{Y}_t$ is given in (15). Subsection 3.3 presents the specification retained in our empirical analysis. The present subsection details the matrices $\Phi_\mathcal{Y}$, Θ, $\Gamma_{\mathcal{Y},0}$, and $\Gamma_{\mathcal{Y},1}$ that prevail in the context of Subsection 3.3. We have:

$$\Phi_\mathcal{Y} = \begin{bmatrix} \phi_{1,1} & 0 & 0 & 0 \\ 0 & \phi_{2,2} & 0 & 0 \\ 0 & 0 & \phi_{3,3} & 0 \\ 0 & 0 & 0 & \phi_{4,4} \end{bmatrix}, \quad \Theta = \begin{bmatrix} \theta^s & -\theta^s & 0 & 0 & 0 \\ 0 & 0 & \theta^d & -\theta^d & 0 \\ 0 & 0 & 0 & 0 & 0 \\ \vdots & \vdots & \vdots & \vdots & \vdots \\ 0 & 0 & 0 & 0 & 0 \end{bmatrix},$$

$$\Gamma_{\mathcal{Y},0} = \begin{bmatrix} \Gamma_{1,\mathcal{Y},0} \\ \Gamma_{2,\mathcal{Y},0} \\ \Gamma_{3,\mathcal{Y},0} \\ \Gamma_{4,\mathcal{Y},0} \end{bmatrix}, \quad \text{and} \quad \Gamma'_{\mathcal{Y},1} = \begin{bmatrix} 0 & 0 & 0 & 0 & 0 \\ 0 & 0 & 0 & 0 & 0 \\ 0 & 0 & 0 & 0 & \Gamma_{[3,5],\mathcal{Y},1} \\ 0 & 0 & 0 & 0 & \Gamma_{[4,5],\mathcal{Y},1} \end{bmatrix}.$$

Besides, the specific model described in Subsection 3.3 also implies that the vector autoregressive gamma process z_t is characterized by:

$$\varphi = \begin{bmatrix} \varphi_p^s & 0 & 0 & 0 & 0 \\ 0 & \varphi_n^s & 0 & 0 & 0 \\ 0 & 0 & \varphi_p^d & 0 & 0 \\ 0 & 0 & 0 & \varphi_n^d & 0 \\ 0 & 0 & 0 & 0 & \varphi_v \end{bmatrix}, \quad \text{and} \quad \nu = \begin{bmatrix} \nu_p^s \\ \nu_n^s \\ \nu_p^d \\ \nu_n^d \\ \nu_v \end{bmatrix}.$$

Moreover, the specification presented in Subsection 3.3 is such that the δ vectors— that relate the components of $\mathcal{Y}_t$ to the trend and cyclical parts of the GDP and of the price index (see eqs. 9 and 10)—are as follows:

$$\delta_T^{(\pi)} = \begin{bmatrix} 0 \\ 0 \\ \delta_{3,T}^{(\pi)} \\ \delta_{4,T}^{(\pi)} \end{bmatrix}, \quad \delta_C^{(\pi)} = \begin{bmatrix} -1 \\ +\delta_{2,C}^{(\pi)} \\ \delta_{3,C}^{(\pi)} \\ \delta_{4,C}^{(\pi)} \end{bmatrix}, \quad \delta_T^{(\Delta y)} = \begin{bmatrix} 0 \\ 0 \\ \delta_{3,T}^{(\Delta y)} \\ \delta_{4,T}^{(\Delta y)} \end{bmatrix}, \quad \delta_C^{(\Delta y)} = \begin{bmatrix} +\delta_{1,C}^{(\Delta y)} \\ 1 \\ 1 \\ 1 \end{bmatrix}.$$

Some of the parameters of the previous vectors are equal to one (or minus) for identification reasons.

Appendix E. Computing the multi-horizon conditional moments of X_t

This appendix details the computation of the first- to fourth-order multi-horizon conditional moments of vector X_t, whose dynamics is presented in Subsection 3.2 (see also Appendix D for details regarding the matrices defining the dynamics of the state vector). Subsection E.1 provides recursive formulas to compute the multi-horizon conditional moments of a

generic affine process. Subsection E.2 focuses on the state vector X_t considered in the present paper (see Subsection 3.2).

E.1. **First- to fourth-order multi-horizon conditional moments of a generic affine process.** In this appendix, we derive the multi-horizon conditional moments of a generic affine process X_t (based on its one-period-ahead conditional moments).

Proposition 5. *Consider a vector affine process X_t that is such that:*

$$\mathbb{E}_t(u'X_{t+1}) = \alpha_1(u) + \beta_1(u)'X_t.$$

Then, we have:

$$\mathbb{E}_t\left(\sum_{i=1}^{h}\gamma_i'X_{t+i}\right) = \alpha_h(\gamma_1,\ldots,\gamma_h) + \beta_h(\gamma_1,\ldots,\gamma_h)'X_t,$$

with

$$\begin{cases}\alpha_h(\gamma_1,\ldots,\gamma_h) = \alpha_{h-1}(\gamma_2,\ldots,\gamma_h) + \alpha_1(\gamma_1 + \beta_{h-1}(\gamma_2,\ldots,\gamma_h))\\ \beta_h(\gamma_1,\ldots,\gamma_h) = \beta_1(\gamma_1 + \beta_{h-1}(\gamma_2,\ldots,\gamma_h)).\end{cases}$$

Proof. We have:

$$\begin{aligned}\mathbb{E}_t\left(\sum_{i=1}^{h}\gamma_i'X_{t+i}\right) &= \mathbb{E}_t\left(\mathbb{E}_{t+1}\left[\sum_{i=1}^{h}\gamma_i'X_{t+i}\right]\right) = \mathbb{E}_t\left(\gamma_1'X_{t+1} + \mathbb{E}_{t+1}\left[\sum_{i=2}^{h}\gamma_i'X_{t+i}\right]\right)\\ &= \mathbb{E}_t\left(\gamma_1'X_{t+1} + \alpha_{h-1}(\gamma_2,\ldots,\gamma_h) + \beta_{h-1}(\gamma_2,\ldots,\gamma_h)'X_{t+1}\right)\\ &= \alpha_{h-1}(\gamma_2,\ldots,\gamma_h) + \alpha_1(\gamma_1 + \beta_{h-1}(\gamma_2,\ldots,\gamma_h))\\ &\quad + \beta_1(\gamma_1 + \beta_{h-1}(\gamma_2,\ldots,\gamma_h))'X_t,\end{aligned}$$

which leads to the result. □

Proposition 6. *Consider a vector affine process X_t that is such that*

$$\mathbb{E}_t(u'X_{t+1}) = \alpha_1(u) + \beta_1(u)'X_t, \quad \textit{and} \quad \mathbb{V}_t(u'X_{t+1}) = \dot{\alpha}_1(u) + \dot{\beta}_1(u)'X_t.$$

Then, for $h \geq 2$:

$$\mathbb{V}_t\left(\sum_{i=1}^{h}\gamma_i' X_{t+i}\right) = \dot{\alpha}_h(\gamma_1,\ldots,\gamma_h) + \dot{\beta}_h(\gamma_1,\ldots,\gamma_h)' X_t,$$

with

$$\begin{cases} \dot{\alpha}_h(\gamma_1,\ldots,\gamma_h) = \dot{\alpha}_1(\gamma_1 + \beta_{h-1}(\gamma_2,\ldots,\gamma_h)) + \dot{\alpha}_{h-1}(\gamma_2,\ldots,\gamma_h) \\ \qquad\qquad\qquad + \alpha_1(\dot{\beta}_{h-1}(\gamma_2,\ldots,\gamma_h)) \\ \dot{\beta}_h(\gamma_1,\ldots,\gamma_h) = \dot{\beta}_1(\gamma_1 + \beta_{h-1}(\gamma_2,\ldots,\gamma_h)) + \beta_1(\dot{\beta}_{h-1}(\gamma_2,\ldots,\gamma_h)). \end{cases}$$

Proof. We have:

$$\begin{aligned} \mathbb{V}_t\left(\sum_{i=1}^{h}\gamma_i' X_{t+i}\right) &= \mathbb{V}_t\left(\mathbb{E}_{t+1}\left[\sum_{i=1}^{h}\gamma_i' X_{t+i}\right]\right) + \mathbb{E}_t\left(\mathbb{V}_{t+1}\left[\sum_{i=1}^{h}\gamma_i' X_{t+i}\right]\right) \\ &= \mathbb{V}_t\left(\gamma_1' X_{t+1} + \mathbb{E}_{t+1}\left[\sum_{i=2}^{h}\gamma_i' X_{t+i}\right]\right) + \mathbb{E}_t\left(\mathbb{V}_{t+1}\left[\sum_{i=2}^{h}\gamma_i' X_{t+i}\right]\right). \end{aligned}$$

That is:

$$\begin{aligned} \mathbb{V}_t\left(\sum_{i=1}^{h}\gamma_i' X_{t+i}\right) &= \mathbb{V}_t\left(\gamma_1' X_{t+1} + \alpha_{h-1}(\gamma_2,\ldots,\gamma_h) + \beta_{h-1}(\gamma_2,\ldots,\gamma_h)' X_{t+1}\right) \\ &\quad + \mathbb{E}_t\left(\dot{\alpha}_{h-1}(\gamma_2,\ldots,\gamma_h) + \dot{\beta}_{h-1}(\gamma_2,\ldots,\gamma_h)' X_{t+1}\right) \\ &= \dot{\alpha}_1(\gamma_1 + \beta_{h-1}(\gamma_2,\ldots,\gamma_h)) + \dot{\beta}_1(\gamma_1 + \beta_{h-1}(\gamma_2,\ldots,\gamma_h))' X_t \\ &\quad + \dot{\alpha}_{h-1}(\gamma_2,\ldots,\gamma_h) + \alpha_1(\dot{\beta}_{h-1}(\gamma_2,\ldots,\gamma_h)) \\ &\quad + \beta_1(\dot{\beta}_{h-1}(\gamma_2,\ldots,\gamma_h))' X_{t+1}, \end{aligned}$$

which leads to the result. □

Proposition 7. *Consider a vector affine process X_t that is such that*

$$\begin{aligned}
\mathbb{E}_t(u'X_{t+1}) &= \alpha_1(u) + \beta_1(u)'X_t, \\
\mathbb{V}_t(u'X_{t+1}) &= \dot{\alpha}_1(u) + \dot{\beta}_1(u)'X_t, \\
\mu_{3,t}(u'X_{t+1}) &= \ddot{\alpha}_1(u) + \ddot{\beta}_1(u)'X_t.
\end{aligned}$$

We also use the following notation:

$$vec\Big(\mathbb{V}_t(X_{t+1})\Big) = \Lambda_0 + \Lambda_1 X_t. \tag{30}$$

Then, for $h \geq 2$:

$$\mu_{3,t}\left(\sum_{i=1}^{h} \gamma_i' X_{t+i}\right) = \ddot{\alpha}_h(\gamma_1, \ldots, \gamma_h) + \ddot{\beta}_h(\gamma_1, \ldots, \gamma_h)'X_t,$$

with

$$\begin{cases}
\ddot{\alpha}_h(\gamma_1, \ldots, \gamma_h) = \ddot{\alpha}_{h-1}(\gamma_2, \ldots, \gamma_h) + \alpha_1(\ddot{\beta}_{h-1}(\gamma_2, \ldots, \gamma_h)) + \ddot{\alpha}_1(\beta_{h-1}(\gamma_2, \ldots, \gamma_h) + \gamma_1) \\
\qquad\qquad + 3\left(\dot{\beta}_{h-1}(\gamma_2, \ldots, \gamma_h) \otimes \Big[\gamma_1 + \beta_{h-1}(\gamma_2, \ldots, \gamma_h)\Big]\right)' \Lambda_0 \\
\ddot{\beta}_h(\gamma_1, \ldots, \gamma_h) = \beta_1(\ddot{\beta}_{h-1}(\gamma_2, \ldots, \gamma_h)) + \ddot{\beta}_1(\beta_{h-1}(\gamma_2, \ldots, \gamma_h) + \gamma_1) \\
\qquad\qquad + 3\Lambda_1'\left(\dot{\beta}_{h-1}(\gamma_2, \ldots, \gamma_h) \otimes \Big[\gamma_1 + \beta_{h-1}(\gamma_2, \ldots, \gamma_h)\Big]\right).
\end{cases}$$

Proof. By the law of total cumulance (see Prop. 19), we have:

$$\begin{aligned}
\mu_{3,t}\left(\sum_{i=1}^{h} \gamma_i' X_{t+i}\right) = \mathbb{E}_t\left(\mu_{3,t+1}\left[\sum_{i=1}^{h} \gamma_i' X_{t+i}\right]\right) + \mu_{3,t}\left(\mathbb{E}_{t+1}\left[\sum_{i=1}^{h} \gamma_i' X_{t+i}\right]\right) \\
+ 3\mathbb{C}ov_t\left(\mathbb{E}_{t+1}\left[\sum_{i=1}^{h} \gamma_i' X_{t+i}\right], \mathbb{V}_{t+1}\left[\sum_{i=1}^{h} \gamma_i' X_{t+i}\right]\right).
\end{aligned}$$

That is:

$$\begin{aligned}\mu_{3,t}\left(\sum_{i=1}^{h}\gamma_i'X_{t+i}\right) &= \mathbb{E}_t\left(\mu_{3,t+1}\left[\sum_{i=2}^{h}\gamma_i'X_{t+i}\right]\right)+\mu_{3,t}\left(\gamma_1'X_{t+1}+\mathbb{E}_{t+1}\left[\sum_{i=2}^{h}\gamma_i'X_{t+i}\right]\right)\\ &\quad+3\mathbb{C}ov_t\Bigg(\Big[\gamma_1'X_{t+1}+\alpha_{h-1}(\gamma_2,\ldots,\gamma_h)+\beta_{h-1}(\gamma_2,\ldots,\gamma_h)'X_{t+1}\Big],\\ &\qquad\Big[\dot\alpha_{h-1}(\gamma_2,\ldots,\gamma_h)+\dot\beta_{h-1}(\gamma_2,\ldots,\gamma_h)'X_{t+1}\Big]\Bigg)\\ &= \mathbb{E}_t\left(\ddot\alpha_{h-1}(\gamma_2,\ldots,\gamma_h)+\ddot\beta_{h-1}(\gamma_2,\ldots,\gamma_h)'X_{t+1}\right)\\ &\quad+\mu_{3,t}\Big(\gamma_1'X_{t+1}+\alpha_{h-1}(\gamma_2,\ldots,\gamma_h)+\beta_{h-1}(\gamma_2,\ldots,\gamma_h)'X_{t+1}\Big)\\ &\quad+3\Big(\gamma_1+\beta_{h-1}(\gamma_2,\ldots,\gamma_h)\Big)'\mathbb{V}_t(X_{t+1})\dot\beta_{h-1}(\gamma_2,\ldots,\gamma_h).\end{aligned}$$

Using $vec(PQR)=(R'\otimes P)vec(Q)$ for the last term (that is a scalar), we have:

$$\begin{aligned}&\Big(\gamma_1+\beta_{h-1}(\gamma_2,\ldots,\gamma_h)\Big)'\mathbb{V}_t(X_{t+1})\dot\beta_{h-1}(\gamma_2,\ldots,\gamma_h)\\ &=\left(\dot\beta_{h-1}(\gamma_2,\ldots,\gamma_h)'\otimes\Big[\gamma_1+\beta_{h-1}(\gamma_2,\ldots,\gamma_h)\Big]'\right)vec\Big(\mathbb{V}_t(X_{t+1})\Big).\end{aligned}$$

This gives:

$$\begin{aligned}\mu_{3,t}\left(\sum_{i=1}^{h}\gamma_i'X_{t+i}\right) &= \ddot\alpha_{h-1}(\gamma_2,\ldots,\gamma_h)+\alpha_1(\ddot\beta_{h-1}(\gamma_2,\ldots,\gamma_h))+\beta_1(\ddot\beta_{h-1}(\gamma_2,\ldots,\gamma_h))'X_t\\ &\quad+\ddot\alpha_1(\beta_{h-1}(\gamma_2,\ldots,\gamma_h)+\gamma_1)+\ddot\beta_1(\beta_{h-1}(\gamma_2,\ldots,\gamma_h)+\gamma_1)'X_t\\ &\quad+3\left(\dot\beta_{h-1}(\gamma_2,\ldots,\gamma_h)\otimes\Big[\gamma_1+\beta_{h-1}(\gamma_2,\ldots,\gamma_h)\Big]\right)'\Big(\Lambda_0+\Lambda_1X_t\Big),\end{aligned}$$

which leads to the result. □

Proposition 8. *Consider a vectorial affine process X_t that is such that*

$$\begin{aligned}
\mathbb{E}_t(u'X_{t+1}) &= \alpha_1(u) + \beta_1(u)'X_t, \\
\mathbb{V}_t(u'X_{t+1}) &= \dot{\alpha}_1(u) + \dot{\beta}_1(u)'X_t, \\
\mu_{3,t}(u'X_{t+1}) &= \ddot{\alpha}_1(u) + \ddot{\beta}_1(u)'X_t \\
\mu_{4,t}\left(u'X_{t+1}\right) &= \dddot{\alpha}_1(u) + \dddot{\beta}_1(u)'X_t.
\end{aligned}$$

We also use the following notations:

$$\left\{\begin{array}{rcl}
vec\Big(\mathbb{V}_t(X_{t+1})\Big) &=& \Lambda_0 + \Lambda_1 X_t \\
vec\Big(\mu_{3,t}(X_{t+1})\Big) &=& M_0 + M_1 X_t.
\end{array}\right. \tag{31}$$

Then, we have, for $h \geq 2$:

$$\mu_{4,t}\left(\sum_{i=1}^{h} \gamma_i' X_{t+i}\right) = \dddot{\alpha}_h(\gamma_1, \ldots, \gamma_h) + \dddot{\beta}_h(\gamma_1, \ldots, \gamma_h)'X_t,$$

with

$$\left\{\begin{array}{l}
\dddot{\alpha}_h(\gamma_1, \ldots, \gamma_h) = \dddot{\alpha}_{h-1}(\gamma_2, \ldots, \gamma_h) + \alpha_1(\dddot{\beta}_{h-1}(\gamma_2, \ldots, \gamma_h)) + \ddot{\alpha}_1(\beta_{h-1}(\gamma_2, \ldots, \gamma_h) + \gamma_1) \\
\qquad + 4\left(\ddot{\beta}_{h-1}(\gamma_2, \ldots, \gamma_h) \otimes \Big[\beta_{h-1}(\gamma_2, \ldots, \gamma_h) + \gamma_1\Big]\right)' \Lambda_0 \\
\qquad + 3\dot{\alpha}_1(\dot{\beta}_{h-1}(\gamma_2, \ldots, \gamma_h)) + 6\Big((\beta_{h-1} + \gamma_1) \otimes (\dot{\beta}_{h-1} \otimes (\beta_{h-1} + \gamma_1))\Big)' M_0 \\
\dddot{\beta}_h(\gamma_1, \ldots, \gamma_h) = \beta_1(\dddot{\beta}_{h-1}(\gamma_2, \ldots, \gamma_h)) + \dddot{\beta}_1(\beta_{h-1}(\gamma_2, \ldots, \gamma_h) + \gamma_1) \\
\qquad 4\Lambda_1'\left(\ddot{\beta}_{h-1}(\gamma_2, \ldots, \gamma_h) \otimes \Big[\beta_{h-1}(\gamma_2, \ldots, \gamma_h) + \gamma_1\Big]\right) \\
\qquad + 3\dot{\beta}_1(\dot{\beta}_{h-1}(\gamma_2, \ldots, \gamma_h)) + 6M_1'\Big((\beta_{h-1} + \gamma_1) \otimes (\dot{\beta}_{h-1} \otimes (\beta_{h-1} + \gamma_1))\Big).
\end{array}\right.$$

Proof. By the Law of total cumulance, we have:

$$\begin{aligned}\mu_{4,t}\left(\sum_{i=1}^{h}\gamma_i'X_{t+i}\right) &= \mathbb{E}_t\left(\mu_{4,t+1}\left[\sum_{i=1}^{h}\gamma_i'X_{t+i}\right]\right)+\mu_{4,t}\left(\mathbb{E}_{t+1}\left[\sum_{i=1}^{h}\gamma_i'X_{t+i}\right]\right)\\ &\quad+4\mathbb{C}ov_t\left(\mu_{3,t+1}\left[\sum_{i=1}^{h}\gamma_i'X_{t+i}\right],\mathbb{E}_{t+1}\left[\sum_{i=1}^{h}\gamma_i'X_{t+i}\right]\right)\\ &\quad+3\mathbb{V}_t\left(\mathbb{V}_{t+1}\left[\sum_{i=1}^{h}\gamma_i'X_{t+i}\right]\right)\\ &\quad+6\kappa_t\left(\mathbb{V}_{t+1}\left[\sum_{i=1}^{h}\gamma_i'X_{t+i}\right],\mathbb{E}_{t+1}\left[\sum_{i=1}^{h}\gamma_i'X_{t+i}\right],\mathbb{E}_{t+1}\left[\sum_{i=1}^{h}\gamma_i'X_{t+i}\right]\right).\end{aligned}$$

Let's examine each term in turn.

First:

$$\begin{aligned}\mathbb{E}_t\left(\mu_{4,t+1}\left[\sum_{i=1}^{h}\gamma_i'X_{t+i}\right]\right) &= \mathbb{E}_t\left(\mu_{4,t+1}\left[\sum_{i=2}^{h}\gamma_i'X_{t+i}\right]\right)\\ &= \mathbb{E}_t\left(\ddot{\alpha}_{h-1}(\gamma_2,\ldots,\gamma_h)+\dddot{\beta}_{h-1}(\gamma_2,\ldots,\gamma_h)X_{t+1}\right)\\ &= \ddot{\alpha}_{h-1}(\gamma_2,\ldots,\gamma_h)+\alpha_1(\dddot{\beta}_{h-1}(\gamma_2,\ldots,\gamma_h))\\ &\quad+\beta_1(\dddot{\beta}_{h-1}(\gamma_2,\ldots,\gamma_h))'X_t.\end{aligned}$$

Second:

$$\begin{aligned}\mu_{4,t}\left(\mathbb{E}_{t+1}\left[\sum_{i=1}^{h}\gamma_i'X_{t+i}\right]\right) &= \mu_{4,t}\left(\gamma_1'X_{t+1}+\mathbb{E}_{t+1}\left[\sum_{i=2}^{h}\gamma_i'X_{t+i}\right]\right)\\ &= \mu_{4,t}\Big(\gamma_1'X_{t+1}+\alpha_{h-1}(\gamma_2,\ldots,\gamma_h)+\beta_{h-1}(\gamma_2,\ldots,\gamma_h)'X_{t+1}\Big)\\ &= \ddot{\alpha}_1(\beta_{h-1}(\gamma_2,\ldots,\gamma_h)+\gamma_1)+\dddot{\beta}_1(\beta_{h-1}(\gamma_2,\ldots,\gamma_h)+\gamma_1)'X_t.\end{aligned}$$

Third:

$$\begin{aligned}
& 4\mathbb{C}ov_t\left(\mu_{3,t+1}\left[\sum_{i=1}^{h}\gamma_i' X_{t+i}\right], \mathbb{E}_{t+1}\left[\sum_{i=1}^{h}\gamma_i' X_{t+i}\right]\right) \\
= \; & 4\mathbb{C}ov_t\left(\ddot{\beta}_{h-1}(\gamma_2,\ldots,\gamma_h)X_{t+1}, (\beta_{h-1}(\gamma_2,\ldots,\gamma_h)+\gamma_1)X_{t+1}\right) \\
= \; & 4\Big(\beta_{h-1}(\gamma_2,\ldots,\gamma_h)+\gamma_1\Big)'\mathbb{V}_t(X_{t+1})\ddot{\beta}_{h-1}(\gamma_2,\ldots,\gamma_h) \\
= \; & 4\left(\ddot{\beta}_{h-1}(\gamma_2,\ldots,\gamma_h)\otimes\Big[\beta_{h-1}(\gamma_2,\ldots,\gamma_h)+\gamma_1\Big]\right)'\Big(\Lambda_0+\Lambda_1 X_t\Big).
\end{aligned}$$

Fourth:

$$\begin{aligned}
3\mathbb{V}_t\left(\mathbb{V}_{t+1}\left[\sum_{i=1}^{h}\gamma_i' X_{t+i}\right]\right) &= 3\mathbb{V}_t\left(\mathbb{V}_{t+1}\left[\sum_{i=2}^{h}\gamma_i' X_{t+i}\right]\right) \\
&= 3\mathbb{V}_t\left(\dot{\alpha}_{h-1}(\gamma_2,\ldots,\gamma_h)+\dot{\beta}_{h-1}(\gamma_2,\ldots,\gamma_h)X_{t+1}\right) \\
&= 3\left(\dot{\alpha}_1(\dot{\beta}_{h-1}(\gamma_2,\ldots,\gamma_h))+\dot{\beta}_1(\dot{\beta}_{h-1}(\gamma_2,\ldots,\gamma_h))'X_t\right).
\end{aligned}$$

Fifth:

$$\begin{aligned}
& 6\kappa_t\left(\mathbb{V}_{t+1}\left[\sum_{i=1}^{h}\gamma_i' X_{t+i}\right], \mathbb{E}_{t+1}\left[\sum_{i=1}^{h}\gamma_i' X_{t+i}\right], \mathbb{E}_{t+1}\left[\sum_{i=1}^{h}\gamma_i' X_{t+i}\right]\right) \\
= \; & 6\kappa_t\left(\dot{\beta}_{h-1}' X_{t+1}, (\beta_{h-1}+\gamma_1)' X_{t+1}), (\beta_{h-1}+\gamma_1)' X_{t+1})\right) \\
= \; & 6(\dot{\beta}_{h-1}\otimes(\beta_{h-1}+\gamma_1))'\mu_{3,t}(X_{t+1})(\beta_{h-1}+\gamma_1) \\
= \; & 6(\beta_{h-1}+\gamma_1)'\otimes(\dot{\beta}_{h-1}\otimes(\beta_{h-1}+\gamma_1))'vec(\mu_{3,t}(X_{t+1})) \\
= \; & 6(\beta_{h-1}+\gamma_1)'\otimes(\dot{\beta}_{h-1}\otimes(\beta_{h-1}+\gamma_1))'(M_0+M_1 X_t).
\end{aligned}$$

This leads to the result. □

E.2. **First- to fourth-order conditional moments of X_t.** In this subsection, we derive quasi-analytical formulas to compute the first- to fourth-order conditional moments of vector X_t in the context of the model described in Section 3. The expanded representation of the different

matrices involved in the formulas is given in Appendix D.

Proposition 9. *In the context of the model defined in Section 3, $\mathbb{E}_t(X_{t+h})$ is affine in X_t, that is:*

$$\mathbb{E}_t(X_{t+h}) = a_h + b_h X_t,$$

with:

$$\begin{cases} a_h &= (I - \Phi_X)^{-1}(I - \Phi_X^h)\mu_X \\ b_h &= \Phi_X^h, \end{cases}$$

where μ_X and Φ_X are defined in (28).

Proof. Given (18), we have:

$$\mathbb{E}_t(X_{t+h}) = \mu_X + \Phi_X\mu_X + \cdots + \Phi_X^{h-1}\mu_X + \Phi_X^h X_t,$$

which leads to the result. □

Corollary 1. *In the context of the model defined in Section 3, $\mathbb{E}_t(\gamma' X_{t+1})$ is affine in X_t. More precisely:*

$$\mathbb{E}_t(\gamma' X_{t+1}) = \alpha_1(\gamma) + \beta_1(\gamma)' X_t.$$

with

$$\alpha_1(\gamma) = \gamma'\mu_X \quad \textit{and} \quad \beta_1(\gamma) = \Phi_X'\gamma,$$

μ_X and Φ_X being defined in (28).

Proposition 10. *In the context of the model defined in Section 3, $\mathbb{V}_t(\gamma' X_{t+1})$ is affine in X_t. More precisely:*

$$\mathbb{V}_t(\gamma' X_{t+1}) = \dot{\alpha}_1(\gamma) + \dot{\beta}_1(\gamma)' X_t,$$

with

$$\begin{cases} \dot{\alpha}_1(\gamma) &= (\gamma_Y \otimes \gamma_Y)' \left[(\Theta \otimes \Theta) S_q \Gamma_{z,0} + S_n \Gamma_{Y,0} + S_n \Gamma'_{Y,1} \mu_z \right] \\ & \quad + (\gamma_z \otimes \gamma_z)' S_q \Gamma_{z,0} + 2(\gamma_z \otimes \gamma_Y)' (I_q \otimes \Theta) S_q \Gamma_{z,0} \\ \dot{\beta}_1(\gamma) &= \Pi' \Big((\gamma_Y \otimes \gamma_Y)' \left[(\Theta \otimes \Theta) S_q \Gamma'_{z,1} + S_n \Gamma'_{Y,1} \Phi_z \right] + (\gamma_z \otimes \gamma_z)' S_q \Gamma'_{z,1} \\ & \quad + 2(\gamma_z \otimes \gamma_Y)' (I_q \otimes \Theta) S_q \Gamma'_{z,1} \Big)', \end{cases}$$

with $\gamma = [\gamma'_Y, \gamma'_z]'$*, where* Π *is such that* $z_t = \Pi X_t$*, that is* $\Pi = [\ \mathbf{0}_{q \times n} \quad Id_{q \times q}\ ]$*, and where* S_p *is an* $p^2 \times p$ *matrix that is such that* $vec(M) = S_p diag(M)$ *for a diagonal matrix* M *of dimension* p*. Specifically:*

$$S_p = \sum_{i=1}^{p} \left[e_i^{(p)} \otimes e_i^{(p)} \right] e_i^{(p)'},$$

where $e_i^{(p)}$ *is* i^{th} *column of the identity matrix of dimension* $p \times p$*.*

Proof. We have:

$$\begin{aligned} \mathbb{V}_t \left(\gamma' X_{t+1} \right) &= \mathbb{V}_t \left(\gamma'_Y Y_{t+1} + \gamma'_z z_{t+1} \right) \\ &= \mathbb{V}_t \left(\gamma'_Y Y_{t+1} \right) + \mathbb{V}_t \left(\gamma'_z z_{t+1} \right) + 2\mathbb{C}ov_t \left(\gamma'_Y Y_{t+1}, \gamma'_z z_{t+1} \right). \end{aligned}$$

Let's now focus on each of the three terms above. Consider the first term:

$$\begin{aligned} \mathbb{V}_t \left(\gamma'_Y Y_{t+1} \right) &= \mathbb{E}_t \left(\mathbb{V}_t \left[\gamma'_Y Y_{t+1} | z_{t+1} \right] \right) + \mathbb{V}_t \left(\mathbb{E}_t \left[\gamma'_Y Y_{t+1} | z_{t+1} \right] \right) \\ &= \mathbb{E}_t \left(\mathbb{V}_t \left[\gamma'_Y (\Phi_Y Y_t + \Theta(z_{t+1} - \bar{z}) + \text{diag} \left(\sqrt{\Gamma_{Y,0} + \Gamma'_{Y,1} z_{t+1}} \right) \varepsilon_{Y,t+1}) | z_{t+1} \right] \right) \\ &\quad + \mathbb{V}_t \left(\mathbb{E}_t \left[\gamma'_Y (\Phi_Y Y_t + \Theta(z_{t+1} - \bar{z}) + \text{diag} \left(\sqrt{\Gamma_{Y,0} + \Gamma'_{Y,1} z_{t+1}} \right) \varepsilon_{Y,t+1}) | z_{t+1} \right] \right) \\ &= \mathbb{E}_t \left(\gamma'_Y \text{diag} \left(\Gamma_{Y,0} + \Gamma'_{Y,1} z_{t+1} \right) \gamma_Y \right) + \mathbb{V}_t \left(\gamma'_Y \Theta z_{t+1} \right). \end{aligned}$$

That is:

$$\begin{aligned}\mathbb{V}_t\left(\gamma_Y' Y_{t+1}\right) &= \mathbb{E}_t\Big((\gamma_Y' \otimes \gamma_Y') vec\left(\text{diag}(\Gamma_{Y,0} + \Gamma_{Y,1}' z_{t+1})\right)\Big) \\ &\quad + \Big((\gamma_Y'\Theta) \otimes (\gamma_Y'\Theta)\Big) vec\left(\text{diag}(\Gamma_{z,0} + \Gamma_{z,1}' z_t)\right) \\ &= (\gamma_Y' \otimes \gamma_Y') S_n\left(\Gamma_{Y,0} + \Gamma_{Y,1}\mathbb{E}_t(z_{t+1})\right) + \left((\gamma_Y'\Theta) \otimes (\gamma_Y'\Theta)\right) S_q\left(\Gamma_{z,0} + \Gamma_{z,1}' z_t\right) \\ &= (\gamma_Y \otimes \gamma_Y)' S_n\left(\Gamma_{Y,0} + \Gamma_{Y,1}(\mu_z + \phi_z z_t)\right) + \left((\gamma_Y \otimes \gamma_Y)'(\Theta \otimes \Theta)\right) S_q\left(\Gamma_{z,0} + \Gamma_{z,1}' z_t\right).\end{aligned}$$

The second term can also be simplified as follows:

$$\mathbb{V}_t\left(\gamma_z' z_{t+1}\right) = (\gamma_z' \otimes \gamma_z') vec\left(\text{diag}(\Gamma_{z,0} + \Gamma_{z,1}' z_t)\right) = (\gamma_z \otimes \gamma_z)' S_q\left(\Gamma_{z,0} + \Gamma_{z,1}' z_t\right).$$

Finally, the last term can be written as:

$$\begin{aligned}2\mathbb{C}ov_t\left(\gamma_Y' Y_{t+1}, \gamma_z' z_{t+1}\right) &= 2\mathbb{E}_t(\mathbb{C}ov_t\left(\gamma_Y' Y_{t+1}, \gamma_z' z_{t+1} | z_{t+1}\right)) \\ &\quad + 2\mathbb{C}ov_t\Big(\mathbb{E}_t\left(\gamma_Y' Y_{t+1} | z_{t+1}\right), \mathbb{E}_t\left(\gamma_z' z_{t+1} | z_{t+1}\right)\Big) \\ &= 2\mathbb{C}ov_t\Big(\gamma_Y'(\Phi_Y Y_t + \Theta(z_{t+1} - \bar{z})), \gamma_z' z_{t+1}\Big) \\ &= 2\gamma_Y'\Theta\mathbb{V}_t(z_{t+1})\gamma_z = 2(\gamma_z' \otimes \gamma_Y'\Theta) S_q\left(\Gamma_{z,0} + \Gamma_{z,1}' z_t\right) \\ &= 2(\gamma_z \otimes \gamma_Y)'(I_q \otimes \Theta) S_q\left(\Gamma_{z,0} + \Gamma_{z,1}' z_t\right).\end{aligned}$$

Putting these three expressions together leads to the result. □

Proposition 11. *In the context of the model defined in Section 3, $\mu_{3,t}(\gamma' X_{t+1})$ is affine in X_t. More precisely:*

$$\mu_{3,t}(\gamma' X_{t+1}) = \ddot{\alpha}_1(\gamma) + \ddot{\beta}_1(\gamma)' X_t,$$

with

$$\begin{cases} \ddot{\alpha}_1(\gamma) &= 2\Big((\gamma_Y'\Theta+\gamma_z')^3\Big)(\nu\odot\mu^3)+3\left[\Big(\Gamma_{Y,1}\gamma_Y^2\Big)'\otimes(\gamma_Y'\Theta+\gamma_z')\right]S_q\Gamma_{z,0} \\ \ddot{\beta}_1(\gamma) &= \Pi'\left\{6\Big((\gamma_Y'\Theta+\gamma_z')^3\Big)diag(\mu^3)\varphi'+3\left[\Big(\Gamma_{Y,1}\gamma_Y^2\Big)'\otimes(\gamma_Y'\Theta+\gamma_z')\right]S_q\Gamma_{z,1}'\right\}', \end{cases}$$

with $\gamma=[\gamma_Y',\gamma_z']'$, *and where* Π *is such that* $z_t=\Pi X_t$, *that is* $\Pi=[\ \mathbf{0}_{q\times n}\quad Id_{q\times q}\ ]$.

Proof. By the law of total cumulance, we have:

$$\begin{aligned}\mu_{3,t}\left(\gamma'X_{t+1}\right) &= \mathbb{E}_t\Big(\mu_{3,t}\left[\gamma'X_{t+1}|z_{t+1}\right]\Big)+\mu_{3,t}\Big(\mathbb{E}_t\left[\gamma'X_{t+1}|z_{t+1}\right]\Big)\\ &\quad+3\mathbb{C}ov_t\Big(\mathbb{E}_t\left[\gamma'X_{t+1}|z_{t+1}\right],\mathbb{V}_t\left[\gamma'X_{t+1}|z_{t+1}\right]\Big)\\ &= \mathbb{E}_t\Big(\mu_{3,t}\left[\gamma_Y'Y_{t+1}+\gamma_z'z_{t+1}|z_{t+1}\right]\Big)+\mu_{3,t}\Big(\mathbb{E}_t\left[\gamma_Y'Y_{t+1}+\gamma_z'z_{t+1}|z_{t+1}\right]\Big)\\ &\quad+3\mathbb{C}ov_t\Big(\mathbb{E}_t\left[\gamma_Y'Y_{t+1}+\gamma_z'z_{t+1}|z_{t+1}\right],\mathbb{V}_t\left[\gamma_Y'Y_{t+1}+\gamma_z'z_{t+1}|z_{t+1}\right]\Big).\end{aligned}$$

The first term being equal to zero, let's focus on the last two terms above:

$$\begin{aligned}&\mu_{3,t}\Big(\mathbb{E}_t\left[\gamma_Y'Y_{t+1}+\gamma_z'z_{t+1}|z_{t+1}\right]\Big)\\ &=\mu_{3,t}\Big(\gamma_Y'(\Phi_YY_t+\Theta(z_{t+1}-\bar{z}))+\gamma_z'z_{t+1}\Big)=\mu_{3,t}\Big((\gamma_Y'\Theta+\gamma_z')z_{t+1}\Big)\\ &=2\Big((\gamma_Y'\Theta+\gamma_z')^3\Big)(\nu\odot\mu^3)+6\Big((\gamma_Y'\Theta+\gamma_z')^3\Big)\mathrm{diag}(\mu^3)\varphi'z_t,\end{aligned}$$

and,

$$\begin{aligned}&3\mathbb{C}ov_t\Big(\mathbb{E}_t\left[\gamma'X_{t+1}|z_{t+1}\right],\mathbb{V}_t\left[\gamma'X_{t+1}|z_{t+1}\right]\Big)\\ &=3\mathbb{C}ov_t\Big((\gamma_Y'\Theta+\gamma_z')z_{t+1},\mathbb{V}_t\left[\gamma_Y'Y_{t+1}|z_{t+1}\right]\Big)\\ &=3\mathbb{C}ov_t\Big((\gamma_Y'\Theta+\gamma_z')z_{t+1},(\gamma_Y'\odot\gamma_Y')\left(\Gamma_{Y,0}+\Gamma_{Y,1}'z_{t+1}\right)\Big)=3(\gamma_Y'\Theta+\gamma_z')\mathbb{V}_t(z_{t+1})\Gamma_{Y,1}\gamma_Y^2\\ &=3\left[\Big(\Gamma_{Y,1}\gamma_Y^2\Big)'\otimes(\gamma_Y'\Theta+\gamma_z')\right]S_q\Big(\Gamma_{z,0}+\Gamma_{z,1}'z_t\Big).\end{aligned}$$

Putting these expressions together leads to the result. □

Proposition 12. *In the context of the model defined in Section 3, $\mu_{4,t}(\gamma' X_{t+1})$ is affine in X_t. More precisely:*

$$\mu_{4,t}(\gamma' X_{t+1}) = \ddot{\alpha}_1(\gamma) + \dddot{\beta}_1(\gamma)' X_t,$$

with

$$\begin{cases} \ddot{\alpha}_1(\gamma) &= 6\Big((\gamma_Y'\Theta + \gamma_z')^4\Big)(\nu \odot \mu^4) + 3\left[\Big(\Gamma_{Y,1}\gamma_Y^2\Big) \otimes (\Gamma_{Y,1}\gamma_Y^2)\right]' S_q \Gamma_{z,0} \\ &\quad +12(\gamma_Y'\Theta + \gamma_z') \otimes \Big((\Gamma_{Y,1}\gamma_Y^2)' \otimes (\gamma_Y'\Theta + \gamma_z')\Big)\tilde{S}_q\Big(\nu \odot \mu^3\Big) \\ \dddot{\beta}_1(\gamma) &= \Pi'\Bigg\{24\Big((\gamma_Y'\Theta + \gamma_z')^4\Big) diag(\mu^4)\varphi' + 3\left[\Big(\Gamma_{Y,1}\gamma_Y^2\Big) \otimes (\Gamma_{Y,1}\gamma_Y^2)\right]' S_q \Gamma_{z,1}' \\ &\quad +36(\gamma_Y'\Theta + \gamma_z') \otimes \Big((\Gamma_{Y,1}\gamma_Y^2)' \otimes (\gamma_Y'\Theta + \gamma_z')\Big)\tilde{S}_q\Big(diag(\mu^3)\varphi'\Big)\Bigg\}', \end{cases}$$

with $\gamma = [\gamma_Y', \gamma_z']'$, and where,

$$\tilde{S}_p = \sum_{i=1}^{p} \left[e_i^{(p)} \otimes e_i^{(p)} \otimes e_i^{(p)}\right] e_i^{(p)'},$$

where $e_i^{(p)}$ denotes the i^{th} column of the identity matrix of dimension $p \times p$.

Proof. By the Law of total cumulance, $\mu_{4,t}\left(\gamma' X_{t+1}\right)$ is equal to:

$$\begin{aligned} &\mathbb{E}_t\Big(\mu_{4,t}\left[\gamma' X_{t+1} | z_{t+1}\right]\Big) + \mu_{4,t}\Big(\mathbb{E}_t\left[\gamma' X_{t+1} | z_{t+1}\right]\Big) \\ &+ 4\mathbb{C}ov_t\Big(\mu_{3,t}\left[\gamma' X_{t+1} | z_{t+1}\right], \mathbb{E}_t\left[\gamma' X_{t+1} | z_{t+1}\right]\Big) \\ &+ 3\mathbb{V}_t\Big(\mathbb{V}_t\left[\gamma' X_{t+1} | z_{t+1}\right]\Big) \\ &+ 6\kappa_t\Big(\mathbb{V}_t\left[\gamma' X_{t+1} | z_{t+1}\right], \mathbb{E}_t\left[\gamma' X_{t+1} | z_{t+1}\right], \mathbb{E}_t\left[\gamma' X_{t+1} | z_{t+1}\right]\Big), \end{aligned}$$

that is,

$$\begin{aligned}
&\mathbb{E}_t\Big(\mu_{4,t}\left[\gamma_Y'Y_{t+1}+\gamma_z'z_{t+1}|z_{t+1}\right]\Big)+\mu_{4,t}\Big(\mathbb{E}_t\left[\gamma_Y'Y_{t+1}+\gamma_z'z_{t+1}|z_{t+1}\right]\Big)\\
&+4\mathbb{C}ov_t\Big(\mu_{3,t}\left[\gamma_Y'Y_{t+1}+\gamma_z'z_{t+1}|z_{t+1}\right],\mathbb{E}_t\left[\gamma_Y'Y_{t+1}+\gamma_z'z_{t+1}|z_{t+1}\right]\Big)\\
&+3\mathbb{V}_t\Big(\mathbb{V}_t\left[\gamma_Y'Y_{t+1}+\gamma_z'z_{t+1}|z_{t+1}\right]\Big)\\
&+6\kappa_t\Big(\mathbb{V}_t\left[\gamma_Y'Y_{t+1}+\gamma_z'z_{t+1}|z_{t+1}\right],\mathbb{E}_t\left[\gamma_Y'Y_{t+1}+\gamma_z'z_{t+1}|z_{t+1}\right],\mathbb{E}_t\left[\gamma_Y'Y_{t+1}+\gamma_z'z_{t+1}|z_{t+1}\right]\Big).
\end{aligned}$$

The first term being equal to zero, let's focus on the four other terms above:

$$\begin{aligned}
&\mu_{4,t}\Big(\mathbb{E}_t\left[\gamma_Y'Y_{t+1}+\gamma_z'z_{t+1}|z_{t+1}\right]\Big)\\
&=\mu_{4,t}\Big(\gamma_Y'(\Phi_Y Y_t+\Theta(z_{t+1}-\bar{z}))+\gamma_z'z_{t+1}\Big)=\mu_{4,t}\Big((\gamma_Y'\Theta+\gamma_z')z_{t+1}\Big)\\
&=6\Big((\gamma_Y'\Theta+\gamma_z')^4\Big)(\nu\odot\mu^4)+24\Big((\gamma_Y'\Theta+\gamma_z')^4\Big)\mathrm{diag}(\mu^4)\varphi' z_t,
\end{aligned}$$

$$\begin{aligned}
&4\mathbb{C}ov_t\Big(\mu_{3,t}\left[\gamma_Y'Y_{t+1}+\gamma_z'z_{t+1}|z_{t+1}\right],\mathbb{E}_t\left[\gamma_Y'Y_{t+1}+\gamma_z'z_{t+1}|z_{t+1}\right]\Big)\\
&=4\mathbb{C}ov_t\Big(\mu_{3,t}\left[\gamma_Y'Y_{t+1}|z_{t+1}\right],(\gamma_Y'\Theta+\gamma_z')z_{t+1}\Big)\\
&=4\mathbb{C}ov_t\Big(0,(\gamma_Y'\Theta+\gamma_z')z_{t+1}\Big)=0,
\end{aligned}$$

$$\begin{aligned}
&3\mathbb{V}_t\Big(\mathbb{V}_t\left[\gamma_Y'Y_{t+1}+\gamma_z'z_{t+1}|z_{t+1}\right]\Big)\\
&=3\mathbb{V}_t\Big(\mathbb{V}_t\left[\gamma_Y'Y_{t+1}|z_{t+1}\right]\Big)=3\mathbb{V}_t\Big((\gamma_Y'\odot\gamma_Y')\left(\Gamma_{Y,0}+\Gamma_{Y,1}'z_{t+1}\right)\Big)\\
&=3(\Gamma_{Y,1}\gamma_Y^2)'\mathbb{V}_t(z_{t+1})\Gamma_{Y,1}\gamma_Y^2=3\left[\Big(\Gamma_{Y,1}\gamma_Y^2\Big)\otimes\Big(\Gamma_{Y,1}\gamma_Y^2\Big)\right]'S_q\Big(\Gamma_{z,0}+\Gamma_{z,1}'z_t\Big),
\end{aligned}$$

and

$$
\begin{aligned}
&6\kappa_t\Big(\mathbb{V}_t\left[\gamma_Y'Y_{t+1}+\gamma_z'z_{t+1}|z_{t+1}\right],\mathbb{E}_t\left[\gamma_Y'Y_{t+1}+\gamma_z'z_{t+1}|z_{t+1}\right],\mathbb{E}_t\left[\gamma_Y'Y_{t+1}+\gamma_z'z_{t+1}|z_{t+1}\right]\Big)\\
&=6\kappa_t\Big(\left(\gamma_Y'\odot\gamma_Y'\right)\left(\Gamma_{Y,0}+\Gamma_{Y,1}'z_{t+1}\right),(\gamma_Y'\Theta+\gamma_z')z_{t+1},(\gamma_Y'\Theta+\gamma_z')z_{t+1}\Big)\\
&=6\Big((\Gamma_{Y,1}\gamma_Y^2)'\otimes(\gamma_Y'\Theta+\gamma_z')\Big)\mu_{3,t}(z_{t+1})(\gamma_Y'\Theta+\gamma_z')'\\
&=6(\gamma_Y'\Theta+\gamma_z')\otimes\Big((\Gamma_{Y,1}\gamma_Y^2)'\otimes(\gamma_Y'\Theta+\gamma_z')\Big)vec(\mu_{3,t}(z_{t+1}))\\
&=6(\gamma_Y'\Theta+\gamma_z')\otimes\Big((\Gamma_{Y,1}\gamma_Y^2)'\otimes(\gamma_Y'\Theta+\gamma_z')\Big)\tilde{S}_q\Big(2(\nu\odot\mu^3)+6\text{diag}(\mu^3)\varphi' z_t\Big).
\end{aligned}
$$

Putting these expressions together leads to the result. □

The following lemma is used in the derivation of Λ_0 and Λ_1, which are needed to use Propositions 7 and 8.

Lemma 1. *If*

$$M=\begin{bmatrix}A & C\\ B & D\end{bmatrix}$$

where A is of dimension $n\times n$ and D is of dimension $q\times q$, then we have

$$vec(M)=\mathcal{S}_1vec(A)+\mathcal{S}_2vec(B)+\mathcal{S}_3vec(C)+\mathcal{S}_4vec(D),$$

where matrices $\mathcal{S}_1$ to $\mathcal{S}_4$ are computed as follows:

- *$\mathcal{S}_1$ is a $(n+q)^2\times n^2$ matrix that is obtained as follows: Take the identity matrix of dimension $(n+q)^2\times(n+q)^2$ and keep only the columns that correspond to 1's in $vec(\tilde{\mathcal{S}}_1)$, where:*

$$\tilde{\mathcal{S}}_1=\begin{bmatrix}\mathbf{1}_{n\times n} & \mathbf{0}_{n\times q}\\ \mathbf{0}_{q\times n} & \mathbf{0}_{q\times q}\end{bmatrix}.$$

- *$\mathcal{S}_2$ is a $(n+q)^2 \times nq$ matrix that is obtained as follows: Take the identity matrix of dimension $(n+q)^2 \times (n+q)^2$ and keep only the columns that correspond to 1's in $vec(\tilde{\mathcal{S}}_2)$, where:*

$$\tilde{\mathcal{S}}_2 = \begin{bmatrix} \mathbf{0}_{n\times n} & \mathbf{0}_{n\times q} \\ \mathbf{1}_{q\times n} & \mathbf{0}_{q\times q} \end{bmatrix}.$$

- *etc.*

The previous lemma is used in the following proposition:

Proposition 13. *In the context of the model defined in n Section 3, we have (consistently with eq. 30):*

$$vec(\mathbb{V}_t(X_{t+1})) = \Lambda_0 + \Lambda_1 X_t,$$

where

$$\begin{aligned} \Lambda_0 &= \mathcal{S}_1\Big[(\Theta\otimes\Theta)S_q\Gamma_{z,0} + S_n(\Gamma_{0,Y} + \Gamma'_{1,Y}\mu_z)\Big] + \\ &\quad \mathcal{S}_2(\Theta\otimes Id_{q\times q})S_q\Gamma_{z,0} + \mathcal{S}_3(Id_{q\times q}\otimes\Theta)S_q\Gamma_{z,0} + \mathcal{S}_4 S_q\Gamma_{z,0}, \end{aligned}$$

$\mathcal{S}_1$, $\mathcal{S}_2$, $\mathcal{S}_3$, and $\mathcal{S}_4$ being defined in Lemma 1, and

$$\begin{aligned} \Lambda_1 &= \Big(\mathcal{S}_1\Big[(\Theta\otimes\Theta)S_q\Gamma_{z,0} + S_n\Gamma'_{1,Y}\Phi_z\Big] + \\ &\quad \mathcal{S}_2(\Theta\otimes Id_{q\times q})S_q\Gamma_{z,1} + \mathcal{S}_3(Id_{q\times q}\otimes\Theta)S_q\Gamma_{z,1} + \mathcal{S}_4 S_q\Gamma_{z,1}\Big)\Pi, \end{aligned}$$

where Π is such that $z_t = \Pi X_t$, that is $\Pi = [\ \mathbf{0}_{q\times n} \quad Id_{q\times q}\ ]$.

Proof. We have

$$vec(\mathbb{V}_t(X_{t+1})) = vec\begin{bmatrix} \mathbb{V}_t(Y_{t+1}) & \mathbb{C}ov_t(Y_{t+1}, z_{t+1}) \\ \mathbb{C}ov_t(z_{t+1}, Y_{t+1}) & \mathbb{V}_t(z_{t+1}) \end{bmatrix}.$$

Let us compute the vectorial versions of $\mathbb{V}_t(Y_{t+1})$, $\mathbb{C}ov_t(Y_{t+1}, z_{t+1})$, $\mathbb{C}ov_t(z_{t+1}, Y_{t+1})$ and $\mathbb{V}_t(z_{t+1})$.

First, we have:

$$\begin{aligned}\mathbb{V}_t(Y_{t+1}) &= \mathbb{V}_t(\mathbb{E}_t(Y_{t+1}|z_{t+1})) + \mathbb{E}_t(\mathbb{V}_t(Y_{t+1}|z_{t+1})) \\ &= \mathbb{V}_t(\Theta z_{t+1})) + \mathbb{E}_t(\text{diag}(\Gamma_{0,Y} + \Gamma'_{1,Y} z_{t+1})) \\ &= \Theta \text{diag}(\Gamma_{z,0} + \Gamma'_{z,1} z_t)\Theta' + \text{diag}(\Gamma_{0,Y}) + \text{diag}(\Gamma'_{1,Y}(\mu_z + \Phi_z z_t)),\end{aligned}$$

which gives

$$vec(\mathbb{V}_t(Y_{t+1})) = (\Theta \otimes \Theta) S_q(\Gamma_{z,0} + \Gamma'_{z,1} z_t) + S_n(\Gamma_{0,Y} + \Gamma'_{1,Y}\mu_z + \Gamma'_{1,Y}\Phi_z z_t)$$

Second, we have:

$$\mathbb{C}ov_t(Y_{t+1}, z_{t+1}) = \Theta \mathbb{V}_t(z_{t+1}) = \Theta \text{diag}(\Gamma_{z,0} + \Gamma'_{z,1} z_t),$$

which gives

$$vec(\mathbb{C}ov_t(Y_{t+1}, z_{t+1})) = (Id_{q\times q} \otimes \Theta) S_q(\Gamma_{z,0} + \Gamma'_{z,1} z_t).$$

Third, we have

$$\mathbb{C}ov_t(z_{t+1}, Y_{t+1}) = \mathbb{V}_t(z_{t+1})\Theta' = \text{diag}(\Gamma_{z,0} + \Gamma'_{z,1} z_t)\Theta',$$

which gives

$$vec(\mathbb{C}ov_t(z_{t+1}, Y_{t+1})) = (\Theta \otimes Id_{q\times q}) S_q(\Gamma_{z,0} + \Gamma'_{z,1} z_t).$$

Finally, we have:

$$vec(\mathbb{V}_t(z_{t+1})) = S_q(\Gamma_{z,0} + \Gamma'_{z,1} z_t).$$

The results follow from Lemma 1. □

Proposition 14. *In the context of the model defined in n Section 3, we have:*

$$vec(\mathbb{V}_t(X_{t+h})) = \Lambda_{0,h} + \Lambda_{1,h} X_t,$$

where $\Lambda_{0,1} = \Lambda_0$ *and* $\Lambda_{1,1} = \Lambda_1$ *(see Proposition 13), and where, for* $h > 1$*:*

$$\begin{cases} \Lambda_{0,h} &= (\Phi_X^{h-1} \otimes \Phi_X^{h-1})\Lambda_0 + \Lambda_{0,h-1} + \Lambda_{1,h-1}\mu_X \\ \Lambda_{1,h} &= (\Phi_X^{h-1} \otimes \Phi_X^{h-1})\Lambda_1 + \Lambda_{1,h-1}\Phi_X. \end{cases}$$

Proof. Proposition 13 proves the result for $h = 1$. Take $h > 1$. By the law of total variance, we have:

$$\begin{aligned} vec(\mathbb{V}_t(X_{t+h})) &= vec(\mathbb{V}_t(\mathbb{E}_{t+1}[X_{t+h}])) + vec(\mathbb{E}_t(\mathbb{V}_{t+1}[X_{t+h}])) \\ &= vec(\mathbb{V}_t(\mu_X + \Phi_X^{h-1}X_{t+1})) + vec(\mathbb{E}_t(\Lambda_{0,h-1} + \Lambda_{1,h-1}X_{t+1})) \\ &= vec(\Phi_X^{h-1}\mathbb{V}_t(X_{t+1})\Phi_X^{h-1'}) + \Lambda_{0,h-1} + vec(\Lambda_{1,h-1}(\mu_X + \Phi_X X_t)) \\ &= \left(\Phi_X^{h-1} \otimes \Phi_X^{h-1}\right) vec(\mathbb{V}_t(X_{t+1})) + \Lambda_{0,h-1} + \Lambda_{1,h-1}\mu_X + \Lambda_{1,h-1}\Phi_X X_t, \end{aligned}$$

which leads to the result, using $vec(\mathbb{V}_t(X_{t+1})) = \Lambda_0 + \Lambda_1 X_t$ (Proposition 13). □

Proposition 15. *Based on the model defined in n Section 3, we have (consistently with eq. 31):*

$$vec(\mu_{3,t}(X_{t+1})) = M_0 + M_1 X_t,$$

where,

$$\begin{aligned} M_0 = {} & (A_2' \otimes A_1)\left[(\Theta \otimes (\Theta \otimes \Theta))\tilde{S}_q\left(2v \odot \mu^3\right) + (S_{z,y,x} + S_{x,z,y} + I_{n^3})S_{n^2,n}\left(\Theta \otimes (S_n\Gamma_{Y,1}')\right)S_q\Gamma_{z,0}\right] \\ & + (B_2' \otimes B_1)\tilde{S}_q\left(2v \odot \mu^3\right) \\ & + \left[(C_2' \otimes C_1) + (D_2' \otimes D_1)S_{x,z,y} + (E_2' \otimes E_1)S_{z,y,x}\right]\left[\left(\Theta \otimes (\Theta \otimes I_q)\right)\tilde{S}_q\left(2v \odot \mu^3\right) + S_{n^2,q}\left(I_q \otimes (S_n\Gamma_{Y,1}')\right)S_q\Gamma_{z,0}\right] \\ & + \left[(F_2' \otimes F_1)S_{z,y,x} + (G_2' \otimes G_1)S_{y,x,z} + (H_2' \otimes H_1)\right]\left[\left(I_q \otimes (\Theta \otimes I_q)\right)\tilde{S}_q\left(2v \odot \mu^3\right)\right], \end{aligned}$$

and

$$
\begin{aligned}
M_1 = \Bigg\{ & (A_2' \otimes A_1)\Big[(\Theta \otimes (\Theta \otimes \Theta))\tilde{S}_q\Big(6diag\left(\mu^3\right)\psi'\Big) + (S_{z,y,x} + S_{x,z,y} + I_{n^3})S_{n^2,n}\Big(\Theta \otimes (S_n\Gamma_{Y,1}')\Big)S_q\Gamma_{z,1}'\Big] \\
& + (B_2' \otimes B_1)\tilde{S}_q\Big(6diag\left(\mu^3\right)\psi'\Big) \\
& + \Big[(C_2' \otimes C_1) + (D_2' \otimes D_1)S_{x,z,y} + (E_2' \otimes E_1)S_{z,y,x}\Big]\Big[\Big(\Theta \otimes (\Theta \otimes I_q)\Big)\tilde{S}_q\Big(6diag\left(\mu^3\right)\psi'\Big) + S_{n^2,q}\Big(I_q \otimes (S_n\Gamma_{Y,1}')\Big)S_q\Gamma_{z,1}'\Big] \\
& + \Big[(F_2' \otimes F_1)S_{z,y,x} + (G_2' \otimes G_1)S_{y,x,z} + (H_2' \otimes H_1)\Big]\Big[\Big(I_q \otimes (\Theta \otimes I_q)\Big)\tilde{S}_q\Big(6diag\left(\mu^3\right)\psi'\Big)\Big]\Bigg\}\Pi,
\end{aligned}
$$

where Π *is such that* $z_t = \Pi X_t$*, that is* $\Pi = \begin{bmatrix} \mathbf{0}_{q\times n} & Id_{q\times q} \end{bmatrix}$*, and where matrices* A_i*,* B_i*,* C_i*,* D_i*,* E_i*,* F_i*,* G_i*,* H_i*,* $i \in \{1,2\}$ *are such that :*

$$
A_1 = \begin{bmatrix} A_{1,1} \\ \mathbf{0}_{q\times n^2} \\ A_{1,2} \\ \mathbf{0}_{q\times n^2} \\ \vdots \\ A_{1,n} \\ \mathbf{0}_{q\times n^2} \\ \mathbf{0}_{(n+q)q\times n^2} \end{bmatrix},\ B_1 = \begin{bmatrix} \mathbf{0}_{(n+q)n\times q^2} \\ \mathbf{0}_{n\times q^2} \\ B_{1,1} \\ \mathbf{0}_{n\times q^2} \\ B_{1,2} \\ \vdots \\ \mathbf{0}_{n\times q^2} \\ B_{1,n} \end{bmatrix},\ C_1 = \begin{bmatrix} C_{1,1} \\ \mathbf{0}_{n\times(n\cdot q)} \\ C_{1,2} \\ \mathbf{0}_{n\times(n\cdot q)} \\ \vdots \\ C_{1,n} \\ \mathbf{0}_{n\times(n\cdot q)} \\ \mathbf{0}_{(n+q)q\times(n\cdot q)} \end{bmatrix},\ E1 = \begin{bmatrix} \mathbf{0}_{(n+q)n\times(q\cdot n)} \\ E_{1,1} \\ \mathbf{0}_{q\times(q\cdot n)} \\ E_{1,2} \\ \mathbf{0}_{q\times q^2} \\ \vdots \\ E_{1,n} \\ \mathbf{0}_{q\times q^2} \end{bmatrix},
$$

where

$$
\begin{cases}
A_{1,i} = [\mathbf{0}_{n\times n(i-1)} \quad \mathbf{I}_n \quad \mathbf{0}_{n\times n(n-i)}] \quad i = 1,\dots,n, & A_2 = [I_n \ \ 0_{n\times q}], \\
B_{1,i} = [\mathbf{0}_{q\times q(i-1)} \quad \mathbf{I}_q \quad \mathbf{0}_{q\times q(q-i)}] \quad i = 1,\dots,q, & B_2 = [0_{q\times n} \ \ I_q], \\
C_{1,i} = [\mathbf{0}_{q\times q(i-1)} \quad \mathbf{I}_q \quad \mathbf{0}_{q\times q(n-i)}] \quad i = 1,\dots,n, & \\
E_{1,i} = [\mathbf{0}_{n\times n(i-1)} \quad \mathbf{I}_n \quad \mathbf{0}_{n\times n(q-i)}] \quad i = 1,\dots,q, &
\end{cases}
$$

and $D_1 = A_1$*,* $C_2 = E_2 = G_2 = A_2$*,* $F_1 = E_1$*,* $D_2 = F_2 = H_2 = B_2$*,* $G_1 = B_1$*, and* $H_1 = C_1$*.*

Proof. We have

$$vec(\mu_{3,t}(X_{t+1})) = vec\begin{bmatrix} \kappa_t(Y_{1,t+1}, Y_{t+1}, Y_{t+1}) & \kappa_t(Y_{1,t+1}, z_{t+1}, Y_{t+1}) \\ \kappa_t(Y_{1,t+1}, Y_{t+1}, z_{t+1}) & \kappa_t(Y_{1,t+1}, z_{t+1}, z_{t+1}) \\ \cdots & \cdots \\ \kappa_t(Y_{n,t+1}, Y_{t+1}, Y_{t+1}) & \kappa_t(Y_{n,t+1}, z_{t+1}, , Y_{t+1}) \\ \kappa_t(Y_{n,t+1}, Y_{t+1}, z_{t+1}) & \kappa_t(Y_{n,t+1}, z_{t+1}, z_{t+1}) \\ \kappa_t(z_{1,t+1}, Y_{t+1}, Y_{t+1}) & \kappa_t(z_{1,t+1}, z_{t+1}, Y_{t+1}) \\ \kappa_t(z_{1,t+1}, Y_{t+1}, z_{t+1}) & \kappa_t(z_{1,t+1}, z_{t+1}, z_{t+1}) \\ \cdots & \cdots \\ \kappa_t(z_{n,t+1}, Y_{t+1}, Y_{t+1}) & \kappa_t(z_{n,t+1}, z_{t+1}, Y_{t+1}) \\ \kappa_t(z_{n,t+1}, Y_{t+1}, z_{t+1}) & \kappa_t(z_{n,t+1}, z_{t+1}, z_{t+1}) \end{bmatrix}.$$

That is:

$$\begin{aligned} vec(\mu_{3,t}(X_{t+1})) &= vec(A_1\mu_{3,t}(Y_{t+1})A_2) + vec(B_1\mu_{3,t}(z_{t+1})B_2) + vec(C_1\kappa_t(Y_{t+1}, Y_{t+1}, z_{t+1})C_2) \\ &\quad + vec(D_1\kappa_t(Y_{t+1}, z_{t+1}, Y_{t+1})D_2) + vec(E_1\kappa_t(z_{t+1}, Y_{t+1}, Y_{t+1})E_2) \\ &\quad + vec(F_1\kappa_t(z_{t+1}, z_{t+1}, Y_{t+1})F_2) + vec(G_1\kappa_t(z_{t+1}, Y_{t+1}, z_{t+1})G_2) \\ &\quad + vec(H_1\kappa_t(Y_{t+1}, z_{t+1}, z_{t+1})H_2) \\ &= (A_2' \otimes A_1)vec(\mu_{3,t}(Y_{t+1})) + (B_2' \otimes B_1)vec(\mu_{3,t}(z_{t+1})) \\ &\quad + (C_2' \otimes C_1)vec(\kappa_t(Y_{t+1}, Y_{t+1}, z_{t+1})) + (D_2' \otimes D_1)vec(\kappa_t(Y_{t+1}, z_{t+1}, Y_{t+1})) \\ &\quad + (E_2' \otimes E_1)vec(\kappa_t(z_{t+1}, Y_{t+1}, Y_{t+1})) + (F_2' \otimes F_1)vec(\kappa_t(z_{t+1}, z_{t+1}, Y_{t+1})) \\ &\quad + (G_2' \otimes G_1)vec(\kappa_t(z_{t+1}, Y_{t+1}, z_{t+1})) + (H_2' \otimes H_1)vec(\kappa_t(Y_{t+1}, z_{t+1}, z_{t+1})). \end{aligned}$$

Using that $vec(z \otimes y' \otimes x) = S_{z,y,x} vec(x \otimes y' \otimes z)$, $vec(y \otimes x' \otimes z) = S_{y,x,z} vec(x \otimes y' \otimes z)$ and $vec(x \otimes z' \otimes y) = S_{x,z,y} vec(x \otimes y' \otimes z)$, we get:

$$\begin{aligned} vec(\mu_{3,t}(X_{t+1})) &= (A_2' \otimes A_1) vec(\mu_{3,t}(Y_{t+1})) + (B_2' \otimes B_1) vec(\mu_{3,t}(z_{t+1})) \\ &+ \Big[(C_2' \otimes C_1) + (D_2' \otimes D_1) S_{x,z,y} + (E_2' \otimes E_1) S_{z,y,x} \Big] vec(\kappa_t(Y_{t+1}, Y_{t+1}, z_{t+1})) \\ &+ \Big[(F_2' \otimes F_1) S_{z,y,x} + (G_2' \otimes G_1) S_{y,x,z} + (H_2' \otimes H_1) \Big] vec(\kappa_t(Y_{t+1}, z_{t+1}, z_{t+1})). \end{aligned}$$

Using Proposition 4, we have that:

$$vec(\mu_{3,t}(z_{t+1})) = \tilde{S}_q \Big[2v \odot \mu^3 + 6 \text{diag}\left(\mu^3\right) \psi' z_t \Big].$$

We then have:

$$\begin{aligned} \mu_{3,t}(Y_{t+1}) &= \mathbb{E}_t \Big[\mu_{3,t}(Y_{t+1}|z_{t+1}) \Big] + \mu_{3,t} \Big[\mathbb{E}_t(Y_{t+1}|z_{t+1}) \Big] \\ &+ \mathbb{E}_t \left[\mathbb{E}_t\Big(Y_{t+1}|z_{t+1}\Big) \otimes \mathbb{V}_t\Big(Y_{t+1}|z_{t+1}\Big) \right] \\ &+ \mathbb{E}_t \left[\mathbb{E}_t\Big(Y_{t+1} \otimes \mathbb{E}_t(Y_{t+1}|z_{t+1}) \otimes Y_{t+1}|z_{t+1}\Big) \right] \\ &+ \mathbb{E}_t \left[\mathbb{V}_t\Big(Y_{t+1}|z_{t+1}\Big) \otimes \mathbb{E}_t\Big(Y_{t+1}|z_{t+1}\Big) \right]. \end{aligned}$$

Applying the *vec* operator, we get:

$$\begin{aligned} vec(\mu_{3,t}(Y_{t+1})) &= vec\Big[\mu_{3,t}(\Theta z_{t+1})\Big] + S_{z,y,x} vec\left\{ \mathbb{E}_t \left[\left[\mathbb{V}_t\Big(Y_{t+1}|z_{t+1}\Big) \otimes \mathbb{E}_t\Big(Y_{t+1}|z_{t+1}\Big) \right] \right] \right\} \\ &+ S_{x,z,y} vec\left\{ \mathbb{E}_t \left[\left[\mathbb{V}_t\Big(Y_{t+1}|z_{t+1}\Big) \otimes \mathbb{E}_t\Big(Y_{t+1}|z_{t+1}\Big) \right] \right] \right\} \\ &+ vec\left\{ \mathbb{E}_t \left[\mathbb{V}_t\Big(Y_{t+1}|z_{t+1}\Big) \otimes \mathbb{E}_t\Big(Y_{t+1}|z_{t+1}\Big) \right] \right\}. \end{aligned}$$

Since $vec(M_1 \otimes m_1) = vec(M_1) \otimes m_1$, for any matrix M_1 and any vector m_1, we can write:

$$\begin{aligned}
vec(\mu_{3,t}(Y_{t+1})) &= (\Theta \otimes (\Theta \otimes \Theta))\tilde{S}_q \left[2v \odot \mu^3 + 6\text{diag}\left(\mu^3\right)\psi' z_t\right] \\
&\quad + (S_{z,y,x} + S_{x,z,y} + I_{n^3})\mathbb{E}_t\left[vec\left(\text{diag}\left(\Gamma_{Y,0} + \Gamma'_{Y,1} z_{t+1}\right)\right) \otimes \mathbb{E}_t\left(Y_{t+1}|z_{t+1}\right)\right] \\
&= (\Theta \otimes (\Theta \otimes \Theta))\tilde{S}_q \left[2v \odot \mu^3 + 6\text{diag}\left(\mu^3\right)\psi' z_t\right] \\
&\quad + (S_{z,y,x} + S_{x,z,y} + I_{n^3})\mathbb{E}_t\left[\left(S_n\left(\Gamma_{Y,0} + \Gamma'_{Y,1} z_{t+1}\right)\right) \otimes \mathbb{E}_t\left(Y_{t+1}|z_{t+1}\right)\right].
\end{aligned}$$

Then, as $\mathbb{E}_t(x \otimes (y - \mathbb{E}(y)) = S_{n,q} vec(\mathbb{C}ov_t(x, y))$, we obtain:

$$\begin{aligned}
vec(\mu_{3,t}(Y_{t+1})) &= (\Theta \otimes (\Theta \otimes \Theta))\tilde{S}_q \left[2v \odot \mu^3 + 6\text{diag}\left(\mu^3\right)\psi' z_t\right] \\
&\quad + (S_{z,y,x} + S_{x,z,y} + I_{n^3}) S_{n^2,n} vec(\mathbb{C}ov_t(S_n\left(\Gamma_{Y,0} + \Gamma'_{Y,1} z_{t+1}\right), \mathbb{E}_t(Y_{t+1}|z_{t+1}))) \\
&= (\Theta \otimes (\Theta \otimes \Theta))\tilde{S}_q \left[2v \odot \mu^3 + 6\text{diag}\left(\mu^3\right)\psi' z_t\right] \\
&\quad + (S_{z,y,x} + S_{x,z,y} + I_{n^3}) S_{n^2,n} vec(S_n \Gamma'_{Y,1} \mathbb{V}_t(z_{t+1})\Theta')) \\
&= (\Theta \otimes (\Theta \otimes \Theta))\tilde{S}_q \left[2v \odot \mu^3 + 6\text{diag}\left(\mu^3\right)\psi' z_t\right] \\
&\quad + (S_{z,y,x} + S_{x,z,y} + I_{n^3}) S_{n^2,n}\left(\Theta \otimes (S_n \Gamma'_{Y,1})\right) S_q(\Gamma_{z,0} + \Gamma'_{z,1} z_t).
\end{aligned}$$

We also have

$$\begin{aligned}\kappa_{3,t}(Y_{t+1}, Y_{t+1}, z_{t+1})) &= \mathbb{E}_t\left[\kappa_t(Y_{t+1}, Y_{t+1}, z_{t+1})\right] + \kappa_t\left[\mathbb{E}_t(Y_{t+1}|z_{t+1}), \mathbb{E}_t(Y_{t+1}|z_{t+1}), z_{t+1}\right] \\ &+ \mathbb{E}_t\left[\mathbb{E}_t\left[Y_{t+1}|z_{t+1}\right] \otimes \mathbb{C}ov_t\left[Y_{t+1}, z_{t+1}|z_{t+1}\right]\right] \\ &+ \mathbb{E}_t\left[\mathbb{E}_t\left[Y_{t+1} \otimes \mathbb{E}_t(Y_{t+1}|z_{t+1}) \otimes (z_{t+1} - \bar{z})|z_{t+1}\right]\right] \\ &+ \mathbb{E}_t\left[\mathbb{V}ar_t\left[Y_{t+1}|z_{t+1}\right] \otimes \mathbb{E}_t\left[z_{t+1} - \bar{z}|z_{t+1}\right]\right] \\ &= \kappa_t\left[\theta z_{t+1}, \theta z_{t+1}, z_{t+1}\right] + \mathbb{E}_t\left[\mathbb{V}ar_t\left[Y_{t+1}|z_{t+1}\right] \otimes \mathbb{E}_t\left[z_{t+1} - \bar{z}|z_{t+1}\right]\right]\end{aligned}$$

$$\kappa_{3,t}(Y_{t+1}, Y_{t+1}, z_{t+1})) = (\Theta \otimes I_q)\mu_{3,t}(z_{t+1})\Theta' + \mathbb{E}_t\left[\text{diag}\left(\Gamma_{Y,0} + \Gamma'_{Y,1}z_{t+1}\right) \otimes \left(z_{t+1} - \bar{z}\right)\right].$$

Since $vec(M_1 \otimes m_1) = vec(M_1) \otimes m_1$, for any matrix M_1 and any vector m_1, we can write:

$$\begin{aligned}vec(\kappa_{3,t}(Y_{t+1}, Y_{t+1}, z_{t+1}))) &= \left[\Theta \otimes (\Theta \otimes I_q)\right]\tilde{S}_q\left[2v \odot \mu^3 + 6\text{diag}\left(\mu^3\right)\psi' z_t\right] \\ &+ \mathbb{E}_t\left[vec\left(\text{diag}\left(\Gamma_{Y,0} + \Gamma'_{Y,1}z_{t+1}\right)\right) \otimes \left(z_{t+1} - \bar{z}\right)\right] \\ &= \left[\Theta \otimes (\Theta \otimes I_q)\right]\tilde{S}_q\left[2v \odot \mu^3 + 6\text{diag}\left(\mu^3\right)\psi' z_t\right] \\ &+ \mathbb{E}_t\left[\left(S_n\left(\Gamma_{Y,0} + \Gamma'_{Y,1}z_{t+1}\right)\right) \otimes \left(z_{t+1} - \bar{z}\right)\right].\end{aligned}$$

Then, as $\mathbb{E}_t(x \otimes (y - \mathbb{E}(y)) = S_{n,q} vec(\mathbb{C}ov_t(x, y))$, we obtain:

$$\begin{aligned} vec(\kappa_{3,t}(Y_{t+1}, Y_{t+1}, z_{t+1}))) &= \Big[\Theta \otimes (\Theta \otimes I_q)\Big] \tilde{S}_q \Big[2v \odot \mu^3 + 6\text{diag}\left(\mu^3\right) \psi' z_t\Big] \\ &\quad + S_{n^2,q} vec(\mathbb{C}ov_t(S_n \left(\Gamma_{Y,0} + \Gamma'_{Y,1} z_{t+1}\right), z_{t+1})) \\ &= \Big[\Theta \otimes (\Theta \otimes I_q)\Big] \tilde{S}_q \Big[2v \odot \mu^3 + 6\text{diag}\left(\mu^3\right) \psi' z_t\Big] \\ &\quad + S_{n^2,q} \Big(I_q \otimes (S_n \Gamma'_{Y,1})\Big) S_q (\Gamma_{z,0} + \Gamma'_{z,1} z_t). \end{aligned}$$

Finally, we have:

$$\begin{aligned} \kappa_{3,t}(Y_{t+1}, z_{t+1}, z_{t+1})) &= \mathbb{E}_t \Big[\kappa_t(Y_{t+1}, z_{t+1}, z_{t+1})\Big] + \kappa_t \Big[\mathbb{E}_t(Y_{t+1}|z_{t+1}), z_{t+1}, z_{t+1}\Big] \\ &\quad + \mathbb{E}_t \Big[\mathbb{E}_t \Big[Y_{t+1}|z_{t+1}\Big] \otimes \mathbb{V}_t \Big[z_{t+1}|z_{t+1}\Big]\Big] \\ &\quad + \mathbb{E}_t \Big[\mathbb{E}_t \Big[Y_{t+1} \otimes \mathbb{E}_t(z_{t+1} - \bar{z}|z_{t+1}) \otimes (z_{t+1} - \bar{z})|z_{t+1}\Big]\Big] \\ &\quad + \mathbb{E}_t \Big[\mathbb{C}ov_t \Big[Y_{t+1}, z_{t+1}|z_{t+1}\Big] \otimes \mathbb{E}_t \Big[z_{t+1} - \bar{z}|z_{t+1}\Big]\Big] \\ &= \kappa_t \Big[\Theta z_{t+1}, z_{t+1}, z_{t+1}\Big] \end{aligned}$$

and hence,

$$vec(\kappa_{3,t}(Y_{t+1}, z_{t+1}, z_{t+1}))) = [I_q \otimes (\Theta \otimes I_q)] \tilde{S}_q \Big[2v \odot \mu^3 + 6\text{diag}\left(\mu^3\right) \psi' z_t\Big].$$

Putting all together leads to the result. □

Proposition 16. *In the context of the model defined in Section 3, the expectation and the variance of the fourth conditional cumulant of X_t are such that:*

$$\mathbb{E}\left(\mu_{4,t}\left(\sum_{i=1}^{h}\gamma_i' X_{t+i}\right)\right) = \dddot{\alpha}_h(\gamma_1,\ldots,\gamma_h) + \dddot{\beta}_h(\gamma_1,\ldots,\gamma_h)'\mathbb{E}(X_t)$$
$$\mathbb{V}\left(\mu_{4,t}\left(\sum_{i=1}^{h}\gamma_i' X_{t+i}\right)\right) = \dddot{\beta}_h(\gamma_1,\ldots,\gamma_h)'\mathbb{V}(X_t)\,\dddot{\beta}_h(\gamma_1,\ldots,\gamma_h)$$

where $\dddot{\beta}_h(\gamma_1,\ldots,\gamma_h)$, $\mathbb{E}(X_t)$ and $\mathbb{V}(X_t)$ given by:

$$\mathbb{E}(X_t) = (I-\Phi_X)^{-1}\mu_X$$
$$vec(\mathbb{V}(X_t)) = (I-\Phi_X\otimes\Phi_X)^{-1}vec\Big(\Sigma_X\big(\mathbb{E}(z_t)\big)\Sigma_X'\big(\mathbb{E}(z_t)\big)\Big)$$

where μ_X and Φ_X are defined in (28), and $\Sigma_X\big(\mathbb{E}(z_t)\big)\Sigma_X'\big(\mathbb{E}(z_t)\big)$ is given by in (29), using $\mathbb{E}(z_t)$ instead of z_{t-1}.

Proof. Given Proposition 8, we have:

$$\mu_{4,t}\left(\sum_{i=1}^{h}\gamma_i' X_{t+i}\right) = \dddot{\alpha}_h(\gamma_1,\ldots,\gamma_h) + \dddot{\beta}_h(\gamma_1,\ldots,\gamma_h)'X_t,$$

which leads to the results. □

APPENDIX F. CUMULANTS AND THEIR PROPERTIES

Definition 4. *Consider a random variable W characterized by a log-Laplace transform ψ_W, i.e.,:*

$$\psi_W(u) := \log \mathbb{E}(\exp(uW)).$$

The kth order cumulant of W, denoted by μ_k, is defined as the kth derivative of ψ evaluated at zero:

$$\mu_k(W) = \frac{\partial}{\partial u}\psi_W(u)\Big|_{u=0}.$$

The following proposition relates the first three cumulants to the first- to third-order moments:

Proposition 17. *Denoting the kth non-central moments by μ'_k, we have:*

$$\begin{aligned}
\mu_1 &= \mu'_1 \\
\mu_2 &= \mu'_2 - {\mu'_1}^2 \equiv \sigma^2 \\
\mu_3 &= \mu'_3 - 3\mu'_2\mu'_1 + 2{\mu'_1}^3 \equiv \tilde{\mu}_3\sigma^3,
\end{aligned}$$

where σ^2 is the variance and $\tilde{\mu}_3$ is the third standardized moment, that is the skewness.

Proof. Consider a random variable W, we have

$$\psi'_W(u) = \frac{\mathbb{E}(W\exp(uW))}{\mathbb{E}(\exp(uW))},$$

which gives $\mu_1(W) = \mathbb{E}(W)$ (taking $u = 0$). Next, we have

$$\psi^{(2)}_W(u) = \frac{\mathbb{E}(W^2\exp(uW))\mathbb{E}(\exp(uW)) - \mathbb{E}(W\exp(uW))\mathbb{E}(W\exp(uW))}{\mathbb{E}(\exp(uW))},$$

which gives $\mu_2(W) = \mathbb{V}(W)$. The same kind of computation gives the last equality. □

Proposition 18. *Consider two random variables X and Y admitting third-order moments. We have, for any scalars a and b:*

$$\begin{aligned}\mu_3(a+bX) &= b^3\mu_3(X)\\ \mu_3(X+Y) &= \mu_3(X)+3\mathbb{C}ov(X^2,Y)+3\mathbb{C}ov(X,Y^2)+\mu_3(Y).\end{aligned}$$

Proof. This results from $\mu_3 = \mu'_3 - 3\mu'_2\mu'_1 + 2{\mu'_1}^3$, where μ'_k denotes the non-central moment of order k. □

Proposition 19. *We have:*

$$\mu_3(X) = \mathbb{E}[\mu_3(X|Y)] + \mu_3[\mathbb{E}(X|Y)] + \mathbb{C}ov[\mathbb{E}(X|Y), \mathbb{V}(X|Y)].$$

Proof. This follows from the law of total cumulance. □

Proposition 20. *The third moment matrix of a p-dimensional random vector X with finite third-order moments is as follows:*

$$\mu_3(X) = \mathbb{E}\left[(X-\mu)\otimes(X-\mu)'\otimes(X-\mu)\right] = \mathbb{E}\left[(X-\mu)\otimes(X-\mu)(X-\mu)'\right].$$

Proof. For any pair of vectors (a,b), we have $ab' = a\otimes b' = b'\otimes a$. This leads to the result. □

Definition 5. *Consider three scalar random variables X, Y, and Z with finite third-order moments. The second- and third-order joint cumulants are defined as follows:*

$$\begin{aligned}\kappa(X,Y) &= \mathbb{C}ov(X,Y) = \mathbb{E}(XY) - \mathbb{E}(X)\mathbb{E}(Y)\\ \kappa(X,Y,Z) &= \mathbb{E}(XYZ) - \mathbb{E}(XY)\mathbb{E}(Z) - \mathbb{E}(XZ)\mathbb{E}(Y) - \mathbb{E}(YZ)\mathbb{E}(X) + 2\mathbb{E}(X)\mathbb{E}(Y)\mathbb{E}(Z).\end{aligned}$$

It is easily seen that:

$$\kappa(X,X) = \mathbb{V}(X)$$

$$\kappa(X,X,X) = \mu_3(X).$$

Moreover:

$$\kappa(a + bX, c + dY, e + fZ) = b \cdot d \cdot f \cdot \kappa(X, Y, Z).$$

Definition 6. *Consider three p-dimensional random vector X, Y, and Z with finite third-order moments. The second- and third-order joint cumulant matrices are defined as follows:*

$$\begin{aligned}
\kappa(X, Y) &= \mathbb{C}ov(X, Y) = \mathbb{E}(XY') - \mathbb{E}(X)\mathbb{E}(Y)' \\
\kappa(X, Y, Z) &= \mathbb{E}(X \otimes Y' \otimes Z) - \mathbb{E}(X \otimes \mathbb{E}(Y)' \otimes Z) - \mathbb{E}(X \otimes Y') \otimes \mathbb{E}(Z) \\
&\quad -\mathbb{E}(X) \otimes \mathbb{E}(Y' \otimes Z) + 2\mathbb{E}(X) \otimes \mathbb{E}(Y)' \otimes \mathbb{E}(Z).
\end{aligned}$$

It is easily seen that:

$$\kappa(X, X) = \mathbb{V}(X)$$

$$\kappa(X, X, X) = \mu_3(X).$$

Moreover:

$$\kappa(A + BX, C + DX, E + FX) = (B \otimes F)\mu_3(X)D'.$$

Appendix G. Robustness: Results under different specifications of the model

For robustness purposes, we compare our baseline decompositions for inflation and GDP growth with those obtained using two specifications of our model. First, we reduce our baseline model to allow for time variation only in the mean and variance. Second, we augment the baseline model to allow for time-variation in the fourth cumulant. Hence the latter model attempts to fit all four first conditional moments for inflation and growth expectations.

The results of these decompositions for GDP growth and inflation are reported in Figures 17 and 18, respectively. Overall, we observe that these decompositions are very similar, which highlights their robustness. However, there are meaningful differences that arise especially in periods when higher-order moments (asymmetry) gain traction, such as up to the

early 1990s and in the post-pandemic period. Specifically, models that account for asymmetry (our baseline model in Panel (B) and the augmented model that includes all four conditional moments in Panel (C)) can enrich the decompositions with tail risk information. This provides a different interpretation of the key drivers of the real economy and inflation during periods with high tail risk. Notably, using higher-order moment information allows for the role of supply drivers on inflation in the 1990s (following the Kuwait invasion) to have magnitudes that are much more realistic in comparison to the Great Recession, when the oil price increase more than doubles. Similarly, accounting for asymmetry leads to demand drivers being more pronounced for economic activity during the Great Recession and for inflation during the post-pandemic period.

Our findings are in line with the idea that tail risk is not always informative but can enrich a model in times of high uncertainty (refer to Clark et al., 2022, who employ entropic tilting to bring the density forecast information contained in the SPF's probability bins to bear on their model estimates and find that there can be periods in which tilting to the bin information helps forecast accuracy).

FIGURE 17. Decomposition of real GDP growth

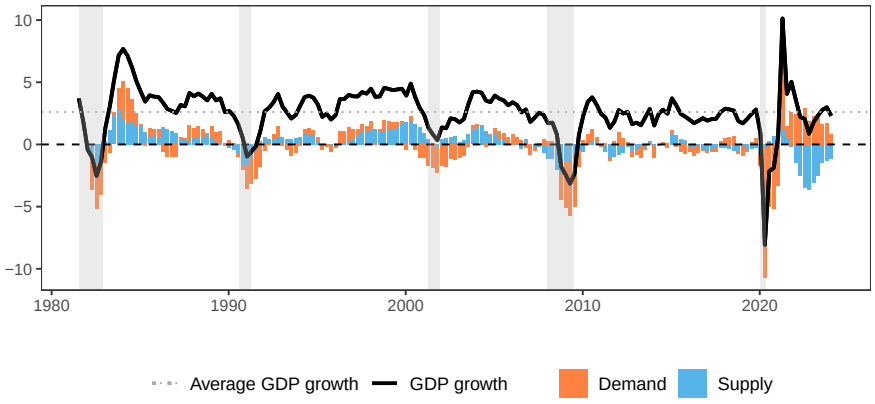

(A) Model with two first conditional moments

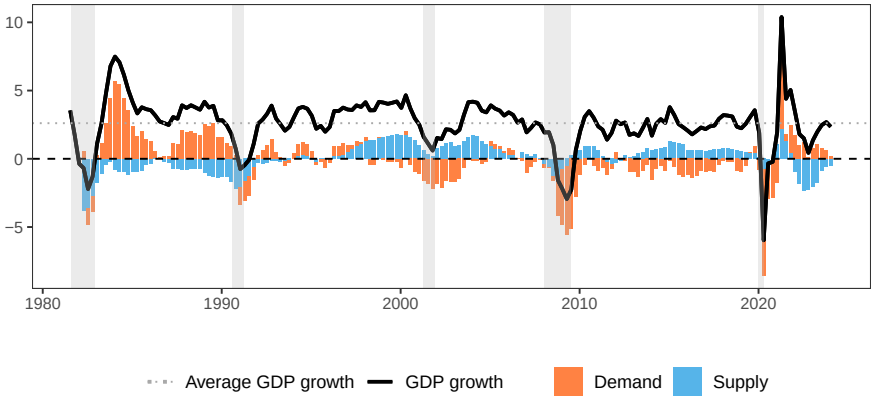

(B) Model with three first conditional moments

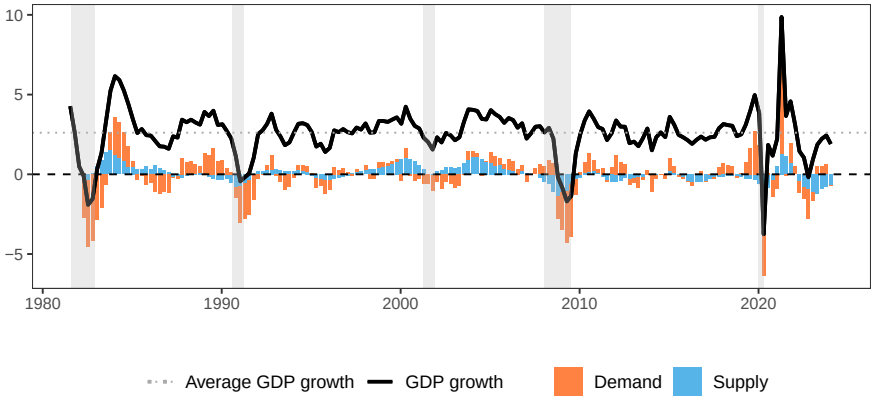

(C) Model with four first conditional moments

Notes: Panel (A), (B) and (C) report the decompositions stemming from (i) a reduced model that allows time variation only in the first two conditional moments, (ii) our baseline model, which accounts for time variation in the three first conditional moments and (iii) an augmented model that allows for the time variation in the four first conditional moments, respectively.

FIGURE 18. Decomposition of inflation

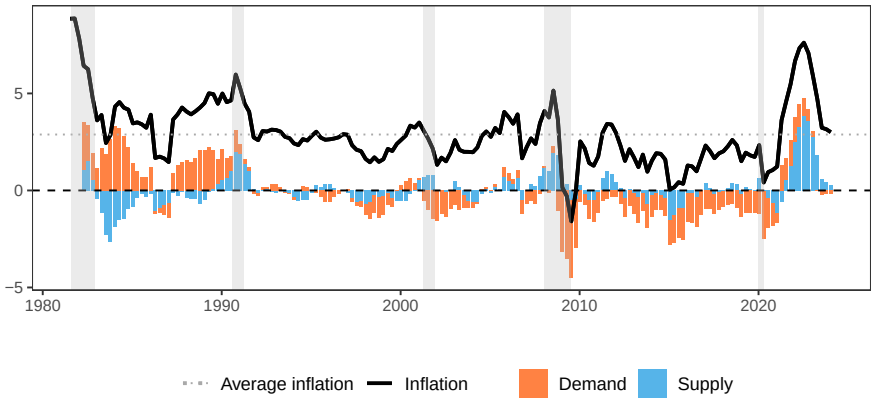

(A) Model with two first conditional moments

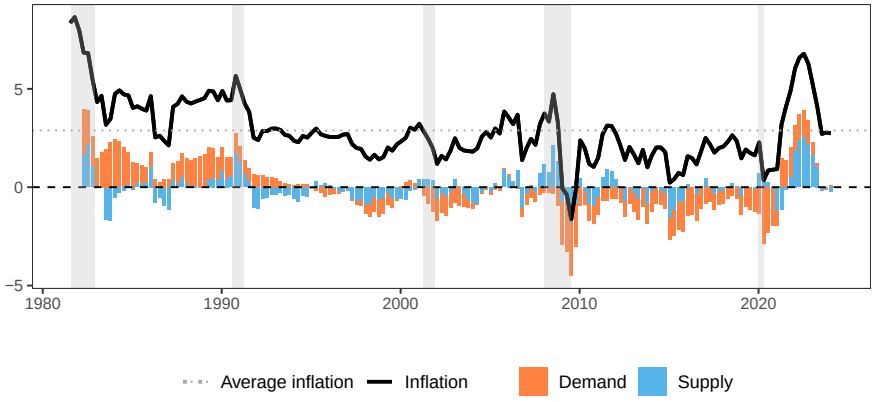

(B) Model with three first conditional moments

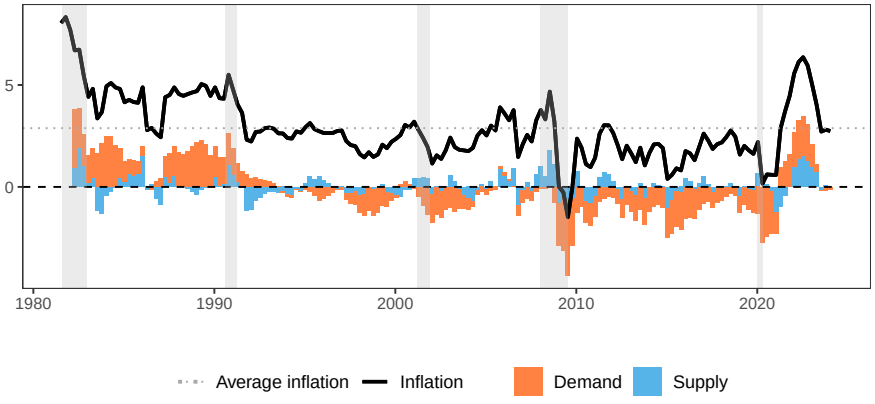

(C) Model with four first conditional moments

Notes: Panel (A), (B) and (C) report the decompositions stemming from (i) a reduced model that allows time variation only in the first two conditional moments, (ii) our baseline model, which accounts for time variation in the three first conditional moments and (iii) an augmented model that allows for the time variation in the four first conditional moments, respectively.